SYNTHESIS OF INNOVATIVE POLYELECTROLYTES USING MONOMERS COMING FROM RENEWABLE SOURCES

Mehmet IŞIK

eman ta zabal zazu
Universidad del País Vasco
Euskal Herriko Unibertsitatea

POLYMAT

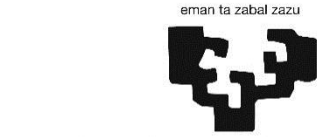

POLYMAT

SYNTHESIS OF INNOVATIVE POLYELECTROLYTES USING MONOMERS COMING FROM RENEWABLE SOURCES

by

MEHMET IŞIK

A thesis submitted in partial fulfillment for the
degree of Doctor of Philosophy
in Applied Chemistry and Polymeric Materials

SUPERVISOR: DR. DAVID MECERREYES

POLYMAT, Institute for Polymer Materials
Faculty of Chemistry, University of the Basque Country (UPV/EHU)

SAN SEBASTIÁN-DONOSTIA, 2016

TABLE OF CONTENTS

CHAPTER 1: INTRODUCTION

1.1. Ionic liquids 1
1.2. Poly(ionic liquid)s 3
1.2.1. Synthesis of poly(ionic liquid)s 5
1.3. Applications of poly(ionic liquid)s 9
1.3.1. Dispersants 9
1.3.2. Sorbents 11
1.3.3. Electrochemical devices 14
1.3.3.1. Ion gels 15
1.4. Deep eutectic solvents (DESs) 23
1.5. Objectives and outline of the thesis 30
1.6. References 34

CHAPTER 2: CHOLINIUM BASED POLY(IONIC LIQUID)S

2.1. Introduction 50
2.2. Experimental 53
2.2.1. Materials 53
2.2.2. Monomer synthesis 53
2.2.3. Synthesis of poly(ionic liquid)s 56
2.2.4. Cholinium lactate ionic liquid preparation 57
2.2.5. Photopolymerization 57
2.2.6. Characterization 58
2.3. Results and Discussion 59
2.3.1. Synthesis and characterization of monomers 59
2.2.2. Synthesis and characterization of poly(ionic liquid)s .. 63
2.4. Conclusions 81
2.5. References 82

CHAPTER 3: AMPHIPHILIC BLOCK COPOLYMERS FROM LACTIC ACID AND CHOLINIUM BUILDING UNITS

3.1. Introduction 86
3.2. Experimental 90
3.2.1. Materials 90
3.2.2. Monomer synthesis 90
3.2.3. Catalyst preparation 91

3.2.4. Macro-RAFT agent synthesis..... 91
3.2.5. Synthesis of the block copolymers..... 92
3.2.6. Preparation of block copolymer nanoparticles..... 92
3.2.7. Characterization..... 93
3.3. Results and Discussion..... 94
3.3.1. Macro-RAFT agent synthesis..... 94
3.3.2. Synthesis of the block copolymers..... 100
3.3.3. Self-assembly in water..... 104
3.4. Conclusions..... 109
3.5. References..... 110

CHAPTER 4: CHOLINIUM BASED ION GELS FOR CUTANEOUS ELECTROPHYSIOLOGY
4.1. Introduction..... 115
4.2. Experimental..... 119
4.2.1. Materials..... 119
4.2.2. Monomer and IL synthesis..... 119
4.2.3. Preparation of ion gels..... 120
4.2.4. Preparation of electrode and ECG measurements..... 121
4.2.5. Characterization..... 123
4.3. Results and Discussion..... 125
4.3.1. Preparation of ion gels..... 125
4.3.2. Rheological properties of ion gels..... 130
4.3.3. Thermal properties of the ion gels..... 133
4.3.4. Electrical properties of the ion gels..... 137
4.3.5. Long term cutaneous recordings..... 139
4.4. Conclusions..... 147
4.5. References..... 149

CHAPTER 5: INNOVATIVE POLY(IONIC LIQUID)S BY THE POLYMERIZATION OF DEEP EUTECTIC MONOMERS
5.1. Introduction..... 153
5.2. Experimental..... 156
5.2.1. Materials..... 156
5.2.2. Preparation of quaternary ammonium compounds..... 156
5.2.3. Preparation of deep eutectic monomers..... 157
5.2.4. Characterization..... 158

5.3. Results and Discussion 160
5.3.1. Deep eutectic monomer preparation 161
5.3.2. Polymerization of deep eutectic monomers 169
5.3.3. CO_2 capture 177
5.4. Conclusions 179
5.5. References 180

CHAPTER 6: DEEP EUTECTIC MONOMER BASED POLY(IONIC LIQUID)S FOR ENHANCED CO_2 CAPTURE
6.1. Introduction 185
6.2. Experimental 189
6.2.1. Materials 189
6.2.2. Deep eutectic monomer preparation 189
6.2.3. Polymerization of DEMs 190
6.2.4. Characterization 191
6.2.5. CO_2 capture 192
6.3. Results and Discussion 193
6.3.1. DEM preparation and characterization 193
6.3.2. PolyDEM preparation and characterization 205
6.3.3. CO_2 capture 215
6.4. Conclusions 220
6.5. References 222

CHAPTER 7: GENERAL CONCLUSIONS 227

ANNEXES 233

VITA 236

1 Introduction

Contents

1.1. Ionic liquids……1
1.2. Poly(ionic liquid)s……..3
1.3. Applications of poly(ionic liquid)s……9
1.4. Deep eutectic solvents (DESs)……23
1.5. Objectives and outline of the thesis……..30
1.6. References……34

Chapter 1

1.1. Ionic liquids

Ionic liquids are described first by Paul Walden in 1914 as salts composed of cations and anions which melt below 100 ºC. This definition was done upon his observations regarding the ethylammonium nitrate salt which displayed a melting point of 14 ºC. This discovery today is acknowledged as the starting point of the ionic liquids.[1] Ionic liquids are generally composed of cations and anions that possess asymmetric character. This asymmetry is the key point to obtain weak coordination between the cation and the anion resulting in a lower melting point than conventional salt systems.[2] Therefore, the choice of the ion couple plays a significant role to design and tailor the properties of the ionic liquids. Today many common ionic liquids include imidazolium, pyridinium, alkylammonium, pyrrolidinium and cholinium cations. The anions are chosen from the broad family of organic or inorganic anions such as halides, polyatomic inorganics and carboxylates. The Chemical structures of some common cations and anions are given in the figure below.

Chapter 1

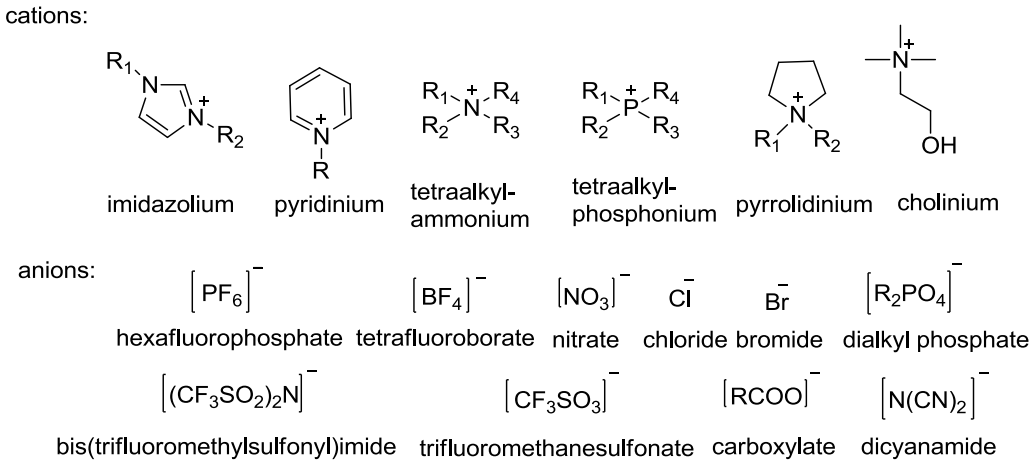

Figure 1.1. Structures of common cations and anions used for ionic liquid preparation

The ultimate property of the ionic liquid can be easily tuned by playing with the cation and anion combination. For instance, ionic liquids bearing bis(trifluoromethylsulfonyl)imide ($TFSI^-$) [$(CF_3SO_2)_2N^-$] anion generally display hydrophobic character making them useful for applications where hydrophobicity is required. On the other hand, in general ionic liquids carrying halide anions are more hydrophilic making them soluble in polar solvents. This flexibility to choose from a variety of anion and cation families renders possible to adjust many properties of ionic liquids such as ion conductivity, thermal stability, heat capacity and solubilization power. In addition, the presence of long range Coulomb interactions endow the ionic liquids with

remarkable physico-chemical properties such as low melting point, non-flammability, wide electrochemical window, thermal stability and negligible vapour pressure.[3-5]

These superior properties make ionic liquids ideal candidates for many different applications. Some of these applications can be listed as solvents[6-11] and catalysts for organic synthesis[12-22], electrochemical devices,[23-27] carbohydrate dissolution and modification[9-11], bioelectronics,[28-32] CO_2 capture and separation,[33-39] fuel cells,[40-42] analytical chemistry[43-45] and nanomedicine.

1.2. Poly(ionic liquid)s

Poly(ionic liquid)s (PILs), also named as polymerized ionic liquids, are polymeric materials which carry ionic species in each of the repeating units. Thus, the backbone of the polymer is composed of cationic or anionic charges to form a macromolecule. Although most of the ionic liquids are liquids at room temperature, most PILs are solids due to its polymeric nature and possess measurable glass transition temperatures. The presence of ionic liquid repeat units within the macromolecular architecture endows the polymer with many unique properties of the ionic liquids. Therefore, these polymeric materials are of great interest to polymer chemists and material scientists to create

new properties and functions by using the great compositional variety of ionic liquids. In addition to the properties of the ionic liquids, PILs possess the superior properties of polymers such as high mechanical stability, improved processability, mouldability and durability. These features of PILs gathered much attention from the scientific community to produce materials with properties that could not be afforded by ionic liquids.[46-50] Currently, scientific research on PILs has increased (figure 1.2) as many new materials are being produced with tailor-designed properties.

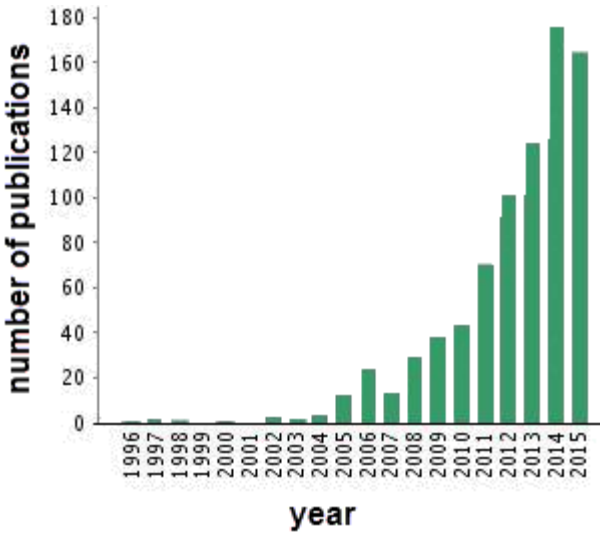

Figure 1.2. Number of publications vs. year. Plot was obtained from Web of Science database by searching for the topics “poly(ionic liquid), “ ionic liquid polymer”, “polymerized ionic liquid”, “polymerizable ionic liquid”, “ionic liquid monomer”.

The intensive studies on PILs expanded many different aspects of these materials such as new structures, properties and applications.

1.2.1. Synthesis of poly(ionic liquid)s

There have been many reports regarding the synthesis of PILs through many different synthetic strategies. These strategies can be categorized into two: 1) polymerization of ionic liquid monomer[51] and 2)

chemical modification of polymers.[52] In each category many different methods can be used such as chain growth, step growth, ring opening and many more. The use of ionic liquid monomers to synthesize poly(ionic liquid)s require the design of monomers by attaching polymerizable groups to the existing ionic liquid structure. The polymerizable group can be attached either to the cation or anion giving rise to cationic or anionic poly(ionic liquid)s. One of the most widely used techniques to synthesize PILs is free radical polymerization of ionic liquid monomers.[53-56] Due to difficulties to purify IL monomers, the tolerance of radical polymerization towards impurities, moisture or other functional groups is the key point in the success of this method. There are three main polymerizable groups utilized in free radical polymerization of ionic liquid monomers. These can be listed as (i) (meth)acryloyl-based,[56] (ii) N-vinylimidazolium-based[52] and (iii) styrenic-based[55] ionic liquid monomer. The general approach to obtain (meth)acryloyl-based ionic liquid monomers is the quaternization of tertiary amines with the methacrylic group to obtain the desired monomer. This chemical strategy is depicted in the scheme below.

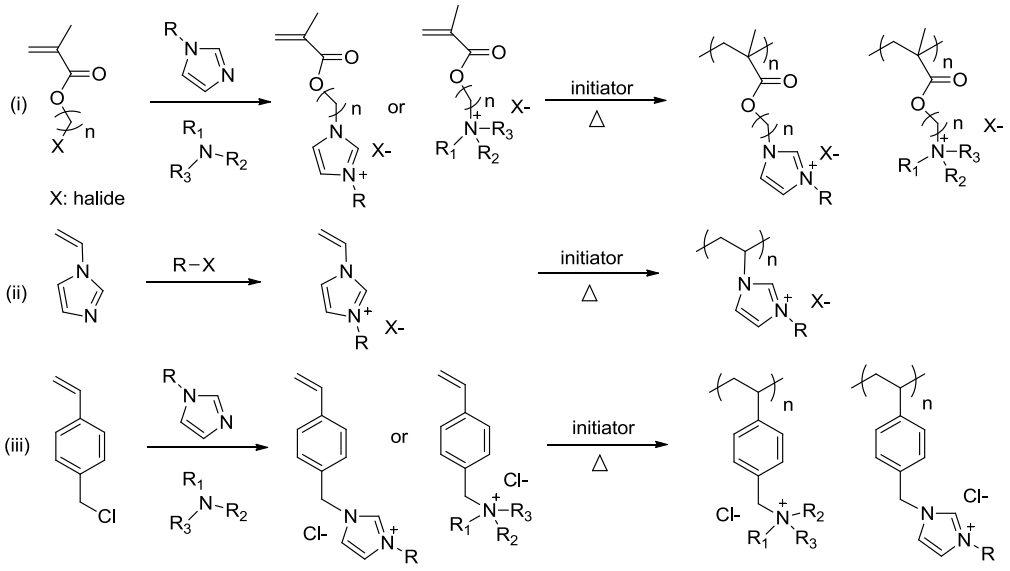

Scheme 1.1. Synthetic routes to obtain IL monomers with different polymerizable groups and the corresponding poly(ionic liquid)s

In the 1st step to prepare IL monomers with methacrylic functionality, halo-alkyl bearing methacrylate monomer is used to quaternize the tertiary amine molecule, either imidazole or N,N,N-trialkylamine. As a result of this simple reaction, IL monomer functionalized with the methacrylic group is obtained. The reaction pathway for the styrenic-based IL monomers is also similar where methylchlorostyrene monomer is used to quaternize the desired tertiary amine molecule. In the 2nd case, already vinyl functionalized imidazole monomer is quaternized with an alkylhalide to obtain the desired IL monomer. All these IL

monomers can be used to perform free radical polymerization to synthesize the desired poly(ionic liquid).[57-59] The synthesis takes place by introducing an initiator to the monomer solution and heating up to complete the polymerization reaction. The alkyl groups denoted as R on the chemical structures allow tailoring many properties of the synthesized poly(ionic liquid)s. In addition, the final properties of the polymers can be tailored through simple anion exchange reactions where the halide anion is exchanged with a desired anion of choice.[52] This strategy opens up the possibility to obtain poly(ionic liquid)s with targeted properties. The 2nd general method to synthesize poly(ionic liquid)s relies on the synthesis of the neutral polymer and quaternization with the desired alkylhalide to obtain the corresponding poly(ionic liquid).[60] Like any other monomeric system, ionic liquids can be copolymerized with different monomers to tailor the final property of the polymer. There are many examples in literature regarding the synthesis of poly(ionic liquid) copolymers for many different applications. [46-50]

The possibility to use radical polymerization for the poly(ionic liquid) synthesis allows using controlled radical polymerization techniques to obtain well-defined polymeric architectures. Among controlled radical polymerization methods atom transfer radical polymerization (ATRP),[61] reversible addition-fragmentation chain transfer (RAFT),[62] nitroxide-mediated radical polymerization (NMP)[63] or cobalt mediated radical

polymerization (CMRP)[64] can be given as examples. The use of these techniques also allows obtaining block copolymers with conventional monomer systems.

1.3. Applications of poly(ionic liquid)s

Unique properties of poly(ionic liquid)s makes them ideal candidates for many different technological fields such as energy and environment, catalysis, analytical chemistry and materials science.

1.3.1. Dispersants

Poly(ionic liquid)s have been used as dispersants to stabilize nanomaterials in aqueous and organic mediums. Recent studies revealed that imidazolium based PILs can efficiently disperse carbon nanotubes or graphene sheets in aqueous medium.[65,66]

PILs can also be used to produce gold and silver nanoparticles for various applications. An interesting example can be given from the work of Fukushima and coworkers where ionic liquid monomers were used to form a soft organic layer on single-wall carbon nanotubes (SWCT). Subsequent polymerization of the monomers resulted in the formation of

bucky gels or bucky plastics with superior mechanical properties and conductivities in comparison to the composite materials obtained with SWCTs.[67] Similarly, PILs were used to stabilize cellulose nanofibers through in-situ polymerization approach. Grygiel et. al. used imidazolium based ionic liquid monomers to graft the corresponding PIL onto the cellulose nanofiber surface. This allowed enhanced stabilization of the fibers and simple anion exchange reactions allowed obtaining solid state mechanically reinforced PIL membranes.[68]

In addition to use PILs as stabilizers for nanomaterials, they have been used for the synthesis of conjugated polymers as stabilizers. Among those polymers, polypyrrole, polyaniline and poly(3,4-ethylenedioxythiophene (PEDOT) can be given as examples. A common method is to polymerize the monomer in the presence of the PIL to end up with dispersion in water as depicted in the following figure.

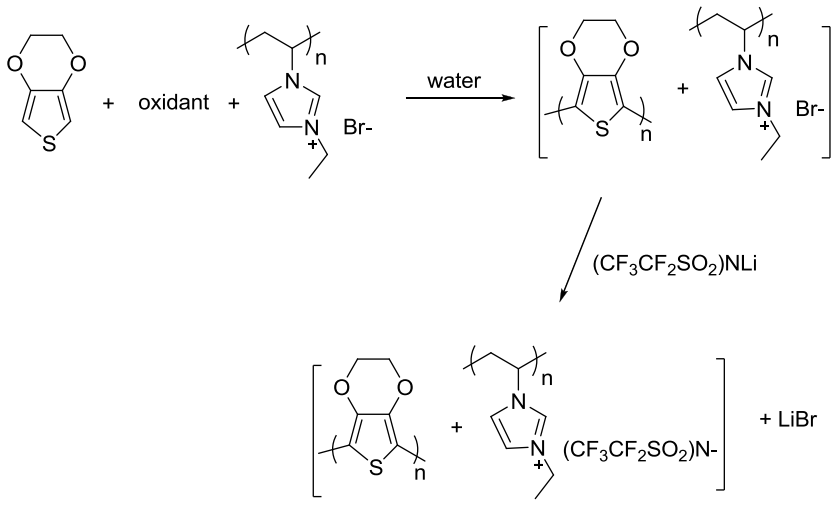

Figure 1.3. Method to obtain PEDOT-PIL dispersions

The substitution of the water soluble anion with a hydrophobic one results in the precipitation of the PIL trapping the conjugated polymer microparticles. The resulting powder can be solubilized in common organic solvents to produce conjugated polymer dispersions in organic solvents.[69,70]

1.3.2. Sorbents

PILs have also been used as sorbents of CO_2 since they exhibit high sorption capacity. The first study to illustrate the CO_2 sorption capability of PILs was reported by Shen and coworkers for poly(1-(4-vinylbenzyl)-

3-butylimidazolium tetrafluoroborate) and poly(1-(4-vinylbenzyl)-3-butyl imidazolium hexafluoro phosphate). The comparison of the CO_2 sorption capabilities of imidazolium and tetraalkylammonium cations by the same group revealed that the tetraalkylammonium cation had a better sorption performance over the imidazolium based systems.[71] The strong interaction of tetraalkylammonium cation with CO_2 is attributed to its high charge density as compared to imidazolium cation since the positive charge in the latter is delocalized.[72,73] Similar studies have been conducted in literature to assess the effect of cation and anion variation on the sorption performance of PILs.[73-75] Tang and coworkers compared different cationic PIL structures and found out that the CO_2 sorption capacity followed the decreasing order: ammonium > pyridinium > phosphonium > imidazolium.[75] The structures of these polycations are displayed in the figure below.

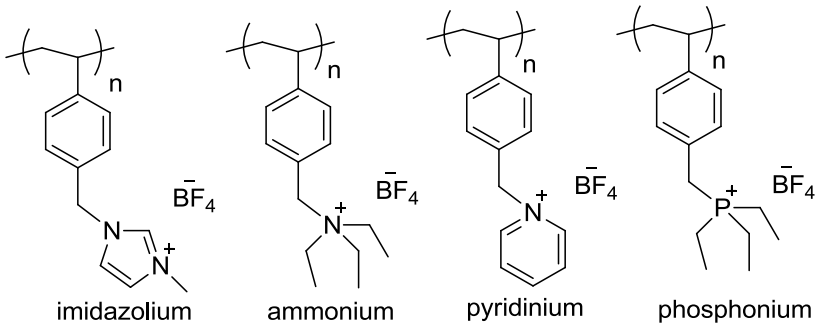

Figure 1.4. Structures of polycations used to compare the effect of cation on CO_2 sorption

As mentioned earlier ammonium based PILs displayed higher CO_2 sorption owing to the presence of sp^3 hybridization in the tetraalkylammonium cations that can rearrange and become more accessible to carbon dioxide. Similarly the anion plays a significant role to have a better CO_2 sorption performance. Organic anions such as carboxylates, sulfonates, imides (NTf_2, Sac) and inorganic anions such as tetrafluorophosphate (PF_6), tetrafluoroborate (BF_4), nitrate (NO_3) and bromide (Br) are some examples from literature. The structures of some of the anions used for CO_2 sorption studies are depicted in the figure below.

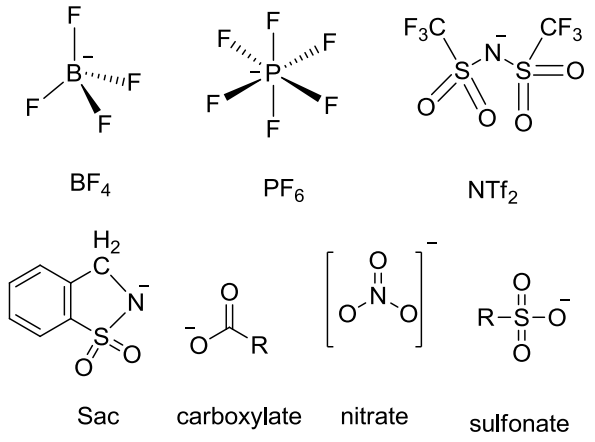

Figure 1.5. Structures of some anions used for CO_2 sorption

Tang and coworkers studied the effect of anion variation on the sorption performance of PILs having similar backbones. It has been

shown that PF_6 and BF_4 anions displayed better performances than NTf_2 and Sac based polymers.[73] Mineo and coworkers did similar experiments and showed that sulfonate anions outperform the carboxylate anions even though they have similar attachments to the anion.[76] Bhavsar et. al. studied the ammonium based PILs having different anions. It was found out that the presence of acetate anion greatly enhanced the CO_2 sorption capability together with the selectivity over N_2. This was correlated with the high basicity of acetate anion giving rise to a strong affinity towards carbon dioxide.[77] Many studies conducted to assess the CO_2 sorption performance of PILs confirmed that the cations and anions play a significant role in the performance of these materials. Based on the studies in literature, incorporation of basic groups and enhanced porosity may lead to improved material design. Therefore, appropriate modifications in their structures by choosing the right cation and anion combinations together with the right polymer backbone and porosity can bring out new materials that outperform the current systems.[78]

1.3.3. Electrochemical devices

Previous studies about the use of ionic liquids for many different applications demonstrated that the applicational perfomances can be

significantly enhanced. However, the liquid nature of ionic liquids presents some drawbacks such as leakage of the electrolyte, hence the need for encapsulation. Therefore, despite its being solid, the ionic nature of PILs makes them ideal candidates as electrolytes for electrochemical devices. They possess many advantages such as mechanical stability, safety and simple processing. The major drawback associated with solid PILs is their low conductivity due to the rigid nature of the polymer. For these reasons, there is a growing interest to design and produce hybrid materials that involve the PIL and IL in one material which are commonly called as ion gels or gel electrolytes.[79]

1.3.3.1. Ion gels

Ion gels are materials composed of an ionic liquid which is stabilized in a solid network such as polymers, ceramics or nanofillers. The stabilization of the ionic liquid in a solid matrix endows the ionic liquid with dimensional stability while preserving its inherent properties. The solid and liquid phases percolate throughout each other and yield a solid-liquid stable system as depicted in the figure below.

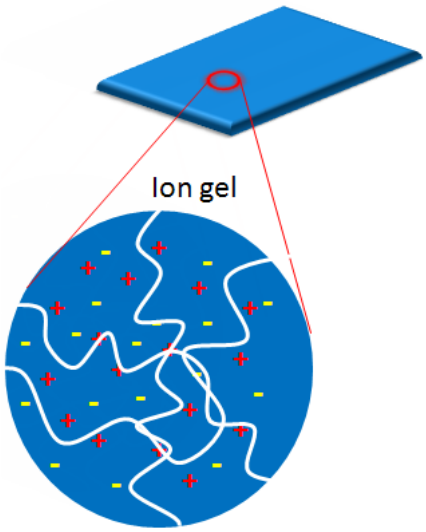

Figure 1.6. Simple illustration of an ion gel

There are several different classes of ion gels which are named as organic ion gels, inorganic ion gels and hybrid ion gels. Synthetic or natural polymers and small molecular weight gelators are used in the case of organic ion gels.[80] The use ceramic nanoparticles or sol/gel chemistry in ionic liquids results in the formation of inorganic ion gels.[81] The use of both organic and inorganic gelators produces hybrid ion gel systems.[82] The matrix nature of the ion gel provides the solid like behavior while preserving the ionic liquid nature of the material. Due to their improved properties compared to pure poly(ionic liquid)s, ion gels have been used for many applications such as batteries,[83,84] actuators,[85]

dye-sensitized solar cells,[86] bioelectronics[87] and electrochromic devices.[79]

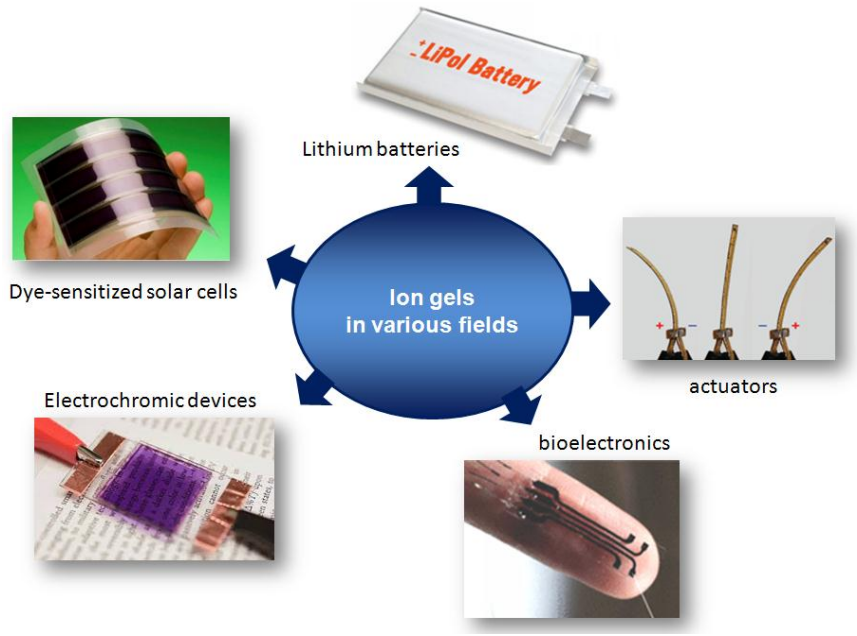

Figure 1.7. Applications of ion gels in different fields

Preparation of ion gels mainly in polymer networks is achieved through several different approaches. One of the 1st examples of ion gels prepared by simple blending of a triblock copolymer where the middle block is miscible with the ionic liquid but the side blocks are not as shown in figure 1.8. The immiscibility of side blocks with the ionic liquids provides the physical crosslinking within the matrix giving the material mechanical strength to produce self-standing membranes.

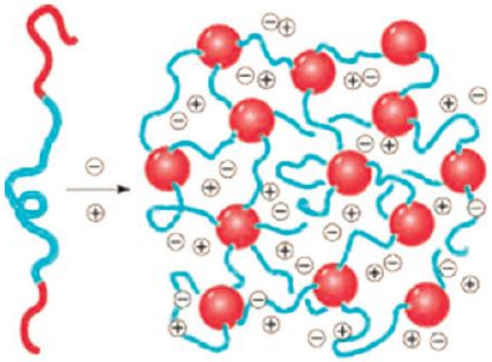

Figure 1.8. Ion gel preparation by mixing with a triblock copolymer having soluble (blue) and insoluble (red) blocks (88)

These ion gels have been investigated deeply for their solid-state self-assembly, ionic conductivity and viscoelastic properties.[88] The tunable nature of the material properties rendered possible to use these ion gels for many different applications such as high capacitance gate dielectrics,[89] thin-film transistors,[90] dye-sensitized solar cells[86] and gas separation membranes.[91]

In addition to block copolymers, biopolymers are also used to prepare ion gels since ionic liquids are miscible with many biopolymer systems. Similarly, a biopolymer of choice is blended with an ionic liquid at a certain ratio to yield a solid membrane material. This concept has been used 1st with cellulose which can be dissolved by using many different ionic liquids. The 1st discovery of gelation of cellulose dissolved

in ionic liquids was coincidental. Kadokawa and coworkers dissolved cellulose in the ionic liquid and left it on the bench. The moisture absorbed by the solution caused to form cellulose nanoaggregates to act as physical crosslinks in the matrix resulting in the formation of an ion gel.[92]

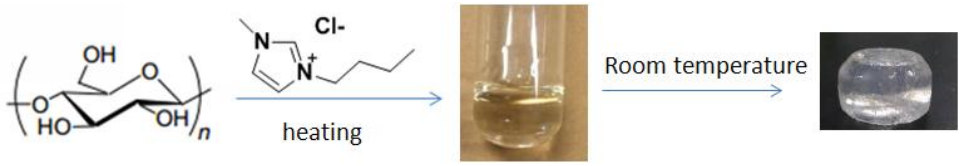

Figure 1.9. Cellulose based ion gel through dissolution and gelation

This approach was later used with many different natural biopolymers such as chitin, amylase, starch, xanthan gum, pullulan, guar gum etc. to produce ion gels based on natural polymers for many different applications.[93]

Another approach to produce ion gels is to use poly(ionic liquid)s as the network to endow some mechanical integrity to the material. This approach has been very successful for the stabilization ionic liquids due to Coulombic interactions between the polymer backbone and the ionic liquid. Within this context, PILs are ideal materials to develop tailor-designed solid electrolytes. Similar to the previous preparation methods, solution of a PIL is mixed with an ionic liquid at a certain ratio. The

evaporation of the solvent yields an ion gel. Due to good compatibility of the components generally transparent films are obtained. The mechanical properties of the final ion gels can be tuned by playing with the amount of the free ionic liquid inside. The material can be tailored from solid-state to sticky gel. The change in the concentration of the ionic liquid also tailors the ionic conductivity. Following figure illustrates the effect of free ionic liquid on the conductivity of the ion gel.[79]

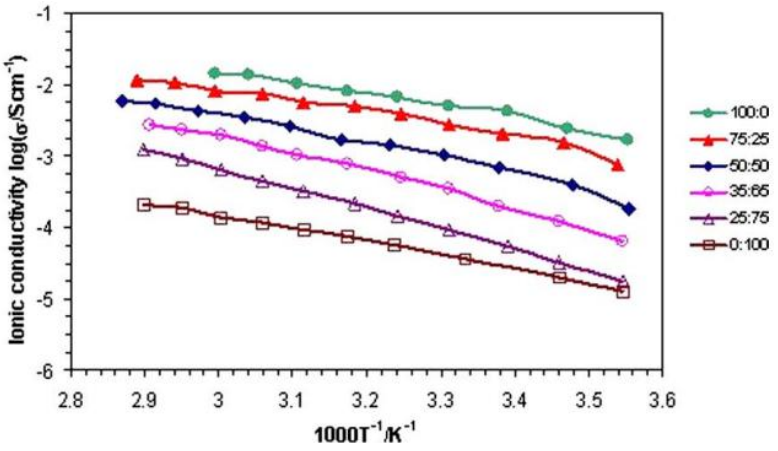

Figure 1.10. Temperature dependence of the conductivity of ion gels prepared with different IL ratios (79)

The poly(1-vinyl-3-ethylimidazolium bis (trifluoromethane sulfonimide) and 1-butyl-3-methyl imidazolium bis (trifluoromethane sulfonamide) mixtures from 100% PIL to 100% IL were analyzed to examine the effect of IL amount on the conductivity with changing

temperature. Addition of IL into the PIL enhanced the conductivity from 10^{-5} Scm^{-1} to 10^{-3} Scm^{-1}.The conductivity value reached to a value of the pure ionic liquid when the IL amount was elevated.[79] Another important advantage of PIL/IL based ion gels is the flexibility to choose the right cation-anion combination for the targeted application. For instance, several groups reported that the imidazolium based PILs bearing iodide anions were better for dye-sensitized solar cells[94-98] whereas electrochromic devices based on PEDOT performed better with imidazolium bearing bromide as the anion. On the other hand, studies showed that pyrrolidinium cation combined with bis(trifluoromethanesulfonimide) anion performs best for lithium batteries.[99,100] This is due to the fact that this cation-anion combination displays superior electrochemical stability compared to similar analogs.

Ion gels based on poly(ionic liquid)/ionic liquid mixtures can also be prepared through the polymerization of ionic liquid monomers in the ionic liquids. Jeremias and coworkers studied the photopolymerization of diallyldimethylammonium bis (trifluoromethane sulfonimide) inside N-butyl-N-methyl pyrrolidonium bis(trifluoromethanesulfon)imide ionic liquid.[101]

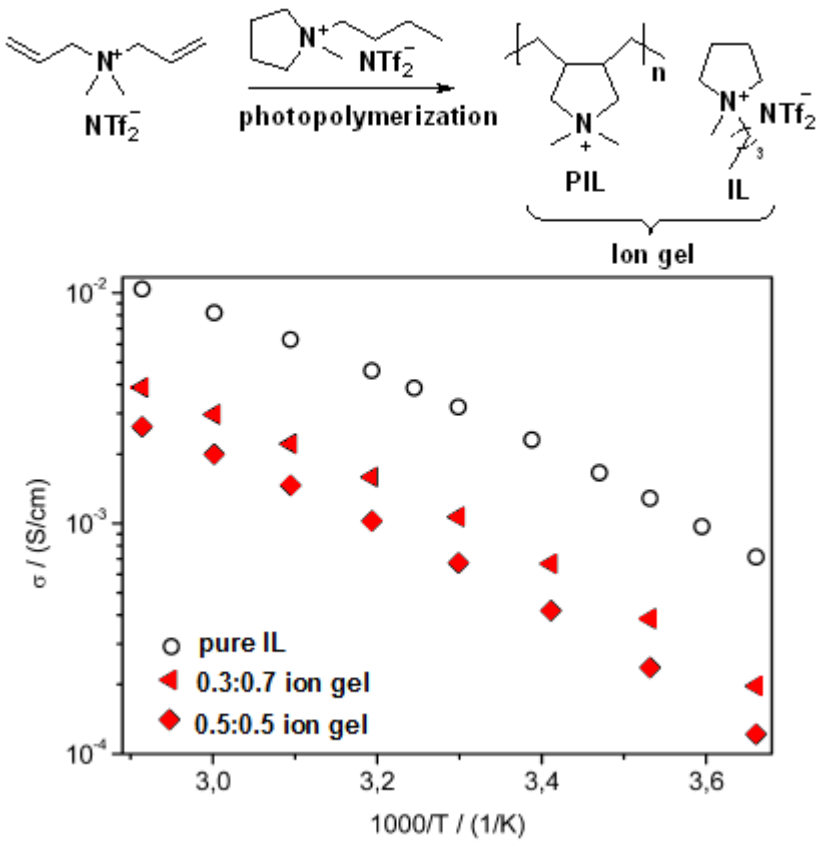

Figure 1.11. Synthesis of the ion gel through photopolymerization and the conductivities of the ion gels prepared (101)

As it is seen from the figure above, the photopolymerization of the monomer in the ionic liquid yielded the ion gels. The conductivities of the ion gels with different IL contents were above 10^{-4} S/cm. They showed similar temperature trend as compared to pure IL.

Owing to the above-mentioned synthetic strategies and structural diversity poly(ionic liquid)s are broadening the applications of conventional polyelectrolytes. Designing new cations and anions that outperform the conventional combinations is still crucial to generate innovative polymeric systems with superior properties.[101,102]

1.4. Deep eutectic solvents (DESs)

Many different solvent systems are used in materials science for different purposes such as organic, inorganic chemistry, polymer synthesis and processing where solvents are needed. The type of the solvent chosen for the process significantly influences the conditions of the process as well as the properties of the final material. The use of solvents in large scale applications reveals the environmental concerns on the selected solvent system. Therefore, considerable attention is paid to the use of green alternatives to the conventional solvent systems. Within this context, ionic liquids have been investigated as alternative solvents due to their unique properties such as nonflammability, chemical stability, high solvation capability, and electrical conductivity and most important of all their negligible vapor pressure which is the main reason why they are considered green. In addition, a subset of ionic liquids are protic ionic liquids. These are

easily formed by combination of a Brønsted acid and a Brønsted base forming the protic ionic liquid through proton transfer.[104,105] Although protic ionic liquids are overlooked as compared to conventional ionic liquid systems, they are relatively easy to prepare since they do not require multistep reactions. The preparation only requires proper mixing of the ingredients to complete the proton transfer reaction. Another important aspect of protic ionic liquids is the possibility to use very cheap and environmentally friendly ingredients such as natural carboxylic acids and amines. This allows facile and economical preparation of protic ionic liquids to be used for various applications. The only possible weak point of protic ionic liquids is the deprotonation to reform the neutral species which lowers the thermal stability. However, recent studies show that protic ionic liquids displaying high thermal stabilities can be prepared.[105] Due to their protic nature, these materials have found use in energy applications, especially in fuel cells as proton conducting materials.[106,107] Recent studies suggest that the cation and anion combination that forms the ionic liquid, either aprotic or protic, is very important for the environmental impact of the ionic liquid.[108,109] Therefore, careful selection of the composition of the ionic liquid and proper recycling is crucial concerns for the use of these types of solvents. For this reason, a new class of ionic liquids named deep eutectic solvents (DESs) emerged as alternatives. DESs are molecular

complexes formed between quaternary ammonium or phosphonium salts and hydrogen bond donor molecules generally chosen from cheap and safe components. The salt acts as the hydrogen bond acceptor to self-associate with the donor molecule to form the DES via hydrogen bonding. The hydrogen bonding formed between the halide anion and the hydrogen donor molecule causes charge delocalization to occur. This strong interaction is responsible for the decrease of the freezing point of the mixture relative to the melting points of the individual components used for the formation of the DES.

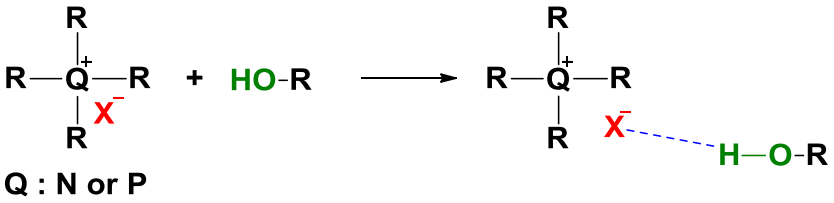

Figure 1.12. Simple illustration of the interaction between the hydrogen bond acceptor and donor moieties.

Deep eutectic solvents possess many common properties with the conventional ionic liquids. As compared to common solvents, DESs are nonvolatile, nonflammable and easy to scale up since no purification is required and synthesis is 100% atom economic making them attractive in large scale industrial applications.

Chapter 1

The very first major studies of ambient temperature salts were reported by Hurley and coworkers about eutectic mixtures of pyridinium halides with metal halides to be used for electrodeposition of metals.[110] These eutectic mixtures contain complex chloroaluminate anions like $AlCl_4^-$ and $Al_2Cl_7^-$ which are large and hence reducing the charge density. The delocalization of the charge decreases the interaction with the cation and eventually results in a lower freezing point. However, due to very sensitive nature of aluminium chloride towards water, these compounds found limited application. Later in 2001 and 2004, Abbott and coworkers showed that similar solvents can be produced with different metal halides like iron, zinc and tin. Since then there have been other reports related to DESs prepared with metal halides.[111-113] In 2002, the same group discovered that the trimethylethanolammonium chloride (choline chloride) urea mixtures form deep eutectic solvents and possess similar properties to ionic liquids.[114] Following this discovery, deep eutectic solvents formed between choline chloride and natural carboxylic acids are reported as versatile alternatives to ionic liquids.[115] Abbott and coworkers divided DESs into 4 different groups as type I, formed between quaternary ammonium and metal halides, type II, formed between quaternary ammonium and metal halide hydrates, type III, formed between quaternary ammonium and hydrogen bond donors and type IV, formed between metal halide and different hydrogen bond

donors such as alcohols and urea.[116] These DESs have been deeply investigated by different groups and proposed for many different applications where ionic liquids or conventional organic solvents are used. Among these applications, CO_2 capture,[117] metal oxide solubilization,[115] drug solubilization,[118] purification,[119] catalysis,[120] electrodeposition,[121] material preparation[122] and biopolymer processing[123] can be given as examples. The use of DES in polymer science is a relatively unexplored topic considering that the 1st article was published in 2011.[124] Morales and coworkers used deep eutectic systems for the frontal polymerization of acrylic monomers. DES was formed between choline chloride and acrylic acid (AA) or methacrylic acid (MAA) monomers. DES assisted frontal polymerization of the monomer was conducted by heating and choline chloride was recovered from the system upon the termination of the polymerization reaction allowing recycling of one component and reutilizing. The use of DES allowed the control of the convection of the heat along the reactor resulting in a better control over the reaction kinetics and the final properties of the polymer without the need to use a common organic solvent.[123,124] Another example to use of DES systems in polymer synthesis is the work of Serrano and coworkers for the synthesis of DES assisted polyesters. In this work, DESs were formed between

quaternary ammonium and phosphonium salts with octanediol. The reaction procedure is depicted below.

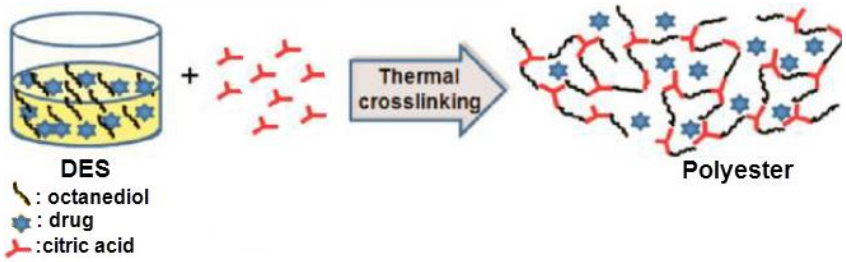

Figure 1.13. DES assisted polyester synthesis (126)

Upon the formation of the DES, citric acid was dissolved in the preformed mixture and the reaction was conducted at 80 ºC for 10 days until the completion of the reaction. The synthesis of these materials through the use of DES as a solvent in the system allowed the use of lower temperatures than conventional systems and also allowed the loading of the polymer with a local anesthetic to use the final material for drug delivery purposes without postsynthetic functionalization of the polymer.[126,127] DES assisted synthesis strategy was also used for the synthesis of crosslinked resorcinol-formaldehyde thermosets for carbonization. Similar to the synthetic procedure used for polyesters, the DESs were prepared with resorcinol and quaternary ammonium salts and the polycondensation reaction was allowed to take place upon the addition of the formaldehyde to the system. The resulting materials were

used to obtain monolithic carbons. One of the main advantages of using DES assisted synthesis of the precursor materials was to avoid the use of additives (e.g., block copolymers) which are difficult to wash out due to the impeded diffusion through small pores. The use of quaternary ammonium salts in the medium allows easy recovery and recycle of the salt. The compositional modifications allow the formation of hierarchical structures and easy manipulation. Moreover, the use of functional molecules in the DES formation allows the preparation of nitrogen or phosphorous doped carbon materials.[128,129] To sum up, the use of DESs in many different fields, especially in polymer science, is flourishing and still unexplored. Therefore, many new advances are to come in forthcoming years.

1.5. Objectives and outline of the thesis

As discussed in the previous parts, there has been a tremendous increase in the research dedicated to the development of polymeric materials composed of ionic building units. These materials find applications in many fields as some examples are given throughout the chapter. However, there is still a need to develop new materials that are safe to use in terms of environmental impact and also easier to manufacture avoiding complicated synthetic strategies to access analogous materials with similar properties considering that many PILs are composed of non-biodegradable and/or high toxicity fluorinated cations and anions.

The synthesis of innovative polyelectrolytes by using renewable sources to prepare state-of-the-art materials based on poly(ionic liquid)s, ion gels or deep eutectic solvents are the main dedication of this work. The scope of this thesis is the introduction of innovative ionic polymers that possess superior properties in terms of environmental impact by using low toxicity ingredients coming from renewable sources and/or easy-to-prepare to avoid multistep and complicated preparation techniques.

To accomplish the main goals various polymeric materials were synthesized. The materials were characterized in terms of chemical

structure, physical properties and possible applications in different fields proposed. As a summary:

In Chapter 1, a general introduction is given about the ionic liquids, polymerized ionic liquids and their applications in different fields.

In Chapter 2, synthesis and characterization of cholinium based poly(ionic liquid)s containing different anions based on natural carboxylic acids was investigated. These polymers were also compared with poly(ionic liquid)s that are carrying a different protic or aprotic cation. Polymer synthesis and properties of the synthesized polymers were reported. The polymers were synthesized by using free radical polymerization in water. It has been seen that the anion and cation combination greatly influences the final properties of the materials. Possible application of these ionic liquid monomers for cellulose coatings and biocompatible ion gels was investigated.

In Chapter 3, amphiphilic block copolymers carrying lactic acid moieties in each repeat unit were synthesized through RAFT polymerization. First, ring-opening polymerization of L-lactide was conducted to obtain well-defined macro-chain transfer agents which were then used to conduct the RAFT polymerization of the cholinium type methacrylic ionic liquid monomer to obtain the block copolymers.

The block copolymers were characterized and their self-assembly in water was investigated.

In Chapter 4, cholinium based ionic liquid monomer and ionic liquid bearing lactate as the anion were used to prepare ion gels through photopolymerization. The ion gels were characterized in terms of their viscoelastic properties, ionic conductivities and thermal properties. These ion gels were used as solid electrolytes in cutaneous electrodes to perform long-term electrocardiography measurements. It was shown that these ion gels were ideal candidates to be used for long-term cutaneous electrophysiology which is not accessible with current electrode systems.

In Chapter 5, deep eutectic monomers (DEM) were prepared by using different quaternary ammonium compounds and various hydrogen bond donors. The resulting DEMs were characterized. These monomers were used for the facile preparation of innovative poly(ionic liquid)s through photopolymerization or polycondensation. Selected sample was used as solid sorbent for carbon dioxide and initial results have shown that this approach can be an alternative to produce materials with environmentally friendly ingredients without complicated synthetic strategies.

In Chapter 6, various natural carboxylic acids were used to prepare deep eutectic monomers. 2-cholinium bromide methacrylate quaternary ammonium monomer was mixed with various carboxylic acids to obtain the desired monomers. Photopolymerization of these monomers yielded homogeneous polymeric materials. Chemical and thermal properties of these materials were investigated and their potential application in carbon dioxide capture was investigated.

In Chapter 7, a general conclusion was drawn including all the findings obtained in this PhD work.

1.6. References

1- Walden, P. Bull. Acad. Imper. Sci. (St. Petersburg) 1914, 1800.

2- A. Stark and K. R. Seddon, in Kirk-Othmer Encyclopedia of Chemical Technology, A. Seidel, John Wiley & Sons, Inc., Hoboken, New Jersey, USA, 5, 2007, **26**, 836-920.

3- M. Galinski, A. Lewandowski and I. Stepniak, Electrochimica Acta, 2006, **51**, 5567-5580.

4- S. Zhang, N. Sun, X. He, X. Lu, X. Zhang, J. Phys. Chem. Ref. Data, 2006, **35**, 1475.

5- J. G. Huddleston, A. E. Visser, W. M. Reichert, H. D. Villauer, G. A. Broker, R. D. Rogers, Green Chem., 2001, **3**, 156-164.

6- C. T. Wu, K. N. Marsh, A. V. Deev, J. A. Boxall, J. Chem. Eng. Data, 2003, **48**, 486.

7- U. Domanska, A. Marciniak, J. Chem. Eng. Data, 2003, **48,** 451.

8- L. A. Blanchard, J. F. Brennecke, Ind. Eng. Chem. Res., 2001, **40**, 287.

9- M. E. Zakrezewska, E. Bogel-Lugasik, R. Bogel-Lukasik, Energy fuels, 2010, **24**, 737-745.

10- H. Zhang, J. Wu, J. Zhang, J. He, Macromolecules, **38**, 8272-8277.

11- D. A. Fort, R. P. Swatloski, P. Moyna, R. D. Rogers, G. Moyna, Chem. Commun., 2006, 714-716.

12- J. A. Boon, J. A. Levisky, J. L. Pflug, J. S. Wilkes, J. Org. Chem., 1986, **51**, 480.

13- D. S. Kim, W. S. Ahn, Korean J. Chem. Eng. 2003, **20**, 39.

14- D. S. Newman, R. E. Winans, R. L. McBeth, J. Electrochem. Soc. 1984, **131**, 1079.

15- T. Fischer, A. Sethi, T. Welton, J. Woolf, Tetrahedron Lett. 1999, **40**, 793.

16- M. J. Earle, P. B. McCormac, K. R. Seddon, Green Chem. 1999, **1**, 517.

17- P. Ludley, N. Karodia, Tetrahedron Lett. 2001, **42**, 2011.

18- S. V. Dzyuba, R. A. Bartsch, Tetrahedron Lett. 2002, **43**, 4657.

19- J. F. Dubreuil, J. P. Bazureau, Tetrahedron Lett. 2000, **41**, 7351.

20- R. T. Dere, R. R. Pal, P. S. Patil, M. M. Salunkhe, Tetrahedron Lett. 2003, **44**, 5351.

21- W. A. Herrmann, V. P. W. Bohm, J. Organomet. Chem., 1999, **572**, 141.

22- V. P. W. Bohm, W. A. Herrmann, Chem. Eur. J., 2000, **6**, 1017.

23- V. R. Koch, C. Nanjundiah, G. B. Appetecchi, B. Scrosati, J. Electrochem. Soc., 1995, **142**, L116.

24- J. S. Wilkes, M. J. Zaworotko, Chem. Commun. 1992, 965.

25- R. T. Carlin, H. C. D. Long, J. Fuller, P. C. Trulove, J. Electrochem. Soc, 1994. **141**, L73

26- P. Bonhoˆte, A.-P. Dias, N. Papageorgiou, K. Kalyanasundaram, M. Gra¨tzel, Inorg. Chem., 1996, **35**, 1168

27- N. Papageorgiou et al., J. Electrochem. Soc., 1996, **143**, 3099

28- M. J. A. Shiddiky and A. A. J. Torriero, Biosens. Bioelectron., 2011,

26, 1775–1787.

29- D. L. Compton and J. A. Laszlo, J. Electroanal. Chem., 2003, **553**, 187–190.

30- S. F. Wang, T. Chen, Z. L. Zhang, X. C. Shen, Z. X. Lu, D. W. Pang and K. Y. Wong, Langmuir, 2005, **21**, 9260–9266.

31- S. F. Wang, T. Chen, Z. L. Zhang, D. W. Pang and K. Y. Wong, Electrochem. Commun., 2007, **9**, 1709–1714.

32- S. Wang, Z. Guo and H. Zhang, Bioelectrochemistry, 2011, **82**, 55–62.

33- M. Ramdin, T.W. de Loos, and T. J.H. Vlugt, Ind. Eng. Chem. Res. 2012, **51**, 8149–8177.

34- M.M. Wan, H.Y.Zhu, Y.Y.Li, J. Ma, S. Liu and J.H.Zhu, ACS Appl. Mater. Interfaces, 2014, **6**, 12947–12955.

35- X. Zhang, X. Zhang, H. Dong,Z. Zhao, S. Zhang and Y. Huang, Energy Environ. Sci., 2012, **5**, 6668–6681.

36- C. Wang, X. Luo, X. Zhu, G. Cui, D. Jiang, D. Deng, H. Li and S. Dai, RSC Adv., 2013, **3**, 15518–15527.

37- J.F.Brennecke and B.E. Gurkan, J. Phys. Chem. Lett., 2010, **1**, 3459–3464.

38- E.D. Bates, R.D. Mayton, I. Ntai and J.R. Davis, J. Am. Chem. Soc., 2002,**124**, 926–927.

39- J.E. Bara, D.E. Camper, D.L. Gin and R.D. Noble, Acc. Chem. Res., 2010, **43**, 152–159.

40- H. Nakamoto, A. Noda, K. Hayamizu, S. Hayashi, H.Hamaguchi, M. Watanabe,J.Phys.Chem.B, 2007, **111**, 1541.

41- A. Noda, M. A. B. Hasan Susan, K. Kudo, S. Mitsushima, K. Hayamizu, M. Watanabe,J.Phys.Chem.B, 2003, **107**, 4024.

42- M. Yoshizawa-Fujita, N. Byrne, M. Forsyth, D. R. MacFarlane, H. Ohno, J.Phys.Chem. B, 2010, **114**, 16373.

43- F. S. Teixeria, N. S. M. Vieira, O. A. Cortes, J. M. M. Araujo, I. M. Marrucho, L. P. N. Rebelo, A. B. Pereiro, J. Chem. Thermodynamics, 2015, **82**, 99-107.

44- P. D. A. Bastos, F. S. Oliveira, L. P. N. Rebelo, A. B. Pereiro, I. M. Marrucho, Fluid Phase Equilibria, 2015, **389**, 48-54.

45- T. Mourao, L. C. Tome, C. Florindo, L. P. N. Rebelo, I. M. Marrucho, ACS Sustainable Chem. Eng., 2014, **2**, 2426-2434.

46- D. Mecerreyes, Prog Polym Sci, 2011, **36**, 1629-48.

47- J. Lu, F. Yan, J. Texter, Prog Polym Sci., 2009, **34**, 431-48.

48- O. Green, S. Grubjesic, S. Lee, M. A. Firestone, Polym Rev., 2009,49,339-60. 49- M. D. Green, T. E. Long, Polym Rev., 2009, **49**, 291-314.

50- J. Yuan, M. Antonietti, Polymer, 2011, **52**, 1469-82.

51- K. Ito, N. Nishina, H. Ohno, Electrochim Acta, 2000, **45**, 1295–8.

52- R. Marcilla, J. A. Blazquez, J. Rodriguez, J. A. Pomposo, D. Mecerreyes, J Polym Sci Part A Polym Chem., 2004, **42**, 208–12.

53- M. Hirao, K. Ito, H. Ohno, Electrochim Acta, 2000, **45**, 1291–4.

54- H. Ohno, K. Ito, Chem Lett., 1998, **6**, 751–2.

55- J. E. Bara, S. Lessmann, C. J. Gabriel, E. S. Hatakeyama, R. D. Noble, D. L. Gin, Ind Eng Chem Res., 2007, **46**, 5397–404.

56- P. Cardiano, P. G. Mineo, F. Neri, S. Lo Schiavo, P. A. Piraino, J Mater Chem., 2008, **18**, 1253–60.

57- S. Ding, H. Tang, M. Radosz, Y. Shen, J Polym Sci Part A Polym Chem., 2004, **42**, 5794–801.

58- B. Yu, F. Zhou, H. Hu, C. Wang, W. Liu, Electrochim Acta, 2007, **53**, 487–94.

59- D. Batra, D. N. T. Hay, M. A. Firestone, Chem. Mater., 2007, **19**, 4423–31.

60- B. P. Mudraboyina, M. M. Obadia, I. Abdelhedi-Miladi, I. Allaoua, E. Drockenmuller, European Polym. J., 2015, **62**, 331-337.

61- H. Tang, J. Tang, S. Ding, M. Radosz, Y. Shen, J Polym Sci Part A Polym Chem., 2005, **43**, 1432-43.

62- K. Tauer, N. Weber, J. Texter, Chem Commun., 2009, **40**, 6065–7.

63- C. M. Stancik, A. R. Lavoie, P. A. Achurra, R. M. Waymouth, A. P. Gast, Langmuir, 2004, **20**, 8975-87.

64- D. Cordella, A. Kermogoret, A. Debuigne, R. Riva, I. German, M. Isik, C. Jerome, D. Mecerreyes, D. Taton, C. Detrembleur, ACS Macro Lett., 2014, **3**, 1276-1280.

65- S. Bellayer, J. Gilman, N. Eidelman, S. Bourbigot, X. Flambard, D. Fox, H. De Long, P. Trulove, Adv Funct Mater., 2005, **15**, 910-6.

66- R. Marcilla, M. Curri, P. Cozzoli, M. Martínez, I. Loinaz, H. Grande, J. Pomposo, D. Mecerreyes, Small, 2006, **2**, 507-12.

67- T. Fukushima, A. Kosaka, Y. Ishimura, T. Yamamoto, T. Takigawa, N. Ishii, T. Aida, Science, 2003, **300**, 2072-4.

68- K. Grygiel, B. Wicklein, Q. Zhao, M. Eder, T. Pettersson, L. Bergstrom, M. Antonietti, J. Yuan, Chem. Commun., 2014, **50**, 12486.

69- R. Marcilla, E. Ochoteco, C. Pozo-Gonzalo, H. Grande, J. A. Pomposo, D. Mecerreyes, Macromol Rapid Commun., 2005, **26**,1122–6.

70- A. Pinkert, K. N. Marsh, S. Pang, M. P. Staiger, Chem Rev., 2009, **109**, 6712–28.

71- J. E. Bara, E. S. Hatakeyama, D. L. Gin, R. D. Noble, Polym Adv Technol., 2008,**19**, 1415-20.

72- J. Tang, W. Sun, H. Tang, M. Radosz and Y. Shen, Macromolecules, 2005, **38**, 2037–2039.

73- J. Tang, H. Tang, W. Sun, M. Radosz and Y. Shen, J. Polym. Sci. Part A: Polym. Chem., 2005, **43**, 5477–5489.

74- J. Tang, H. Tang, W. Sun, M. Radosz and Y. Shen, Polymer, 2005, **46**, 12460–12467.

75- J. Tang, Y. Shen, M. Radosz and W. Sun, Ind. Eng. Chem. Res., 2009, **48**, 9113–9118.

76- P.G. Mineo, L. Livoti, M. Giannetto, A. Gulino, S.L. Schiavo and P. Cardiano, J. Mater. Chem., 2009, **19**, 8861–8870.

77- R.S. Bhavsar, S.C. Kumbharkar and U.K. Kharul, J. Membr. Sci., 2012, **389**, 305–315.

78- S. Zulfiqar, M. I. Sarwar and D. Mecerreyes, Polym. Chem., 2015, **6**, 6435.

79- R. Marcilla, F. Alcaide, H. Sardon, J. A. Pomposo, C. Pozo-Gonzalo, D. Mecerreyes, Electrochem. Commun., 2006, **8**, 482–8.

80- T. Ueki and M. Watanabe, Macromolecules, 2008, 41, 3739.

81- A. Vioux, L. Viau, S. Volland and J. Le Bideau, C. R. Chim., 2010, **13**, 242.

82- F. Gayet, L. Viau, F. Leroux, F. Mabille, S. Monge, J.-J. Robin and A. Vioux, Chem. Mater., 2009, **21**, 5575.

83- M. Armand, F. Endres, D. R. MacFarlane, H. Ohno and B. Scrosati, Nat. Mater., 2009, **8**, 621.

84- A. Guerfi, M. Dontigny, Y. Kobayashi, A. Vijh and K. Zaghib, J. Solid State Electrochem., 2009, **13**, 1003.

85- S. Imaizumi, H. Kokubo, M. Watanabe, Macromolecules, 2012, **45**, 401-409.

86- J. Yoon, D. ki Kang, J. Won, J-Y. Park, Y. S. Kang, J Power Sources, 2012, **201**, 395-401.

87- P. Leleux, C. Johnson, X. Strakosas, J. Rivnay, T. Herve, R. M. Owens, G. G. Malliaras, Adv. Healthcare Mater., 2014, **3**, 1377-1380.

88- T. P. Lodge, Science, 2008, **321**, 50.

89- K. H. Lee, M. S. Kang, S. Zhang, Y. Gu, T. P. Lodge, C. D. Frisbie, Adv. Mater., 2012, **24**, 4457-4462.

90- J. Lee, M. J. Panzer, Y. He, T. P. Lodge, C. D. Frisbie, J. Am. Chem. Soc., 2007, **129**, 432-4533.

91- Y. Gu, E. L. Cussler, T. P. Lodge, J. Membrane Sci., 2012, **423**, 20-26.

92- J-I., Kadokawa, M-A. Murakami, Y. Kaneko, Carbohydrate Res., 2008, **343**, 769-772.

93- A. Takada, J-I. Kadokawa, Biomolecules, 2015, **5**, 244.

94- S. Yanagida, M. Watanabe, H. Matsui, K. Okada, H. Usui, T. Ezure, N. Tanabe, Fujikura Technical Review, 2005, 59-65.

95- R. Kawano, T. Katakabe, H. Shimosawa, Md. K. Nazeeruddin, M. Gratzel, H. Matsui, T. Kitamura, N. Tanabe, M. Watanabe, Phys Chem Chem Phys., 2010, **12**, 1916–21.

96- B. Yu, F. Zho, C. Wang, W. Liu, Eur Polym J., 2007, **43**, 2699.

97- M. Wang, Y. Lin, X. Zhou, X. Xiao, L. Yang, S. Feng, X. Li, Mat. Chem. Phys., 2008, **107**, 61–6.

98- G. Wang, L. Wang, S. Zhuo, S. Fang, Y. Lin, Chem Commun., 2011, **47**, 2700–2.

99- A. L. Pont, R. Marcilla, I. De Meatza, H. Grande, D. Mecerreyes, J Power Sources, 2009, **188**, 558–63.

100- G. B. Appetecchi, G. T. Kim, M. Montanina, M. Carewska, R. Marcilla, D.Mecerreyes, I. De Meatza, J Power Sources, 2010, **195**, 3668–75.

101- S. Jeremias, M. Kunze, S, Passerini, M. Schonhoff, J. Phys. Chem. B., 2013, **117**, 10596-10602.

102- A. S. Shaplov, R. Marcilla, D. Mecerreyes, Electrochimica Acta, 2015, **175**, 18-34.

103- M. Salsamendi, L. Rubatat, D. Mecerreyes, page 283 in Electrochemistry in Ionic Liquids volume 1: Fundamentals, Springer, Switzerland, 2015.

104- T. L. Greaves, C. J. Drummond, Chem. Rev., 2008, **108**, 206-237.

105- T. L. Greaves, C. J. Drummond, Chem. Rev., 2015, **115**, 11379-11448.

106- U. A. Rana, M. Forsyth, D. R. MacFarlane, J. M. Pringle, Electrochimica Acta, 2012, **84**, 213-222.

107- M. Diaz, A. Ortiz, M. Isik, D. Mecerreyes, I. Ortiz, Int. J. Hyd. Energ., 2015, **40**, 11294-11302.

108- S. Stolte, M. Matzke, J. Arning, A. Boschen, W-R. Pitner, U. Wels-Biermann, B. Jastorff, J. Ranke, Green Chem., 2007, **9**, 1170-1179.

109- S. Stolte, J. Arning, U. Bottin-Weber, M. Matzke, F. Stock, K. Thiele, M. Uerdingen, U. Welz-Biermann, B. Jastorff, J. Ranke, Green Chem., 2006, **8**, 621-629.

110- F. H. Hurley, T. P. Wier, J. Electrochem. Soc., 1951, **98**, 203.

111- A. P. Abbott, G. Capper, D. L. Davies, H. L. Munro, R. K. Rasheed, V. Tambyrajah, Chem. Commun., 2001, 2010-2011.

112- A. P. Abbott, G. Capper, D. L. Davies, R. Rasheed, Inorg. Chem., 2004, **43**, 3447-3452.

113- M. S. Sitze, E. R. Schreiter, E. V. Patterson, R. G. Freeman, Inorg. Chem., 2001, **40**, 2298-2304.

114- A. P. Abbott, G. Capper, D. L. Davies, R. K. Rasheed, V. Tambyrajah, Chem. Commun., 2003, 70-71.

115- A. P. Abbott, D. Boothby, G. Capper, D. L. Davies, R. K. Rasheed, J. Am. Chem. Soc., 2004, **126**, 9142-9147.

116- A. P. Abbott, J. C. Barron, K. S. Ryder, D. Wilson, Chem. Eur. J., 2007, **13**, 6495-6501.

117- L. L. Sze, S. Pandey, S. Ravula, S. Pandey, H. Zhao, G. A. Baker, S. N. Baker, ACS Sustainable Chem. Eng., 2014, **2**, 2117-2123.

118- P. M. Pawar, K. J. Jarag and G. S. Shankarling, Green Chem.,

2011, **13**, 2130–2134.

119- A. P. Abbott, P. M. Cullis, M. J. Gibson, R. C. Harris, E. Raven, Green Chem., 2007, **9**, 868-872.

120- S. B. Phadtare and G. S. Shankarling, Green Chem., 2010, **12**, 458–462.

121- E. Gomez, P. Cojocaru, L. Magagnin and E. Valles, J. Electroanalytical Chem., 2011, **658**, 18–24.

122- E. R. Cooper, C. D. Andrews, P. S. Wheatley, P. B. Webb, P. Wormald and R. E. Morris, Nature, 2004, **430**, 1012–1016.

123- M. Francisco, A. van den Bruinhorst, M. C. Kroon, Green Chem., 2012, **14,** 2153.

124- J. D. Mota-Morales, M. C. Gutierrez, I. C. Sanchez, G. Luna-Barcenas, F. del Monte, Chem. Commun., 2011, **47**, 5328-5330.

125- J. D. Mota-Morales, M. C. Gutierrez, M. L. Ferrer, I. C. Sanchez, E. A. Elizalde-Pena, J. A. Pojman, F. del Monte, G. Luna-Barcenas, J. Polym. Sci. Part A: Polym. Chem., 2013, **51**, 1767-1773.

126- S. Garcia-Arguellas, M. C. Serrano, M. C. Gutierrez, M. L. Ferrer, L. Yuste, F. Rojo, F. del Monte, Langmuir, 2013, **29**, 9525-9534.

127- M. C. Serrano, M. C. Gutierrez, R. Jimenez, M. L. Ferrer, F. del Monte, Chem. Commun., 2012, **48**, 579-581.

128- J. Patino, M. C. Gutierrez, D. Carriazo, C. O. Ania, J. L. G. Fierro, M. L. Ferrer, F. del Monte, J. Mater. Chem. A., 2014, **2**, 8719.

129- M. C. Gutierrez, D. Carriazo, C. O. Ania, J. B. Parra, M. L. Ferrer, F. del Monte, Energy Environ. Sci., 2011, **4**, 3535.

2 Cholinium Based Poly(ionic liquid)s

Contents

2.1. Introduction……..50
2.2. Experimental……53
2.3. Results and Discussion……59
2.4. Conclusions……..…81
2.5. References……..……82

Chapter 2

2.1. Introduction

Although ionic liquids are initially defined as green solvents, one of the most actual concerns is their toxicology and safety in terms of environmental impact. Many studies in literature to examine the toxicity, biocompatibility or biodegradability of different ionic liquids combining various cations and anions revealed that some cations and anions display toxicity and some other combinations are considered safer compared to their toxic analogs. Therefore, the choice of the cation and anion combination becomes crucial for the design of new poly(ionic liquid)s.[1-7] In addition, poly(ionic liquid)s are finding applications in many new areas each day, hence there is always a continual need for new cation and anion combinations to be able to access new properties.

Although a large number of ionic liquids have been synthesized to date, most of them were based on halogenated anions such as bis (trifluoromethane sulfonimide) (NTf_2), tetrafluoroborate (BF_4) and hexafluorophosphate (PF_6) or various derivatives of these anions. Due to their low negative charge density, they display low melting point when combined with cations to form the ionic liquid.[8] However, they are highly toxic hence their applications are limited.[3,5] An alternative method to develop safer ILs is to combine components having well-defined toxicological and biodegradation properties. A simple approach can be

the use of carefully selected naturally-derived components which carry lower toxicity and display enhanced bio-degradability.[3,9]

Cholinium, trimethylethanolammonium, is a quaternary ammonium cation which supports several biological functions. In fact, cholinium salicylate was found approximately 55 years ago[10] and choline chloride has been used since 2001 to prepare low melting point deep eutectic solvents due to its low toxicity, biocompatibility, biodegradability and large scale availability.[11] More recently, Ohno and coworkers synthesized cholinium based room temperature ionic liquids, choline cation combined with natural carboxylates through anion exchange reactions. Due to their low toxicity and biodegradability these types of ionic liquids are named as bioionic liquids.[12]

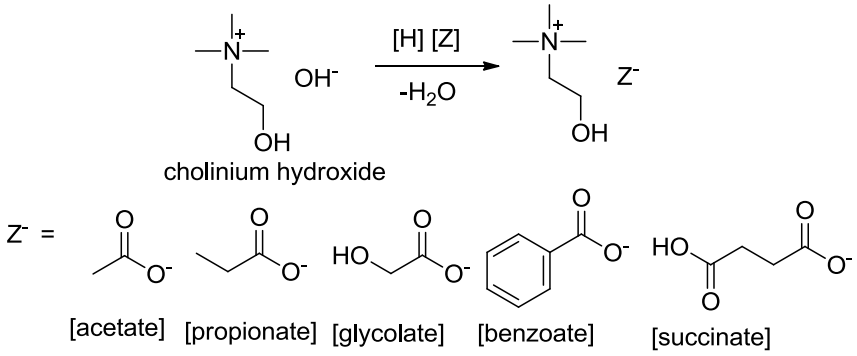

Figure 2.1. Preparation of cholinium ionic liquids with some carboxylate anions (12)

Various properties of these ionic liquids have been studied and reported since the initial report. Petkovic and coworkers studied the toxicity of cholinium ionic liquids containing natural carboxylates. They have found out that the fungi can actively grow in media containing cholinium ionic liquids, hence benign cholinium cation allowed the synthesis of biocompatible ionic liquids.[13]

Owing to its benign character, cholinium ionic liquids have been used for many different applications. Among these applications, aqueous biphasic extraction,[14] dissolution of biomass such as selective dissolution of lignin by using cholinium amino acid ionic liquids,[15] carbon dioxide separation membranes,[16] bioactive polysaccharide film preparation[17] can be given as some example to the applications of cholinium based ionic liquids.

For that purpose, a series of eight different ionic liquid monomers including cholinium ionic liquid monomers were prepared and polymerized by using free radical polymerization. The polymers were characterized and compared in terms of the effect of the cation and the anion. A preliminary study was conducted to use the cholinium ionic liquid monomer for cellulose coatings and biocompatible ion gels through photopolymerization.

Chapter 2

2.2. Experimental

2.2.1. Materials

2-dimethylaminoethylmethacrylate (98%), 2-trimethylammonium-ethyl chloride methacrylate solution (Aldrich 80 wt% in H_2O) were used as received and utilized as starting materials for the synthesis of ionic liquid monomers. 2-bromoethanol (95%, Aldrich), silver lactate (97%, Aldrich), silver acetate (99%, Aldrich), lactic acid (Aldrich 85 wt% in H_2O), acetic acid (99.5%, Fluka), 2,2′-Azobis(2-methylpropionamidine) dihydrochloride (AIBA, 97%, Aldrich), 2,2′-Azobis(2-methylpropionitrile) (AIBN, 98%, Aldrich), trimethylethanol ammonium hydroxide (cholinium hydroxide) (Aldrich 45 wt% in methanol), ethylene glycol dimethacrylate (98%, Aldrich), 2,2-Dimethoxy-2-phenyl-acetophenone (photoinitiator, 99%, Aldrich), ethyl acetate (Aldrich) and cellulose fiber (medium, Aldrich) were used as received without further purification. All the chemicals were high purity.

2.2.2. Monomer synthesis

Ionic liquid monomers were synthesized by using the commercially available 2-dimethylaminoethylmethacrylate as the precursor molecule. To synthesize the cholinium based monomer 2-bromoethanol was used

for the quaternization of the starting monomer. In a typical reaction, 15 grams (95.41 mmol) of 2-dimethylaminoethylmethacrylate was charged into a round-bottom-flask. 14.310 grams (114.51 mmol) of 2-bromoethanol was introduced over the monomer dropwise for the reaction to take place. The stoichiometry of the reaction was adjusted to have the 2-bromoethanol in excess to have a full quaternization of the monomer. The reaction was conducted under continuous stirring at room temperature for 24 hours. As the reaction proceeded, the medium became more viscous and eventually the crude product solidified in the flask. The solid was then dissolved in the minimum amount of methanol and precipitated into excess ethylacetate to get rid of any unreacted starting material. The final 2-cholinium bromide methacrylate powder was filtered and washed again with ethylacetate for further cleaning. The clean product was transferred into vial and dried under vacuum at room temperature and kept in the fridge until use. The yield of the reaction was calculated as 87% at the end. Cholinium based ionic liquid monomers bearing acetate and lactate anions were synthesized by using the previously synthesized 2-cholinium bromide methacrylate ionic liquid monomer through anion exchange reactions by using silver lactate or silver acetate. In a typical reaction, 2-cholinium bromide methacrylate was weighed into a round-bottom-flask. The monomer was dissolved in methanol/water mixture to have a 10% solid concentration. To this

solution, silver lactate or silver acetate dispersed in methanol/water mixture was added dropwise under agitation. The reaction was conducted at room temperature for 24 hours. The crude product was filtered in order to separate the silver bromide from the solution. Then the solution was centrifuged to remove the remaining silver bromide from the system. The final clean solution was dried under pressurized air to remove water and methanol from the system. The corresponding 2-cholinium lactate methacrylate and 2-cholinium acetate methacrylate monomers were obtained with 81% and 78% yields, respectively.

Synthesis of non-cholinium type monomers were conducted through similar anion exchange reaction by using 2-trimethylammoniumethyl chloride methacrylate monomer. The monomer was dissolved in water/methanol mixture to have 10% solid concentration at the end. Then the silver acetate or silver lactate dispersed in the solvent mixture was added dropwise. The reaction was conducted for 24 hours and the monomer was cleaned through filtration and centrifugation. The monomers 2-trimethylammonium ethyl lactate or 2-trimethylammonium ethyl acetate were obtained as viscous liquids. The synthesis of protic non-cholinium type monomers were conducted through the neutralization of the 5 grams (31.8 mmol) of 2-dimethylaminoethyl methacrylate tertiary amine monomer with 2.864 grams (31.8 mmol) of lactic acid or 1.909 grams (31.8 mmol) of acetic acid. The monomer was

weighed into a flask and the corresponding acid was added dropwise on the monomer solution in methanol at room temperature. The solution was dried under vacuum and the 2-dimethyl ammoniumethyl lactate methacrylate and 2-dimethylammoniumethyl acetate methacrylate were obtained as viscous liquid at room temperature.

2.2.3. Synthesis of poly(ionic liquid)s

All the ionic liquid monomers were polymerized through conventional free radical polymerization. In a typical reaction, 2.0 grams of the monomer was weighed into a round-bottom-flask equipped with a magnetic stirrer. The monomer was dissolved in 18 grams of deionized water to have a 10% solid concentration. The solution was bubbled with nitrogen for 20 minutes prior to putting into oil bath. After that the flask was placed into oil bath at 70 °C. The AIBA initiator (1% by weight with respect to the monomer) was dissolved in deionized water, bubbled with nitrogen and added over the monomer solution at 70 °C. The reaction was conducted at this temperature for 24 hours. The polymer was dried under vacuum to remove the water and obtained as a solid product at the end. All the ionic liquid monomers were polymerized by using the same polymerization procedure.

2.2.4. Cholinium lactate ionic liquid preparation

The synthesis of the ionic liquid was conducted by the neutralization of the cholinium hydroxide with lactic acid. To a solution of cholinium hydroxide in methanol, an equivalent of the lactic acid solution was added dropwise. The solution was mixed for 2 hours and the solvent was removed under vacuum at 45 °C. The resulting ionic liquid was slightly yellowish and viscous.

2.2.5. Photopolymerization

A UV chamber (model BS 03, Dr. Gröbel UV-Elektronik GmbH) equipped with 20 UV lamps (wavelength range from 315 to 400 nm with a maximum intensity at 368 nm) was used. The incident light irradiance (ILI) was measured using a radiometer UV sensor (which is part of the chamber) and it was varied in the range of 2.5–7 mW/cm^2. The photopolymerization of ion gel samples was conducted as follows: To the 0.5 g mixture of cholinium lactate ionic liquid (60% by weight) and 2-cholinium lactate methacrylate monomer (40% by weight) either with or without ethylene glycol dimethacrylate, photoinitiator (1% by weight of the monomer) was introduced and stirred prior to photopolymerization. The resulting mixture was casted into Teflon mold having 1x1 cm dimensions. The mold was then placed into UV chamber and kept for 30

minutes. Then the samples were taken out of the mold. A similar procedure was applied for the cellulose coatings. The cellulose-2-cholinium lactate methacrylate solution was mixed with the photoinitiator prior to coating application. The solution was then coated onto a glass substrate and put into UV chamber for 30 minutes.

2.2.6. Characterization

The ^{1}H NMR measurements were carried out on a Bruker AC-500 instrument. The samples were dissolved in deuterium oxide, and the solutions were analyzed. Gel permeation chromatography-size exclusion chromatography (GPC-SEC) with light scattering detection was used to determine the molecular weight of the polymers using a water/acetonitrile (80:20, w/w) eluent with 0.1 M NaCl, 0.03 M NaH_2PO_4 and 0.03 w% NaN_3 at 25 °C at a rate of 1 mL/min by using three columns (Ultrahydrogel 2000, 250, and 150). Thermogravimetric analysis (TGA) was performed by using a TA instruments Q500 device. The samples were heated from room temperature to 600 °C with a heating rate of 10 °C/min under N_2 atmosphere. Differential scanning calorimetry (DSC) experiments were performed on a TA Instruments Q2000. The sample materials were enclosed in non-recyclable aluminum hermetic pans, the sample masses being in the range of 5-10 mg. The samples were first heated to 150 °C with a heating rate of

10 °C/min and kept isothermal for 5 minutes. The samples were then cooled down to -70 °C with a cooling rate of 10 °C/min and kept isothermal for 5 minutes. Second run heating cycles were taken and analyzed for the detection of the glass transition temperature of the polymers. Modulated DSC measurement was applied for 1 sample (poly(2-trimethyl-ammoniumethyl acetate methacrylate) since the glass transition could not be obtained clearly from the normal scan. The measurement was performed with period p=80 s, temperature amplitude A_T= 0.5 °C and an average heating rate of 2 °C/min. Reversing heat flow signal was used for the detection of the glass transition temperature. Rheology measurements on the prepared ion gels were conducted on a Thermo-Haake Rheostress I viscoelastometer using oscillatory tests. Angular frequency sweeps from 0.1 to 10 rad/s at constant strain amplitude (γ = 0.005) were applied at 25 °C. G' and G'' values were plotted versus frequency.

2.3. Results and Discussion

2.3.1. Synthesis and characterization of monomers

All the monomers were synthesized by using commercially available starting materials. The cholinium based monomers were synthesized through the quaternization of tertiary amine containing methacrylic

monomer with 2-bromoethanol. The product, 2-cholinium bromide methacrylate, was obtained in high yields. The reaction schemes to obtain the cholinium monomers are shown below.

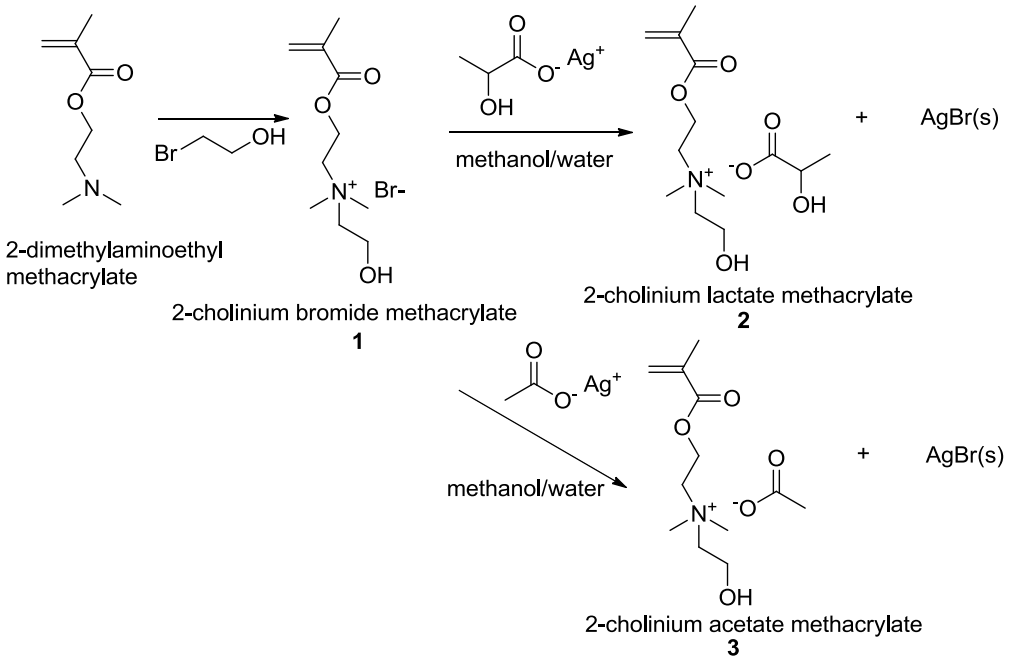

Figure 2.2. Synthesis of cholinium based monomers

The use silver salt for the anion exchange reaction allows easy removal of the silver bromide formed as a byproduct since silver halide has negligible solubility in the reaction medium. The removal silver halide yields the clean monomer solution. Similarly, the protic and aprotic analogs were synthesized through neutralization and anion exchange reactions, respectively. To synthesize protic monomers lactic acid and acetic acid were used for the neutralization of the tertiary

amine monomer. The aprotic monomer synthesis was done by using the same silver chemistry to obtain the monomers with the desired counter anions. The reaction schemes for the synthesis of protic and aprotic monomers are given below.

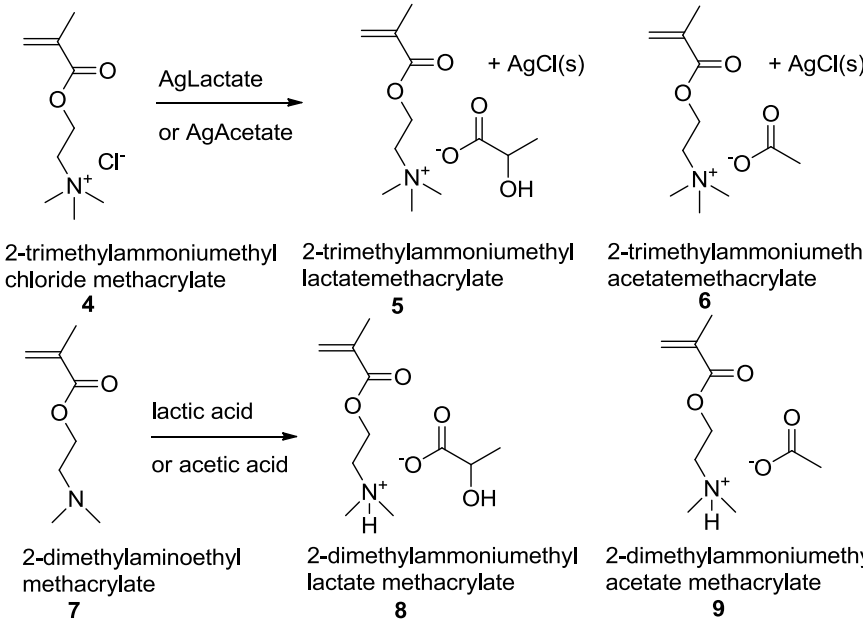

Figure 2.3. Synthesis of protic and aprotic ionic liquid monomers with acetate and lactate anions

All the monomers were obtained as liquids at room temperature. The monomers were characterized by ^{1}H NMR spectroscopy to confirm the structure of the ionic liquid monomers. The spectra are given below.

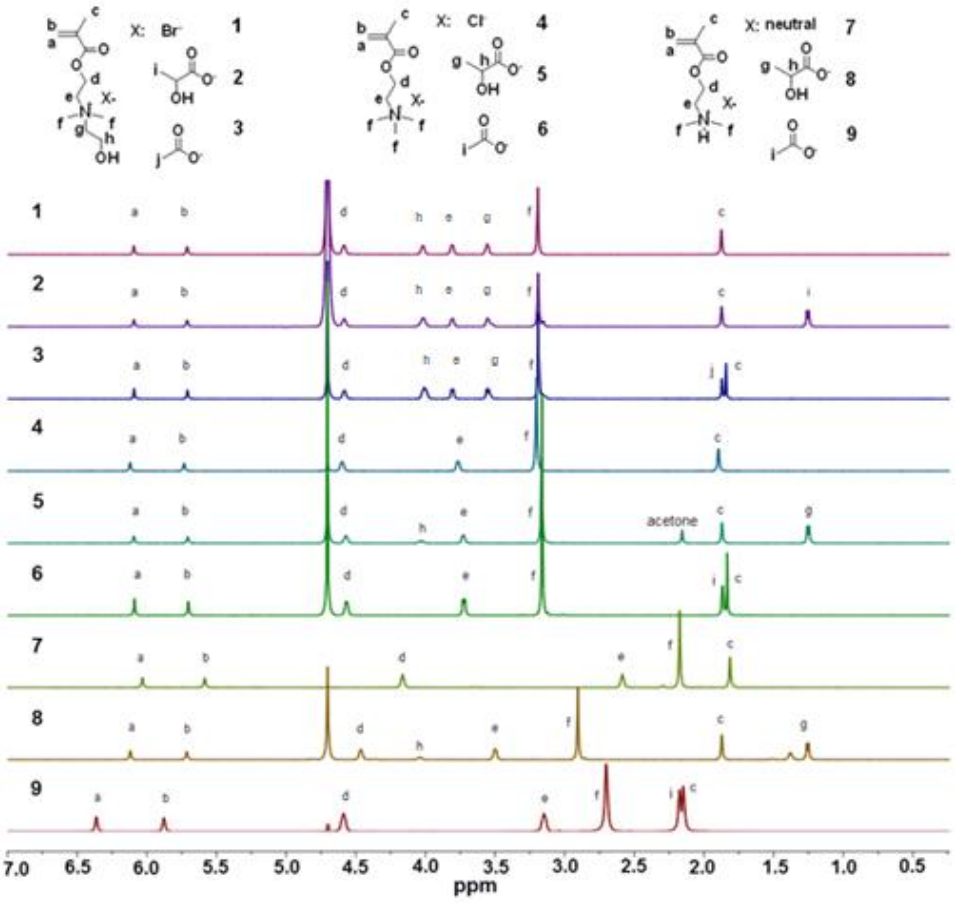

Figure 2.4. ^{1}H NMR spectra of ionic liquid monomers (D_2O)

Structural characterization of the ionic liquid monomers confirmed the formation of the monomers. With the quaternization of the starting monomer (7) with 2-bromoethanol, new peaks were observed between 3.5-4.0 ppm arising from the ethanol attached as a result of the quaternization reaction. The anion exchange reactions resulted in the

signals associated with the protons on the anions as can be seen from the spectra of ionic liquid monomers. In all the cases the monomers were obtained with high purity without any contamination of the starting materials.

2.3.2. Synthesis and characterization of poly(ionic liquid)s

Polymerizations of the ionic liquid monomers were conducted through conventional free radical polymerization by using water as the solvent and 2,2`-azobis(2-methylpropionamidine) dihydrochloride (AIBA) as the thermal initiator. All the polymerizations were conducted for 24 hours and full conversion of the monomer was obtained at the end of the reactions. All the polymerization reactions provided sufficient molecular weight to perform the characterization of the polymers. The polymers were 1st analyzed by ^{1}H NMR to confirm the formation of the poly(ionic liquid)s. The chemical structures of the polymers synthesized are provided in figure 2.5.

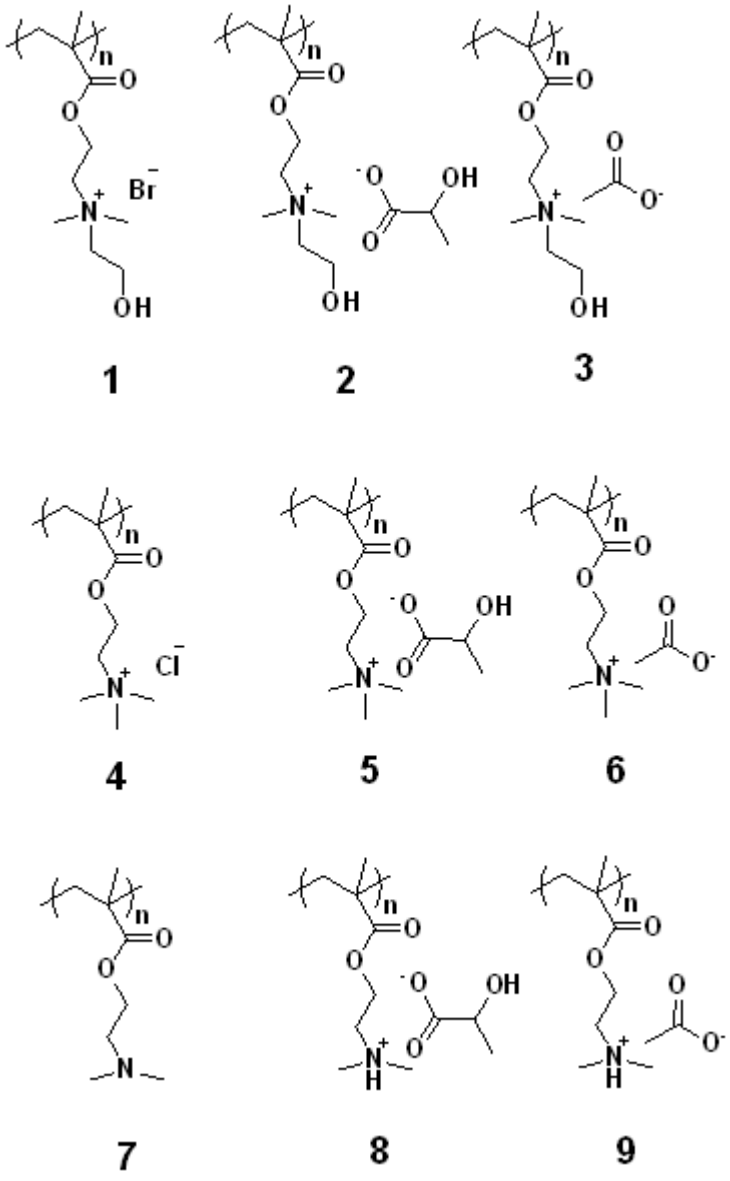

Figure 2.5. Chemical structures of the poly(ionic liquid)s synthesized

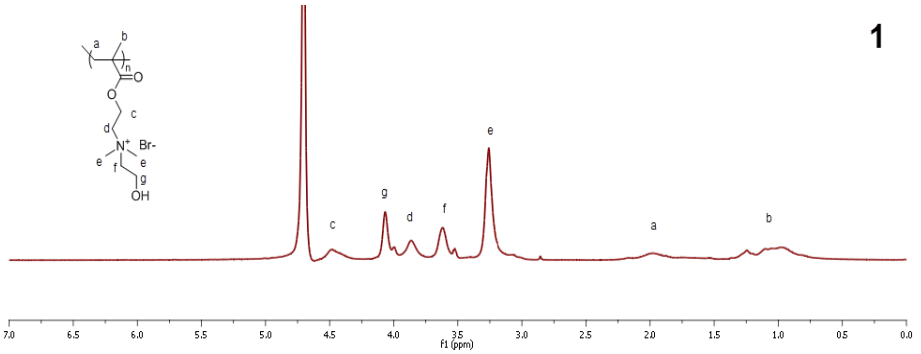
1
a
b
n
O
O
c
d
N+
Br-
e
f
e
g
OH
c
g
d
f
e
a
b
7.0
6.5
6.0
5.5
5.0
4.5
4.0
3.5
3.0
2.5
2.0
1.5
1.0
0.5
0.0
f1 (ppm)

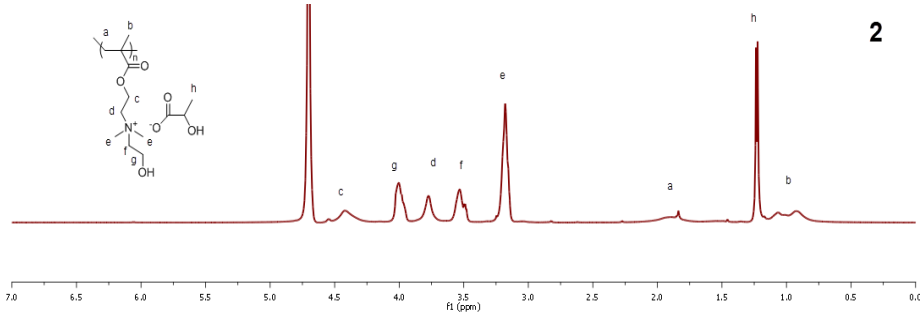
2
a
b
n
O
O
c
d
N+
O
h
O
OH
e
f
e
g
OH
h
e
g
d
f
c
a
b
7.0
6.5
6.0
5.5
5.0
4.5
4.0
3.5
3.0
2.5
2.0
1.5
1.0
0.5
f1 (ppm)

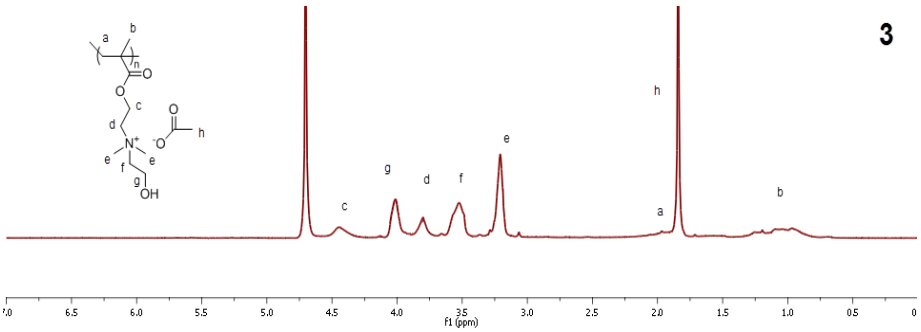
3
a
b
n
O
O
c
d
N+
O
h
e
f
e
g
OH
h
e
g
d
f
c
a
b
6.5
6.0
5.5
5.0
4.5
4.0
3.5
3.0
2.5
2.0
1.5
1.0
0.5
f1 (ppm)

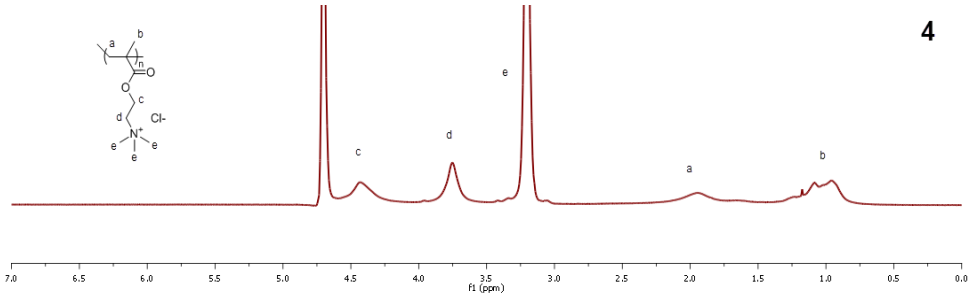
4
a
b
c
d
e
Cl-
c
d
e
a
b
7.0
6.5
6.0
5.5
5.0
4.5
4.0
3.5
3.0
2.5
2.0
1.5
1.0
0.5
0.0
f1 (ppm)

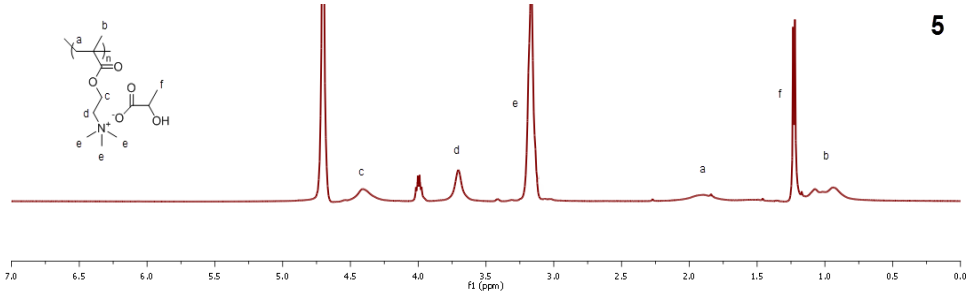
5
a
b
c
d
e
f
OH
c
d
e
f
a
b
7.0
6.5
6.0
5.5
5.0
4.5
4.0
3.5
3.0
2.5
2.0
1.5
1.0
0.5
0.0
f1 (ppm)

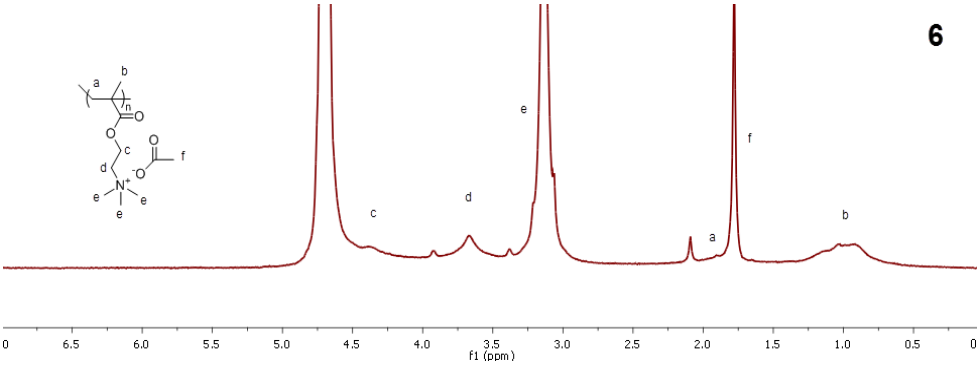
6
a
b
c
d
e
f
c
d
e
f
a
b
0
6.5
6.0
5.5
5.0
4.5
4.0
3.5
3.0
2.5
2.0
1.5
1.0
0.5
0
f1 (ppm)

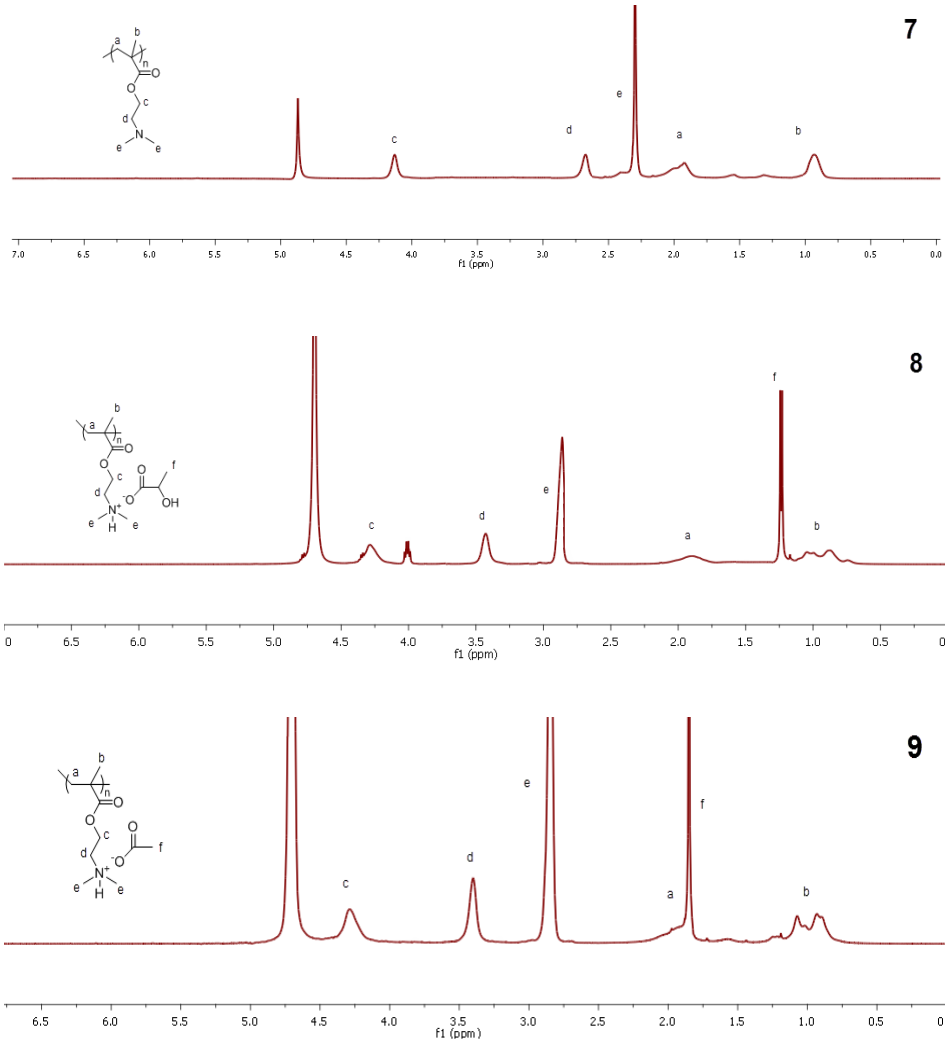

Figure 2.6. ^{1}H NMR spectra of poly(ionic liquid)s by using monomers from 1 to 9 (D_2O)

The ^{1}H NMR spectra confirmed that the monomer reactive groups giving signals between 5.5-6.5 ppm were disappeared indicating that full

conversions were achieved for all the poly(ionic liquid)s synthesized. Other characteristic signals associated with the polymer backbone were also observed around 1.0-2.0 ppm as broad signals as an indication of the formation of a polymeric material. In conclusion, the polymers were obtained free of monomer and used for further characterization to investigate their various properties.

One of the most important properties of a polymer is the molecular weight. Therefore, the molecular weights of the poly(ionic liquid)s were characterized by using an GPC-SEC with light scattering detection in water. The molecular weights determined are given in table below.

Table 2.1. Molecular and thermal properties of the poly(ionic liquid)s prepared

Polymer Code	M_n[a] (kDa)	M_w[b] (kDa)	T^c_{onset} (°C)	T^d_{dec} (°C)	T_g[e] (°C)
1	62.2	100.6	240.0	300.0	80.0
2	38.8	42.3	183.9	253.7	-52.0
3	70.6	80.9	163.9	218.5	-26.0
4	224.3	306.5	243.6	307.5	88.0
5	36.6	57.1	180.4	240.7	-50.0
6	463.6	701.0	160.4	212.5	31.0[δ]
7	nd*	nd*	138.6	387.2	19.0[f]
8	140.8	191.8	173.8	252.4	-36.0
9	405.4	485.9	163.3	327.4	9.0

[a] Number average, [b] weight average molecular weights measured by light scattering detector [c] The temperature value at the point where a sharp decrease in the weight percent starts. [d] The temperature value at which 50% of the weight is lost. [e] The glass transition temperatures are taken as the temperature at the middle point of the glass transition region. [f] The value is taken from literature. [g] The glass temperature for this polymer is obtained from modulated DSC scan.

In the table 2.1., the molecular weights of the polymers synthesized are given. In all the cases, high molecular weight (50K-400K) and polydispersity indexes (1.5-2.0) were obtained as expected by the uncontrolled free radical polymerization in solution. The molecular

weights obtained were sufficient enough to characterize various properties of those polymers. However some trends in the molecular weights can be observed among different counter anions. Although the poly(ionic liquid)s bearing acetate anions showed higher molecular weights than the halide and lactate anions, further analysis is required to assess the effect of the anion in the free radical polymerization process.

Thermal properties of the polymers were analyzed by using thermal gravimetric analysis (TGA) and differential scanning calorimetry (DSC). The degradation profiles of the poly(ionic liquid)s are provided below. The extracted data from the profile are provided in table 2.1.

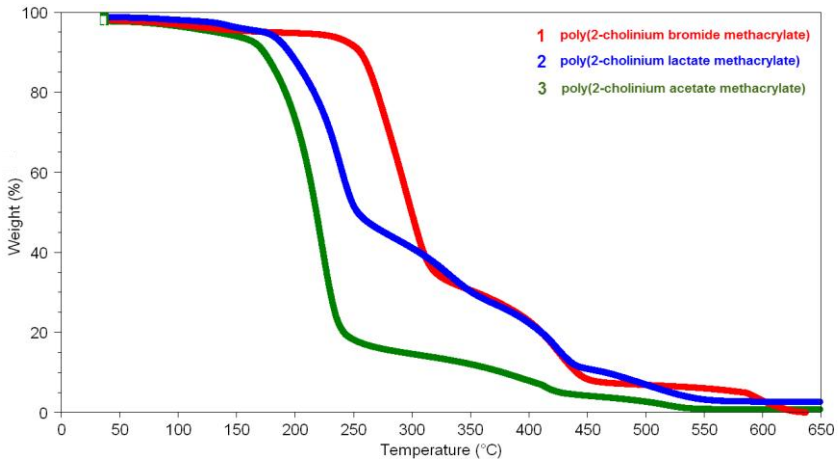

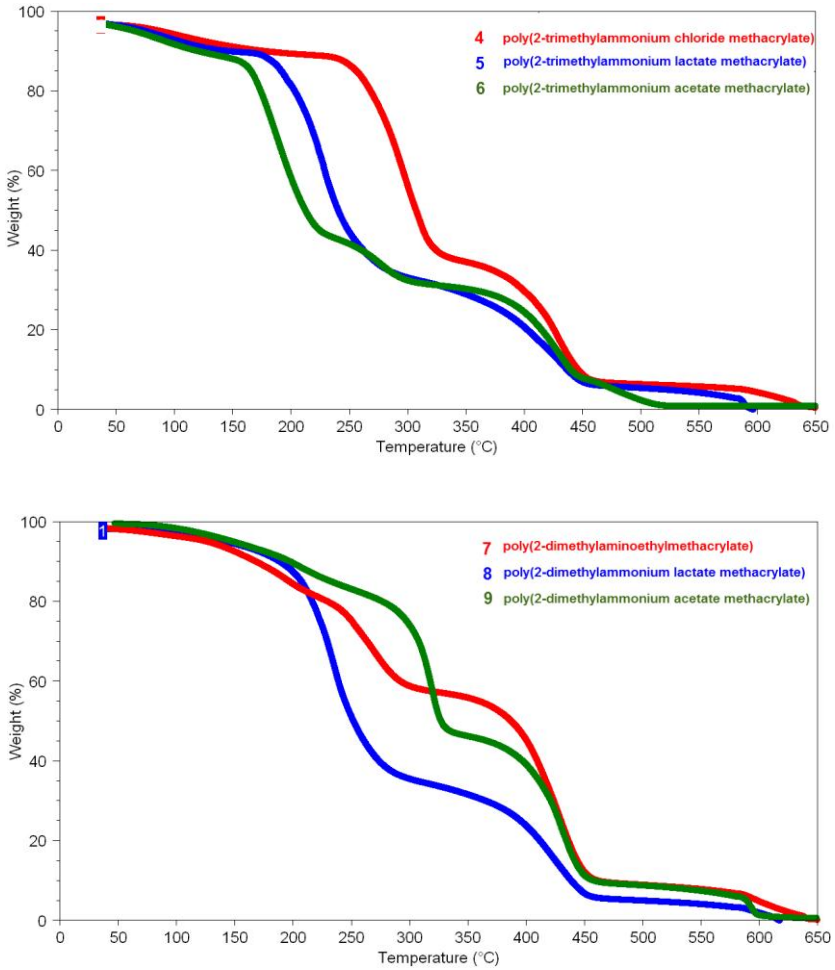

Figure 2.7. TGA profiles of the poly(ionic liquid)s synthesized

When the degradation profiles of all the polymers are analyzed, it can be clearly observed that the polymers displayed a three-step degradation profile. It is well defined in literature that quaternary ammonium species decompose through Hofmann elimination which results in the formation of unsaturated groups and free amine. A

representative mechanism is provided for the decomposition of quaternary ammoniums through Hofmann elimination.

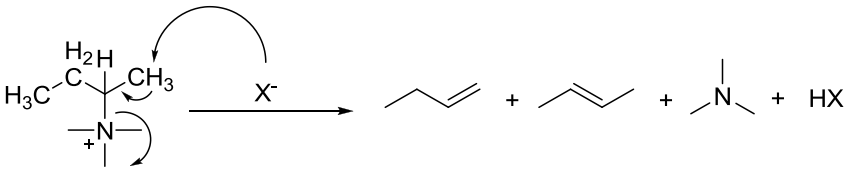

Figure 2.8. Hofmann elimination of quaternary ammonium compound

Hence, the first steps of the TGA signals can be attributed to the degradation of pendant groups on the polymer backbone. On the other hand, a thermal stability trend of poly(ionic liquid)s with different anions was observed in the order of T_{dec} halide > T_{dec} lactate > T_{dec} acetate, except for poly(2-dimethylaminoethyl methacrylate) and the quaternized analogs of the same polymer. This fact may be associated to the self-catalyzed nucleophilic attack of the anions to form the corresponding SN_2 products at high temperatures. For all the polymers having halide, lactate and acetate counteranions, similar onset, and decomposition temperatures were recorded as seen from the table 2.1., the decomposition temperature of poly(2-dimethylammoniumethyl acetate methacrylate) at 327 °C being the only exception.

Another important property that was investigated was the glass transition temperatures of the poly(ionic liquid)s. The DSC signals were recorded and the extracted data is given table 2.1. The DSC profiles are provided in the figure below.

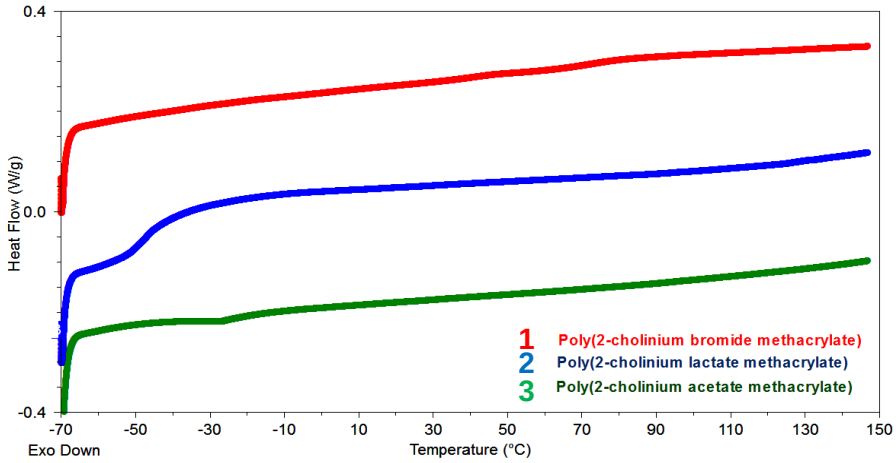

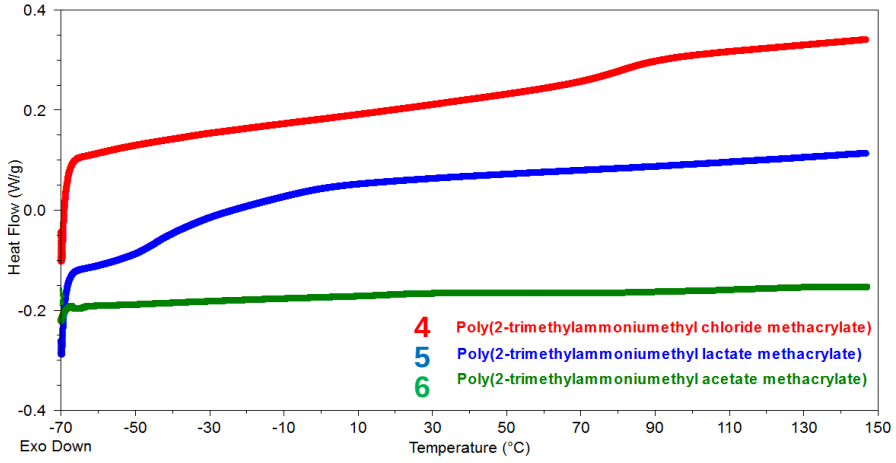

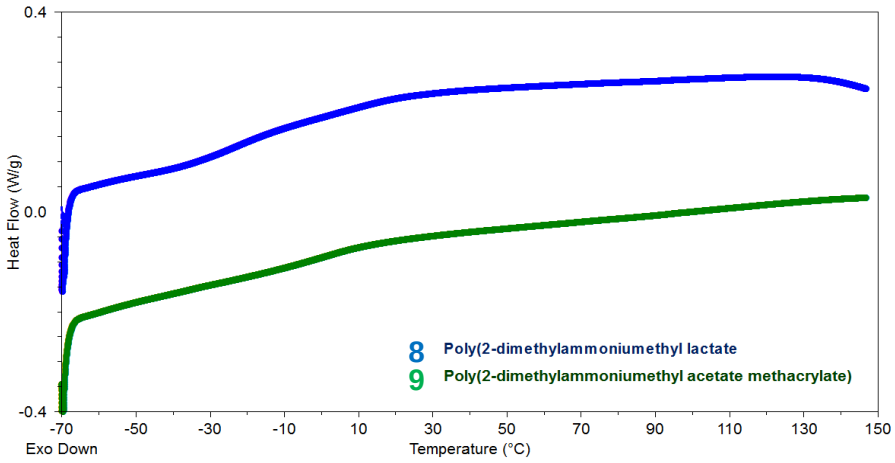

Figure 2.9. DSC signals of the poly(ionic liquid)s from -70 °C to 150 °C

All the polymers were found to be amorphous and displayed glass transition temperatures (T_g) as can be seen from the DSC profiles given in figure 2.9. As it can be seen from extracted data in table 2.1., T_gs of 80, −26, and −52 °C were obtained for poly(2-cholinium bromide methacrylate), poly(2-cholinium acetate methacrylate), and poly(2-cholinium lactate methacrylate), respectively. For 2-trimethylammonium ethyl methacrylate and 2-dimethylaminoethyl methacrylate based polymers, similar trends in the glass transition temperatures were also observed in the order of T_g chloride > T_g acetate > T_g lactate. The lowest T_gs were recorded for the polymers combining lactate as counteranions. Indeed, the lactate has the highest H-bonding ability since it possess a hydroxyl group, which weakens the electrostatic interactions between

the cation and the anion, and consequently lowers the T_g of the polymer. The same explanation is also valid for poly(2-cholinium lactate methacrylate) and poly(2-cholinium acetate methacrylate), which displayed the lowest glass transition temperatures among their analogs. These polymers carry also hydroxyl units, the former has both in the cation and the anion and the latter contains on the cation. The highest glass transition temperatures were obtained for the polymers bearing halide anions which are smaller and display strong Coulombic interactions with the cation resulting in a higher glass transition temperature. It can be concluded that the glass transitions can be tuned by playing with the chemical structures of both the cation and the anion.

One potential application of the cholinium based ionic liquid monomers is to use them for the preparation biocompatible ion gels. As explained in detail in chapter 1, ion gels are materials composed of ionic liquids stabilized in a solid matrix to obtain a self-standing material having the characteristic properties of ionic liquids. Ion gels can be prepared through different methods such as block copolymer gelation, sol-gel technique or simple blending with a matrix material. Within this respect, we have chosen photopolymerization to form the ion gel by using cholinium lactate ionic liquid. The preparation of the ionic liquid is simple and straightforward. Commercially available cholinium hydroxide was let to react with stoichiometric amount of lactic acid to obtain the

corresponding ionic liquid. The structure of the ionic liquid was confirmed by ^{1}H NMR. The spectrum is given in the figure below.

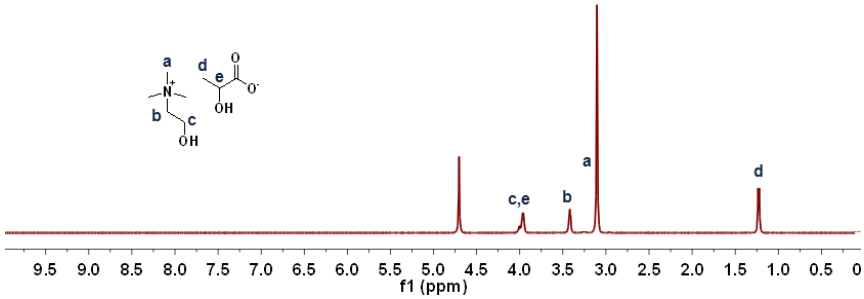

Figure 2.10. ^{1}H NMR spectrum of the cholinium lactate ionic liquid (D_2O)

The spectrum obtained from the ionic liquid confirmed the structure of compound. The signal associated with the lactic acid was observed around 1.2 ppm and the signals associated with the cholinium cation were observed between 3.0 and 4.0 ppm. This ionic liquid was used to prepare the ion gels. As a preliminary study, 2 different ion gels were prepared containing 60% free ionic liquid. In one case, the 2-cholinium lactate methacrylate ionic liquid monomer was photopolymerized in the presence of the photoinitiator and in the 2nd case a crosslinker was introduced to attain more mechanical integrity. The procedure is depicted in the figure below.

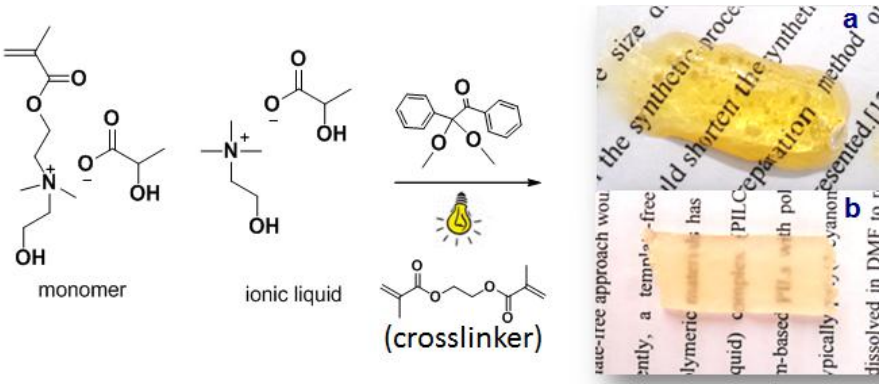

Figure 2.11. Preparation of ion gels by photopolymerization

The photopolymerization of the ionic liquid monomer in the ionic liquid without any crosslinker lead to the formation of a gel which is more like a jelly as clearly seen in figure 2.11a. Addition of 4% crosslinker significantly improved the mechanical integrity of the ion gel leading to a self-standing membrane as seen in figure 2.11b. The viscoelastic properties of the ion gels were examined by rheology measurements.

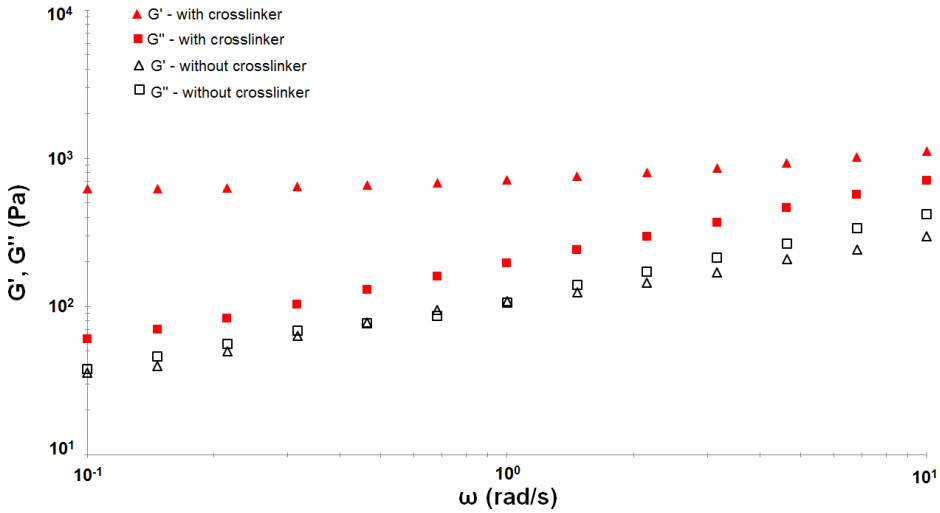

Figure 2.12. Dynamic moduli G' (triangle symbols) and G'' (square symbols) as a function of frequency. Ion gels with (filled symbols) and without (empty symbols) crosslinker.

Elastic (G′) and viscous (G″) moduli of the ion gels were examined as a function of frequency at room temperature. G′ and G″ values were congruent across most frequencies and near parallel indicating that the sample slightly passed the gel point for the ion gel without the cross-linker. G′ became almost independent of frequency over the entire measured range and greater than G″ for the ion gel with 4 wt % difunctional crosslinker indicating that the sample behaves as cross-linked soft solid ion gel. These preliminary examinations on the preparation of ion gels based on cholinium building units were promising

and the experience obtained from these studies were used to make a profound investigation on these material.

As another application, 2-cholinium lactate methacrylate ionic liquid monomer was used to obtain cellulose-poly(ionic liquid) composite coatings by using photopolymerization. During the past decade, a tremendous amount of research has been conducted regarding the dissolution of cellulose in ionic liquids. It is well-known that some ionic liquids are able to efficiently dissolve cellulose.[18] For instance, ionic liquids containing halide, carboxylate, and phosphate anions have been shown to possess high capability to efficiently break the strong inter- and intramolecular H-bonds present in the macromolecular structure of cellulose. Poly(ionic liquid)−cellulose composites have been prepared through the use of cellulose previously dissolved in mixtures of ionic liquids in which one component is a polymerizable ionic liquid monomer.[19] The procedure applied for the composite preparation was very simple and straightforward. Basically, different amounts of cellulose (5 and 10 wt %) were dissolved in 2-cholinium lactate methacrylic monomer by stirring at room temperature for 3 days. Then, the resulting solutions were applied onto glass surfaces and cured by UV light in the presence of the 2,2-dimethoxy-2-phenylacetophenone photo-initiator. The coating obtained on glass surfaces are shown in the following figure.

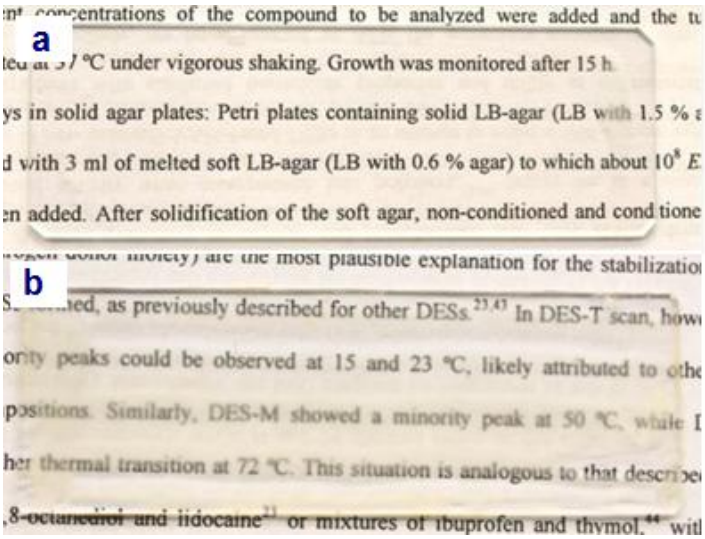

Figure 2.13. Pictures of the cellulose-poly(ionic liquid) coating obtained with a) 5 wt% and b) 10 wt% cellulose

The coating containing 5 wt % of cellulose displayed an excellent optical transparency as it can be clearly seen in figure 2.13a. When the cellulose concentration was increased up to 10 wt %, a slight decrease in the optical transparency of the coating was observed, probably due to the limit of solubility of cellulose in the ionic liquid, which commonly is about 10%.

2.4. Conclusions

Cholinium-based ionic liquid methacrylic monomers having halide, lactate, and acetate counteranions were prepared for the first time and successfully polymerized by using conventional free radical polymerization in water. Their properties were investigated and compared with the non-cholinium type methacrylic analogs. Poly(ionic liquid)s having lactate as counter anion displayed relatively better thermal stability and had lower glass transition temperatures compared to those combining acetate counter anions. Moreover, 2-cholinium lactate methacrylate monomer was used for the preparation of ion gels containing cholinium lactate ionic liquid. The ion gels were prepared to have 60 wt% free ionic liquid inside and their mechanical integrity was easily altered with the addition of a crosslinker. The same monomer was also utilized to prepare cellulose coatings by a fast UV curing process. The hydroxyl functionality attached to the alkyl substituent of ammonium cation of the cholinium ionic liquids in combination to the lactate counter anion makes it liquid at room temperature which facilitates its applications as ion gels or cellulose composites.

Chapter 2

Scientific Contributions

1- Isik M., Gracia R., Kollnus L. C., Tome L. C., Marrucho I. M., Mecerreyes D., *Cholinium based poly(ionic liquid)s: Synthesis, characterization and application as biocompatible ion gels and cellulose coatings*, ACS Macro Lett., **2013**, 2, 975-979.

2- Isik M., Gracia R., Kollnus L. C., Tome L. C., Marrucho I. M., Mecerreyes D., *Cholinium lactate methacrylate: ionic liquid monomer for cellulose composites and biocompatible ion gels*, Macromol. Symp., **2014**, 342, 21-24.

2.5. References

1- S. Stolte, M. Matzke, J. Arning, A. Boschen, W.-R. Pitner, U. Welz-Biermann, B. Jastorff and J. Ranke, Green Chem., 2007, **9**, 1170-1179.

2- B. Jastorff, K. Mölter, P. Behrend, U. Bottin-Weber, J. Filser, A. Heimers, B. Ondruschka, J. Ranke, M. Schaefer, H. Schröder, A. Stark, P. Stepnowski, F. Stock, R. Störmann, S. Stolte, U. Welz-Biermann, S. Ziegert, and J. Thöming., Green Chem., 2005, **7**, 362

3- S. Stolte, J. Arning, U. Bottin-Weber, M. Matzke, F. Stock, K. Thiele, M. Uerdingen, U. Welz-Biermann, B. Jastorff, and J. Ranke., Green Chem. 2006, **8**, 621.

4- J. Neumann, C.-W. Cho, S. Steudte, J. Koser, M. Uerdingen, J. Thoming and Stefan Stolte, Green Chem., 2012, **14**, 410.

5- J. Neumann, S. Steudte, C-W. Cho, J. Thoming and S. Stolte, Green Chem., 2014, **16**, 2174.

6- J. Pernak, N. Borucka, F. Walkiewicz, B. Markiewicz, P. Fochtmann, S. Stolte, S. Steudte and P. Stepnowski, Green Chem., 2011, **13**, 2901.

7- J. Naumann, O. Grundmann, J. Thoming, M. Schulte and S. Stolte, Green Chem., 2010, **12**, 620-627.

8- H. Niedermeyer, C. Ashworth, A. Brandt, T. Welton and P. A. Hunt, Phys. Chem. Chem. Phys., 2013, **15**, 11566.

9- H. Ohno and K. Fukumoto, Acc. Chem. Res., 2007, **40**, 1122-1129.

10- R.H.Broh-Kahn, Int. Rec. Med., 1960, **173**, 217.

11- A. P. Abbott, G. Capper, D. L. Davies, H.L. Munro, R.K. Rasheed and V. Tambyrajah, Chem.Comm., 2001, 2010-2011.

12- Y. Fukaya, Y. Iizuka, K. Sekikawa and H. Ohno, Green Chem., 2007, **9**, 1155-1157.

13- M. Petkovic, J.L. Ferguson, H. Q. N. Gunaratne, R. Ferreira, M. C. Leitao, K. R. Seddon, L. Paulo, N. Rebelo and C. S. Pereira, Green Chem., 2010, **12**, 643-469.

14- S. Shahriari, L. C. Tome, J. M. M. Araujo, L. P. N. Rebelo, J. A. P. Coutinho, I. M. Marrucho and M. G. Freire, RSC Advances, 2013, **3**, 1835-1843.

15- X-D Hou, T. J. Smith, N.Li, M-H. Zong, Biotechnology and Bioengineering, 2012, **109**, 2484.

16- L. C. Tome, D. J.S. Patinha, R. Ferreira, H. Garcia, C. S. Pereira, C. S. R. Freire, L. P. N. Rebelo and I. M. Marrucho, ChemSusChem., 2014, **7**, 110-113.

17- L. C. Tome, N. H. C. S. Silva, H. R. Soares, A. S. Coroadinha, P. Sadocco, I. M. Marrucho and C. S. R. Freire, Green Chem. 2015, **17**, 4291-4299.

18- R. P. Swatloski, S. K. Spear, J. D. Holbrey, R. D. Rogers, J. Am. Chem. Soc. 2002, **124**, 4974−4975.

19- Kadokawa, J. I. In Ionic Liquids: Applications and Perspectives; Kokorin, A., Ed.; InTech: United Kingdom, 2011; p 98.

3 Amphiphilic Block Copolymers from Lactic Acid and Cholinium Building Units

Contents

3.1. Introduction……86

3.2. Experimental……90

3.3. Results and Discussion……94

3.4. Conclusions……109

3.5. References……110

Chapter 3

3.1. Introduction

Polylactide (PLA), biocompatible and biodegradable by enzyme and hydrolysis, is hydrophobic aliphatic polyester and probably the most important biobased synthetic polymer.[1,2] Hydrophobicity of polylactide is a problem for biological and biomedical applications since it will not be applicable in aqueous environment.[3] In order to overcome this problem, one of the main approaches is to combine polylactide with water soluble polymers to form amphiphilic block copolymers which can self-assemble into different morphologies like micelle or vesicle potentially to be used for drug delivery applications.[4] The water soluble block to be combined with PLA can be chosen from either synthetic or natural polymers.

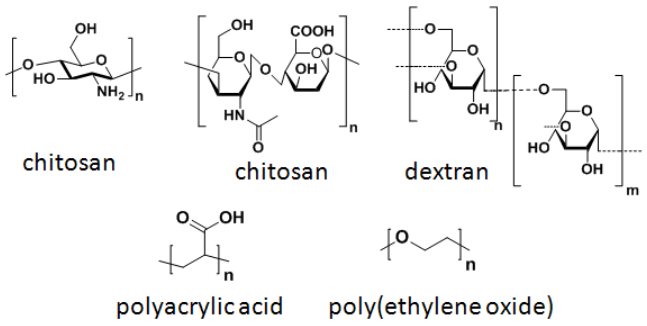

Figure 3.1. Chemical structures of some water soluble natural and synthetic polymers

Among others, poly(acrylic acid) and poly(ethylene oxide) can be given as examples to the important synthetic water soluble polymers that have been utilized for various polylactide based amphiphilic block

copolymers.[5] Natural water soluble polymers are as well used for the synthesis of amphiphilic PLA copolymers. Among those, chitosan,[6] dextran,[7] hyaluronic acid,[8] chondroitin sulfate[9] can be given as examples. Recently, Fajardo et. al synthesized through click chemistry PLA based amphiphilic block copolymers by using chondroitin sulfate as the water soluble block.

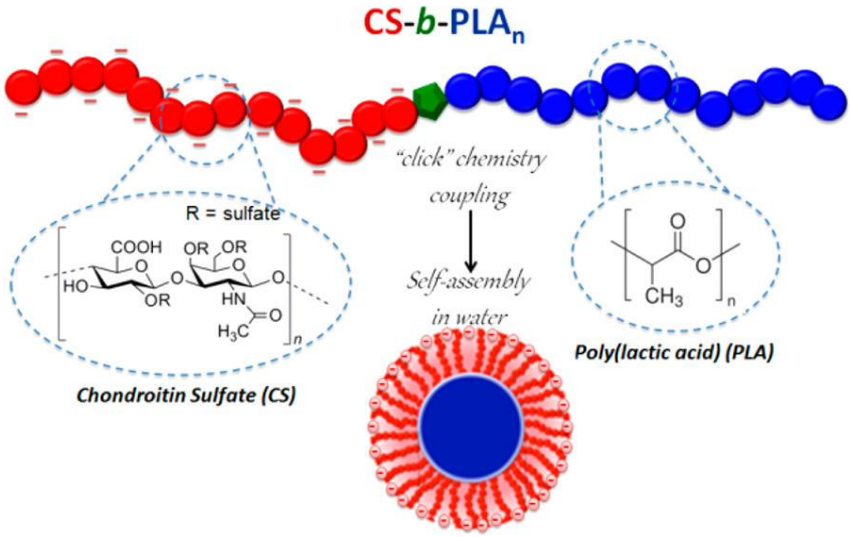

Figure 3.2. Synthesis of PLA-Chondroitin sulfate block copolymers (9)

Block copolymers self assembled in water and displayed spherical micelles that are in the range of 23-31 nm as revealed by TEM and proposed as new drug delivery platforms.[9] Robb et. al synthesized drug delivery vehicles based on polylactide and poly(allyl glycidyl ether).[10] Functional backbone of the PLA allows the attachment of drug molecules co-

valently which are released upon the degradation of the PLA. The proper adjustment of the composition of the block copolymer allows playing with the degradation time to produce materials with the desired release profiles.[10]

A number of applications can be listed for PLA amphiphilic block copolymers.[3] The most widely hypothesized application is the delivery of hydrophobic drugs where drug molecules are encapsulated within the hydrophobic PLA matrix.[11]

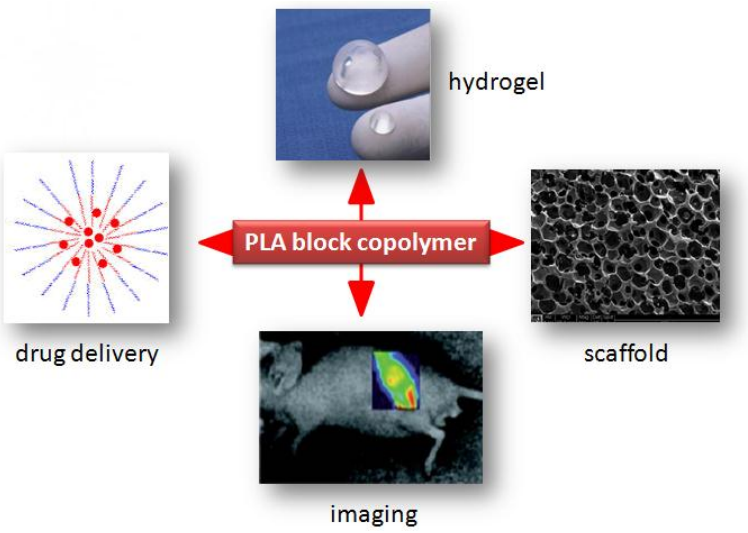

Figure 3.3. Illustrations for some applications of PLA block copolymers

They can also be used as imaging and diagnostic platforms by the use of active agents.[12] Other applications can be the preparation of hydrogels and scaffolds to be used as tissue engineering platforms.[13, 14]

Chapter 3

Cholinium, a quaternary ammonium cation, trimethylethanol ammonium, is an essential micronutrient which supports several biological functions.[15] Due to their particular features, such as biocompatibility, excellent biodegradability, and low toxicity, ionic liquids combining cholinium cation with non-hazardous anions have been used in several applications as diverse as solvents in benign extraction schemes as aqueous biphasic systems, agents for collagen-based materials, or in the pretreatment or the dissolution of biomass.[16-22] More detailed introduction regarding the cholinium based ionic liquids are provided in the previous chapter.

The synthesis of cholinium based poly(ionic liquid)s are already presented previously by the free radical polymerization of the cholinium based ionic liquid monomers. Within this context, we have chosen the same cholinium cation combined with lactate anion to use for the synthesis of copolymers with lactide to obtain new block copolymers. As a result, the amphiphilic block copolymer will be carrying moieties coming from lactic acid (lactide and lactate) in both blocks of the copolymers combined with the cholinium cation. Thus, the synthesis and self-assembly of poly(L-lactide)-poly(2-cholinium lactate methacrylate) block copolymers will be given throughout this chapter.

Chapter 3

3.2. Experimental

3.2.1. Materials

2-dimethylaminoethyl methacrylate (98%, Aldrich), 2-bromoethanol (95%, Aldrich), silver lactate (97%, Aldrich), 4-Cyano-4-[(dodecylsulfanylthiocarbonyl) sulfanyl]pentanol (Aldrich), 2,2′-Azobis(2-methylpropionitrile) (AIBN, 98%, Aldrich), 1,8-Diazabicyclo[5.4.0]undec-7-ene (DBU) (98%, Aldrich), benzoic acid (BA) (99.5%, Aldrich), ethyl acetate (99.5%, Aldrich), dichloromethane (99.5%, Aldrich), methanol (99.8%, Aldrich), diethyl ether (99.5%, Aldrich) were used as received without further purification. L-lactide was kindly provided by Futerro. Di-alysis membranes (Pur-A-Lyzer, MWCO 3.5 kDa, Aldrich) with cut-off molecular weight of 3500 kDa were used.

3.2.2. Monomer synthesis

2-cholinium lactate methacrylate was synthesized by using 2-cholinium bromide methacrylate as the starting material. The detailed procedure for the synthesis of both monomers was given in chapter 2. Shortly, stoichiometric amount of 2-cholinium bromide methacrylate was reacted with silver lactate in water/methanol mixture. After 24 hours the crude product was isolated from the precipitates by centrifugation. The monomer was dried with pressurized air.

3.2.3. Catalyst preparation

To prepare benzoic acid:1,8-Diazabicyclo[5.4.0]undec-7-ene (DBU) salt, benzoic acid (BA) was dissolved in diethyl ether (15% solid) and put into round bottom flask equipped with a dropping funnel containing equimolar amount of DBU dissolved in diethyl ether (20% solid). DBU solution was slowly dropped onto benzoic acid solution to form a white precipitate. The mixture was let to mix for 1 hour after the addition was completed. The salt formed (DBU:BA) was washed with excess diethyl ether and dried under vacuum prior to use. The final product was obtained as a white powder at the end of the drying process.

3.2.4. Macro-RAFT agent synthesis

Ring opening polymerization of L-lactide was conducted by using hydroxyl terminated 4-cyano-4-[(dodecylsulfanylthiocarbonyl)sulfanyl] pentanol chain transfer agent (CTA) as the initiator and DBU:BA salt as the catalyst in the presence of dichloromethane as the solvent at 40 °C. In a typical reaction, 0.3 g of initiator (0.77 mmol), 5.32 g of L-lactide (36.9 mmol), 1.05 g of catalyst and 22.5 g of dichloromethane were mixed in one-neck round bottom flask and the reaction was conducted for 42 hours. Conversion of the monomer to polymer was followed by ^{1}H NMR. Aliquots were taken during the reaction for characterization. Final poly-

mer was precipitated in cold methanol to get rid of unreacted monomer. Two polymers with different molecular weights were prepared, molecular weights being 3500 and 7100 g/mol as calculated from ^{1}H NMR.

3.2.5. Synthesis of the block copolymers

Poly(L-lactide) macro-CTA (MCTA) is used to conduct the polymerization of 2-cholinium lactate methacrylate monomer through RAFT polymerization. In a typical reaction, 0.2 g of MCTA and 0.89 g of ionic liquid monomer were dissolved in methanol/DCM (5.9 ml + 2.0 ml) in a one-neck round-bottom flask. N_2 was purged through the flask and 0.0025 g of AIBN initiator added at 70 °C dissolved in 1.0 ml of methanol. The reactions were conducted for 24 hours. Conversion of the monomer to polymer was followed by ^{1}H NMR. Resulting crude product was washed with acetone and dichloromethane to get rid of any unreacted monomer.

3.2.6. Preparation of block copolymer nanoparticles

Amphiphilic block copolymers were dissolved in deionized water to have a concentration of 5 mg/ml. In a typical preparation, 50 mg of block copolymer was dissolved in 10 ml deionized water and remained under mechanical stirring for 24 hours at room temperature until all material

was completely dissolved. The solutions were then poured into dialysis membranes having 3500 kDa cut-off molecular weight and dialyzed against excess deionized water for 48 hours at room temperature under strong agitation. Dialyzed solutions were poured into vials and diluted dropwise to 1 mg/ml to prevent multiple scattering and analyzed by dynamic light scattering and TEM. Before the analysis, the solutions were filtered through 0.45 µm regenerated cellulose syringe filters.

3.2.7. Characterization

The ^{1}H NMR measurements were carried out on a Bruker AC-400 instrument with the following experimental conditions: spectral width 20 ppm with 32 K data points, flip angle 90, relaxation delay of 18 s, digital resolution of 0.24 Hz/pt. Gel permeation chromatography was conducted on Agilent PL-GPC 50 integrated GPC system with refractive index detector to detect the molecular weights of the polymers. The eluent was THF containing 10 mM of lithium bis(trifluoromethane sulfonyl) imide. Narrow molecular weight polystyrene standards were used for calibration. The mean size of the nanoparticles was determined by dynamic light scattering (DLS) method. The intensity average particle diameter was measured at 25 ºC and 173º backscatter angle by using dynamic light scattering Malvern ZetaSizer Nano-S instrument equipped with a

633 nm red laser. Transmission electron microscopy (TEM) was performed on a TECNAI G^2 20 TWIN (200 kV).

3.3. Results and Discussion

3.3.1. Macro-RAFT agent synthesis

The macro-RAFT agent (macro-CTA) was synthesized by the ring opening polymerization of L-lactide with the dual chain transfer agent (CTA) which bears a hydroxyl group to act as the initiator for the polymerization. The polymerization was conducted in dichloromethane by using benzoic acid: 1,8-Diazabicyclo [5.4.0] undec-7-ene (DBU) salt as the catalyst at 40 °C. The use of an effective catalyst system allows the polymerization to be conducted at mild temperatures. The reaction scheme of the polymerization is provided below.

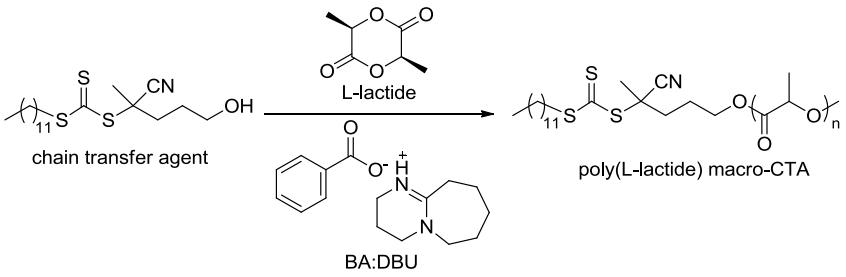

Scheme 3.1. Synthesis pathway of the poly(L-lactide) (PLA) macro-CTA

The controlled nature of the organocatalyzed ring opening polymerization of the L-lactide monomer provides to control the molecular weight of the final product. This can be achieved by adjusting the initial stoichiometry of the reactants. As an example, to obtain a molecular weight of 5000 g/mol, 1 mole of initiator should be reacted with 5 kg of the monomer. Macro-CTAs having two different molecular weights were synthesized by playing with the stoichiometry of the reaction and the conversion of the monomer to polymer was monitored by ^{1}H NMR.

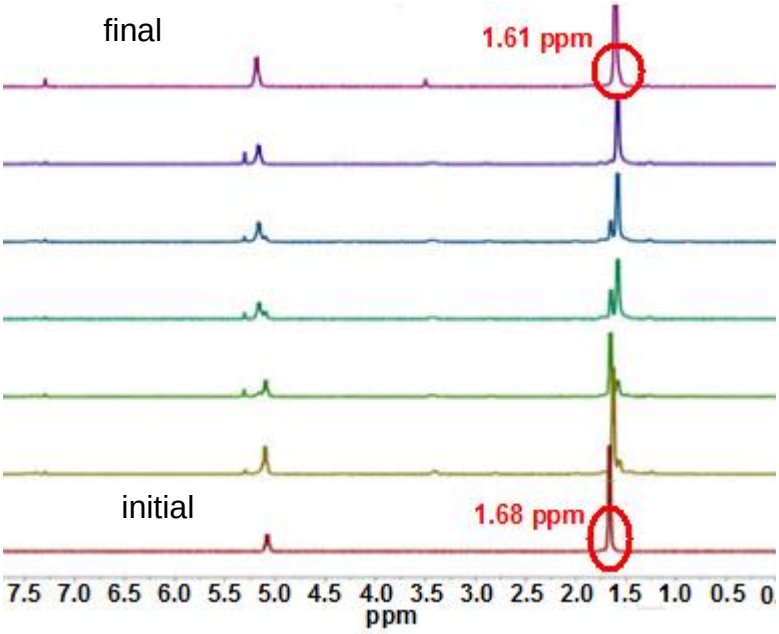

Figure 3.4. ^{1}H NMR spectra taken during the synthesis of the PLA macro-CTA

The methyl proton (-C=OC(-CH_3)O-) signal originating from the lactide monomer at 1.68 ppm disappears as the polymerization reaction proceeds and the methyl signal arising from the polymeric repeat unit appears at 1.61 ppm at the final PLA. The integral ratio of these two peaks during the reaction allows us to determine the conversion of the monomer to polymer. The conversion was calculated by determining the ratio of the integrals of the methyl proton signals of the –C(-CH_3)C(=O)O repeating units in the polymer chains to the corresponding lactide monomer (1.68 ppm and 1.61 ppm). The calculated conversion values were plotted against time and given in the following figure.

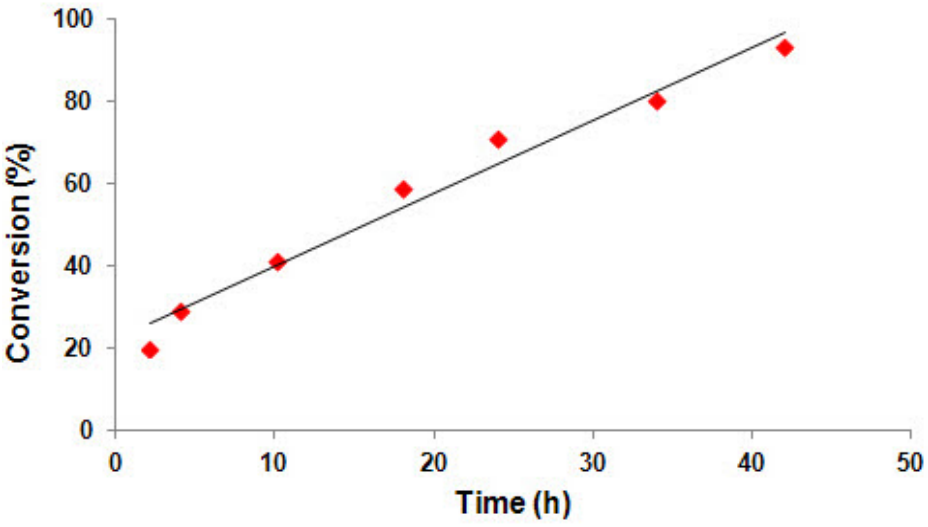

Figure 3.5. Conversion of the monomer to polymer during the course of the polymerization reaction

As seen from the figure given, the conversion of the monomer proceeds linearly as the reaction time passes; indicating that the polymerization was first-order in monomer concentration. In addition, the linearity of this plot points to a rapid initiation and an absence of chain termination, suggesting a living ROP upto 93% of conversion. This methyl signal of the final clean polymer at 1.61 ppm and the methyl proton signal at 0.88 ppm arising from the methyl chain ($CH_3(CH_2)_{11}$-) of the RAFT agent were used to estimate the calculated molecular weight of the PLA. The calculated molecular weights determined from ^{1}H NMR signals correlate well with the expected theoretical molecular weights of the PLA macro RAFT agents. The ^{1}H NMR signals used to determine the calculated molecular weights of the polymers are provided in the following figure together with the ^{13}C NMR spectrum.

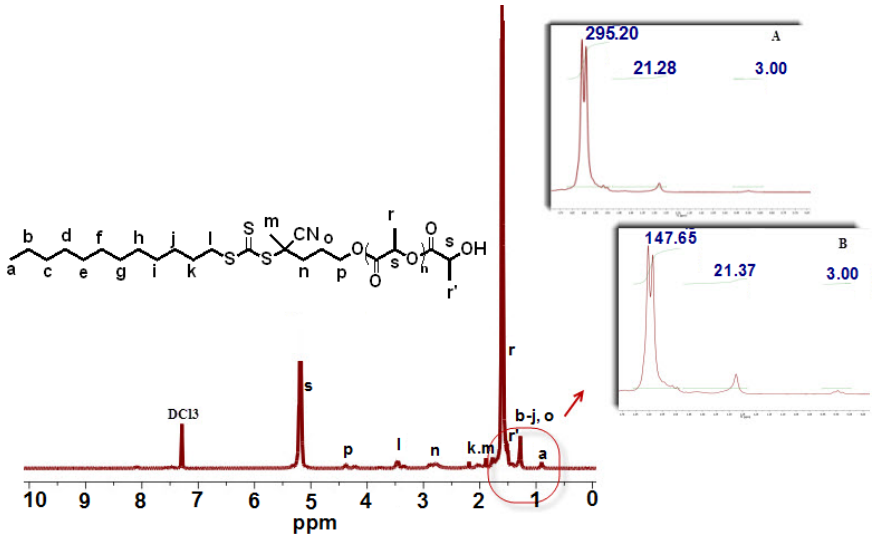

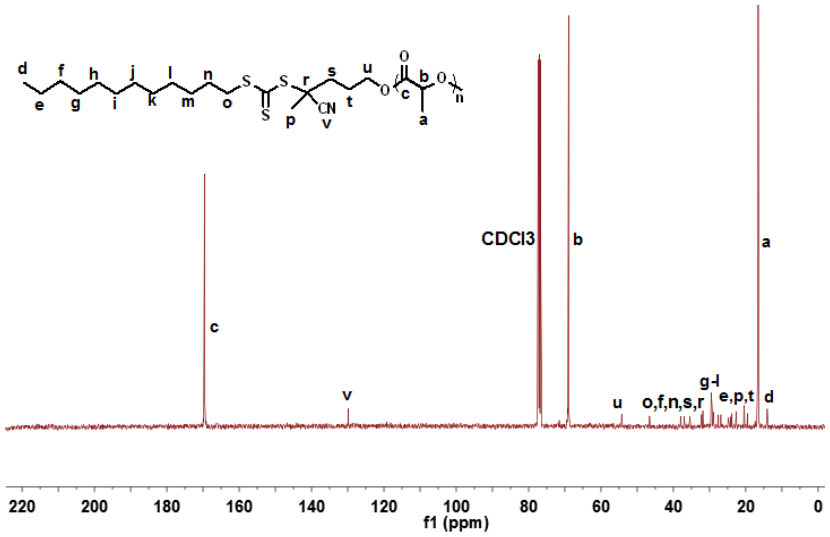

Figure 3.6. ^{1}H NMR spectrum of PLA macro-RAFT agent, inner images shows the integral values used to determine the calculated molecular weights of the polymers. A) PLA7.0K B) PLA3.5K and the ^{13}C NMR spectrum of PLA

The molecular weights of the PLA macro-CTAs were found to be 3500 g/mol and 7100 g/mol for the polymers PLA3.5K and PLA7.0K, respectively. These polylactide macro-RAFT agents are used to synthesize the desired block copolymers. As another characterization, GPC measurements were also performed to confirm the polydispersities of the macro-CTAs. The GPC signals recorded for the homopolymers are provided in the figure below.

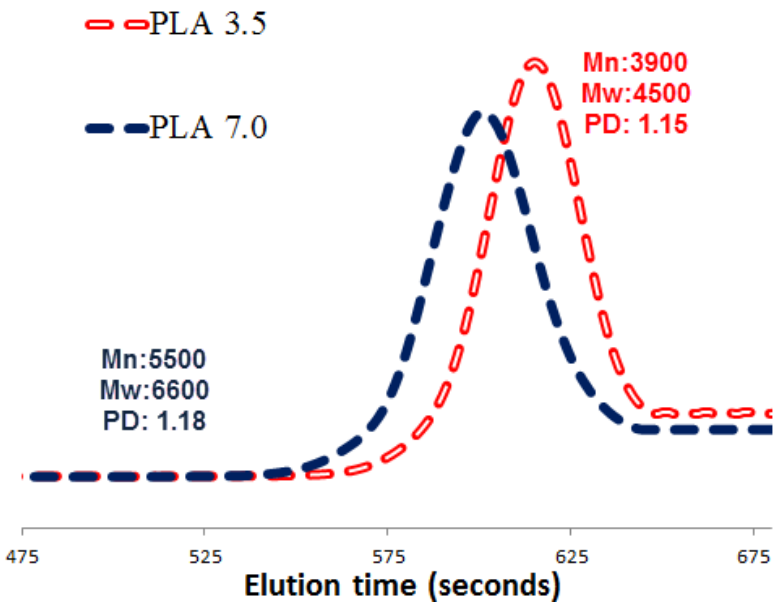

Figure 3.7. GPC-SEC signals recorded for PLA3.5 and PLA7.0 polylactide macro-RAFT agents

As seen from the figure, monomodal GPC signals are obtained with low polydispersities which represent good control over the polymerization of L-lactide. The GPC signals shifts to lower retention times indicating an increase in the molecular weight as expected as the degree of polymerization increases for the polymer with a higher molecular weight. The theoretical, calculated and measured molecular weights of the PLA macro RAFT agents are provided in table 3.1.

3.3.2. Synthesis of the block copolymers

Poly(L-lactide)-poly(2-cholinium lactate methacrylate) block copolymers were synthesized by using the previously synthesized macro-RAFT agents to control the polymerization of the methacrylic monomer.

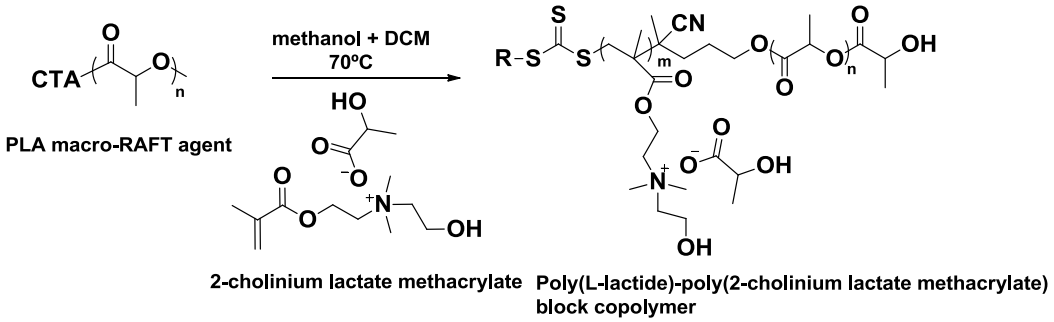

Scheme 3.2. General synthesis scheme of the PLA-PIL block copolymer

All the polymerization reactions were performed in methanol/dichloromethane (5/1 v/v) solvent mixture for 24 hours. The final products were analyzed by ^{1}H NMR to follow the conversion of the monomer to polymer. The crude product was washed sequentially with acetone and dichloromethane to get rid of any unreacted starting material. ^{1}H NMR revealed that the conversion was over 99% after each polymerization.

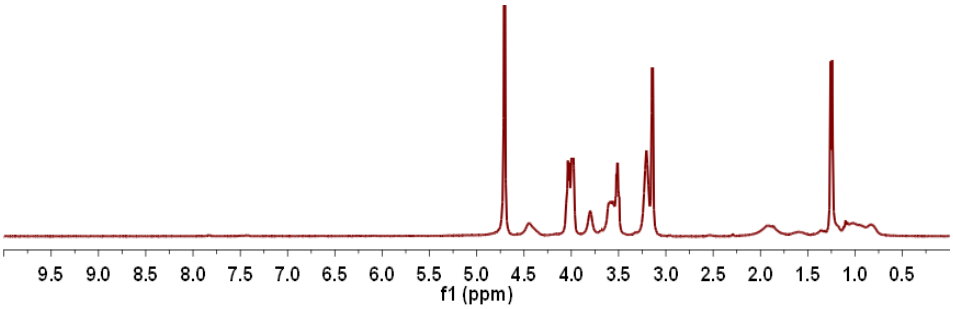

Figure 3.8. ^{1}H NMR spectrum of PLA-PIL given as an example (D_2O)

As it can be seen from the spectrum given, the monomer associated signals between 5.5 and 6.5 ppm were disappeared at the end of the polymerization reaction. This indicates that the monomer was fully converted. The signals observed in the given spectrum as an example refer mainly to the PIL block since the PLA block is shielded by the water soluble PIL block of the block copolymer. The sharp peak at around 1.25 ppm corresponds to the $-CH_3$ proton on the lactate anion. The broad signals at 1.0 ppm and 1.9 ppm are associated with the $-CH_3$ and $-CH_2$ protons on the backbone of the PIL block. The signals between 3.0 and 4.6 ppm are assigned to the protons of the pendant group of the PIL block.

Four different block copolymers were synthesized. The polymers synthesized were denoted as PLA3.5-PIL50, PLA3.5-PIL100, PLA7.0-PIL50, PLA7.0-PIL100 where the PLA denotes the poly(L-lactide) block and the second denotes the poly(2-cholinium lactate methacrylate)

block, the number indicating the degree of polymerization for this block. The list of polymers and molecular properties are provided in table 3.1.

Table 3.1. Polymers synthesized and their properties

Polymer code	M_n[a]	M_n[b]	M_n[c]	M_w[d]	PDI[e]
PLA 3.5	3800	3500	3900	4500	1.15
PLA 7.0	7300	7100	5500	6600	1.18
PLA3.5-PIL50	18300	-	6200	8100	1.30
PLA3.5-PIL100	32900	-	9250	11500	1.25
PLA7.0-PIL50	21800	-	8900	11800	1.32
PLA7.0-PIL100	36400	-	10300	13300	1.29

[a] Theoretical molecular weights. Calculated from the formula: $M_{n,theory}$=(Mass of monomer) x P / $[RAFT]_0$ + Mw_{RAFT}, where P is the fractional conversion, Mw_{RAFT} is the molecular weight of the RAFT agent, $[RAFT]_0$ is the initial concentration of the RAFT agent. [b] Molecular weights calculated from ^{1}H NMR [c,d,e] GPC results based on PS standards in THF containing 10 mM of LiTFSI.

All the block copolymers were analyzed by GPC to follow the formation of the block copolymers. To illustrate this, GPC signals of two different block copolymers are provided below.

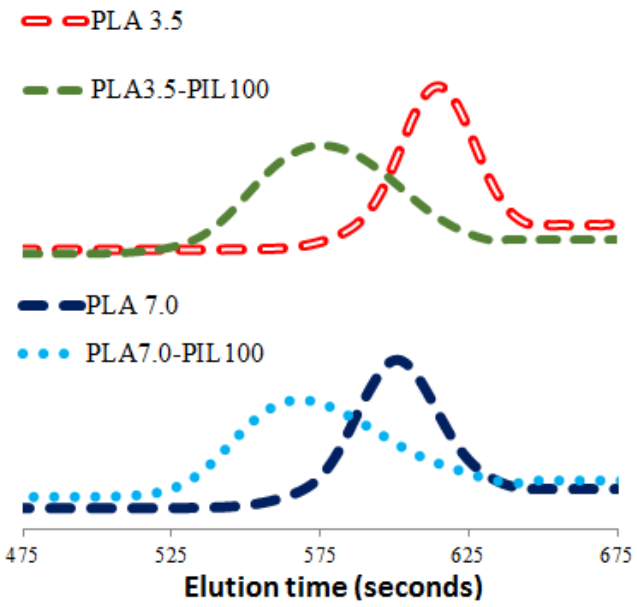

Figure 3.9. GPC signals of block copolymers synthesized by using two different PLA macro RAFT agents

All the polymers displayed monomodal GPC signals with reasonably low polydispersities indicating good control over the polymerization by using PLA macro RAFT agent, showing shifts to lower retention volumes as the molecular weight increases with the formation of the block copolymer.

3.3.3. Self-assembly in water

The amphiphilic nature of block copolymers allows obtaining self-assembled nanostructures in selective mediums. The PIL block of the PLA-PIL block copolymer is highly water soluble due to its ionic nature whereas the PLA block is highly water insoluble. This distinctive pattern allows the polymer backbone to self-assemble to minimize the energy of the system. When the block copolymer is dissolved in aqueous medium, the ionic block stabilizes the hydrophobic part, forming self-assembled structures having PLA core surrounded by PIL outer shell. In order to study the self assembly of the amphiphilic block copolymers in aqueous environment, block copolymers were dissolved in deionized water to have a concentration of 5 mg/ml. Dialyzed solutions were poured into vials and diluted dropwise to 1 mg/ml and analyzed by dynamic light scattering and TEM.

The sizes of the self-assembled structures in water are determined by dynamic light scattering (DLS) and the values are provided in the table below.

Table 3.2. Mean sizes of the self assembled block copolymers from DLS and TEM experiments

Polymer	Intensity avg.(nm) DLS		Number avg.(nm) DLS	TEM (nm)
	1st peak	2nd peak		
PLA3.5-PIL50	22	140	22	17
PLA3.5-PIL100	26	176	26	22
PLA7.0-PIL50	30	200	30	29
PLA7.0-PIL100	37	230	37	35

The DLS revealed for all copolymers a bimodal intensity average size distribution as it can be seen from the figure 3.10a and considering the fully stretched polymer chain, the smallest peaks are attributed to the primary micelles, while the second peaks are considered from the aggregation of the individual micelles since the intensity averaged particle size distributions are extremely sensitive to aggregation.

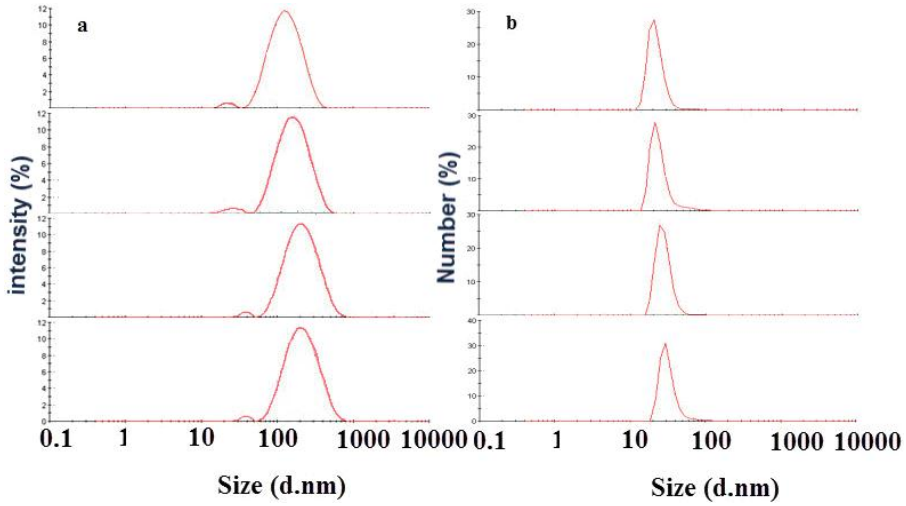

Figure 3.10. a) Intensity and b) number average mean size distribution of the block copolymers in deionized water

Therefore, it can be stated that the number of primary micelles are predominant in the system. This statement can be further verified by analyzing the number averaged size distributions of the self assembled solutions. The profiles are provided in figure 3.10b. As it is clearly seen, the number averaged DLS data represents that the primary micelles are predominant in the system confirming our statement. In order to further analyze the size, morphology and distribution of the self assembled structures, TEM experiments were conducted. TEM images are displayed in figure 3.11 for all the block copolymers that were analyzed.

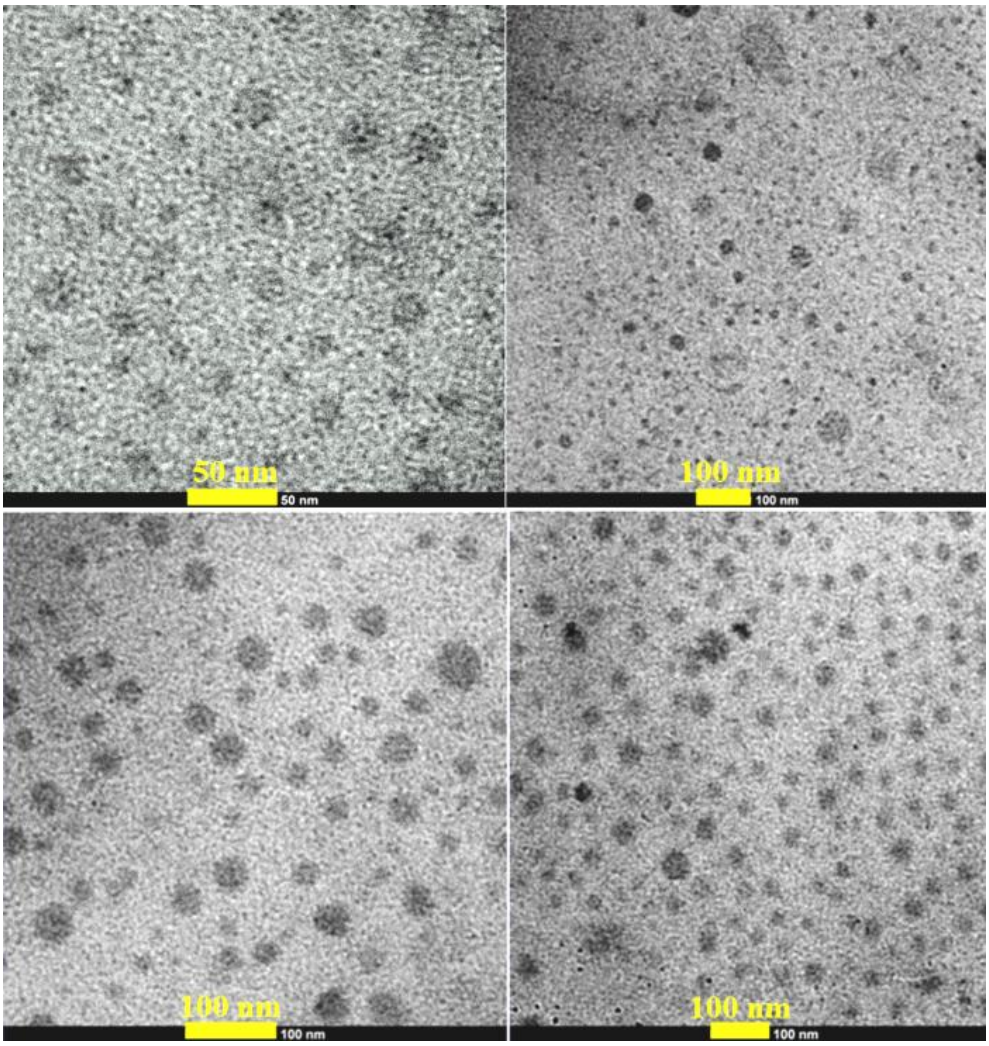

Figure 3.11. TEM images of the block copolymers a) PLA3.5-PIL50 b) PLA3.5-PIL100 c) PLA7.0-PIL50 d) PLA7.0-PIL100

TEM images confirmed the predominant presence of primary spherical micelles in dry state and the mean diameter that is obtained from the

pictures are smaller than those obtained from DLS in swollen state. The average sizes are 17, 22, 29 and 35 nm for PLA3.5-PIL50, PLA3.5-PIL100, PLA7.0-PIL50, PLA7.0-PIL100, respectively. This may be attributed to the fact that the hydrodynamic volume is measured from DLS whereas the size in TEM refers to the dry state where the nanoparticles are collapsed. The mean diameters that are obtained from DLS and TEM are provided in table 3.2. If the mean sizes of the block copolymers are compared, it is clearly seen that the average mean size increases as the molecular weight of the PLA block increases. For the block copolymer having the same PIL degree of polymerization, the size changes from 17 to 29 nm for PLA3.5 and from 22 to 35 nm for PLA7.0. Although the changes are not that dramatic, the same observation is valid for the block copolymers with increasing PIL degree of polymerization. The values determined from TEM reveals that considerably small size micelles can be prepared, sizes going down to approximately 17 nm with a proper design of the composition of the block copolymer.

3.4. Conclusions

Poly(L-lactide)-poly(2-cholinium lactate methacrylate) amphiphilic block copolymers were synthesized by a combination of organocatalyzed ring opening polymerization and controlled radical RAFT polymerizations. These amphiphilic block copolymers contain units coming from lactic acid in both blocks (hydrophilic and hydrophobic) as well as natural cholinium units in the hydrophilic block. Gel permeation chromatography revealed the formation of well-defined block copolymers with relatively low polydispersities. Self-assembly of the amphiphilic block copolymers in aqueous medium was investigated by means of dynamic light scattering and TEM. The block copolymers self-assembled into spherical nanostructures having sizes down to 17 nm as revealed by TEM analysis. The sizes of the nanostructures varied by playing with either PLA or PIL chain lengths, giving opportunity to produce spherical nanostructures in the range of 17-35 nm which makes them of potential interest in nanomedicine.

Scientific contribution

Isik M, Sardon H, Saenz M, Mecerreyes D, *New amphiphilic block copolymers from lactic acid and cholinium building units*, RSC Adv., **2014**, 4, 53407.

3.5. References

1- J. K. Oh, Soft Matter, 2011, 7, 5096; A. P. Gupta and V. Kumar, Eur. Polym. J., 2007, **43**, 4053; E. T. H. Vink, K. R. Rabago, D. A. Glassner and P. R. Gruber, Polym. Degrad. Stab., 2003, **80**, 403; K. M. Nampoothiri, N. R. Nair and R. P. John, Bioresour. Technol., 2010, **101**, 8493.

2- E. Chiellini and R. Solaro, Adv. Mater., 1996, 8, 305–313.

3- N. Nishiyama and K. Kataoka, Adv. Polym. Sci., 2006, **193**, 67.

4- X. Fan, Z. Wang, D. Yuan, Y. Sun, Z. Li and C. He, Polym. Chem., 2014, 5, 4069; B. Jeong, Y. H. Bae, D. S. Lee and S. W. Kim, Nature, 1997, **388**, 860.

5- S. A. Hagan, A. G. A. Coombes, M. C. Garnett, S. E. Dunn, M. C. Davies, L. Illum and S. S. Davis, Langmuir, 1996, **12**, 2153; N. Petzetakis, M. P. Robin, J. P. Patterson, E. G. Kelley, P. Cotanda, P. H. H. Bomans, N. A. J. M. Sommerdijk, A. P. Dove, T. H. Epps and R. K. O'Reilly, ACS Nano, 2013, **7**, 1120.

6- Y. Wu, Y. Zheng, W. Yang, C. Wang, J. Hu and S. Fu, Carbohydr. Polym., 2005, **59**, 165.

7- Z. Zhao, Z. Zhang, L. Chen, Y. Cao, C. He and X. Chen, Langmuir, 2013, **29**, 13072.

8- A. K. Yadav, P. Mishra, A. K. Mishra, P. Mishra, S. Jain and G. P. Agrawal, J. Nanomed. Nanotechnol., 2007, **3**, 246.

9- A. R. Fajardo, A. Guerry, E. A. Britta, C. V. Nakamura, M. E. C. Muniz, R. Borsali and S. Halila, Biomacromolecules, 2014, **15**, 2691.

10- M. J. Robb, L. A. Connal, B. F. Lee, N. A. Lynd and C. J. Hawker, Polym. Chem., 2012, **3**, 1618.

11- E. Jabbari, X. Yang, S. Moeinzadeh and X. He, Eur. J. Pharm. Biopharm., 2013, **84**, 49.

12- J. Lee, J. H. Im, K. M. Huh, Y.-K. Lee and H. Shin, J. Nanosci. Nanotechnol., 2010, **10**, 487.

13- S. K. Agrawal, N. Sanabria-DeLong, G. N. Tew and S. R. Bhatia, Macromolecules, 2008, **41**, 1774.

14- K. Nagahama, T. Ouchi and Y. Ohya, Adv. Funct. Mater., 2008, **18**, 1220.

15- Y. Fukaya, Y. Iizuka, K. Sekikawa and H. Ohno, Green Chem., 2007, **9**, 1155.

16- M. Isik, R. Gracia, L. C. Kollnus, L. C. Tome, M. I. Marrucho and D. Mecerreyes, ACS Macro Lett., 2013, **2**, 975.

17- L. C. Tome, D. J. S. Patinha, R. Freire, H. Garcia, C. S. Pereira, C. S. R. Freire, L. P. N. Rebelo and I. M. Marrucho, ChemSusChem, 2014, **7**, 110; J. M. M. Araujo, C. Florindo, A. B. Pereiro, N. S. M. Vieira, A. A. Matias, C. M. M. Duarte, L. P. N. Rebelo and I. M. Marrucho, RSC Adv., 2014, **4**, 28126.

18- J. Pernak, A. Syguda, I. Mirska, A. Pernak, J. Nawrot, A. Pradzynska, S. T. Griffin and R. D. Rogers, Chem.–Eur. J., 2007, **13**, 6817.

19- X.-D. Hou, Q.-P. Liu, T. J. Smith, N. Li and M.-H. Zong, PLoS One, 2013, **8**, 1.

20- Q.-P. Liu, X.-D. Hou, N. Li and M.-H. Zong, Green Chem., 2012, **14**, 304.

21- M. Petkovic, J. L. Ferguson, H. Q. N. Gunaratne, R. Ferreira, M. C. Leitao, K. R. Seddon, L. P. N. Rebelo and C. S. Pereira, Green Chem., 2010, **12**, 643.

22- H. Garcia, R. Ferreira, M. Petkovic, J. L. Ferguson, M. C. Leitao, H. Q. N. Gunaratne, K. R. Seddon, L. P. N. Rebelo and C. S. Pereira, Green Chem., 2010, **12**, 367.

23-D. J. Coady, K. Fukushima, H. W. Horn, J. E. Rice and J. L. Hedrick, Chem. Commun., 2011, **47**, 3105.

4 Cholinium Based Ion Gels for Cutaneous Electrophysiology

Contents

4.1. Introduction……115

4.2. Experimental……119

4.3. Results and Discussion……125

4.4. Conclusions……147

4.5. References……149

Chapter 4

4.1. Introduction

Among many different methods, electroencephalography (EEG) (brain activity), electrocardiography (ECG) (cardiac activity) or electromyography (muscular response) are important electrophysiological diagnostic procedures where electrodes placed on the skin are used to monitor the electrical activity of specific organs. Electrodes are the most important components in these device applications to monitor and evaluate the biopotential activity. The transduction of potential signals in the tissue to potential signals in the solid state conductor takes place in the electrode.[1-4] There are several factors such as impedance, susceptibility to recording artifact, long term stability, safe contact with the skin and simplicity of application when designing and producing cutaneous electrodes. Another important factor is the top layer of the epidermis, stratum corneum, which acts as a barrier to ionic current. This barrier increases the impedance especially at low frequencies.[5]

Ag/AgCl electrodes are the current gold standard in cutaneous recordings but they require the use of an electrolyte to decrease electrode/skin interface impedance. When exposed to air, the electrolyte dries out after several hours causing an increase in the impedance resulting in the loss of accurate recording.[6] Further addition or refilling of the electrolyte gel to each electrode is time-consuming and causes discomfort to the patient and the caregiver. To enhance the properties of

the hydrogels used for electrodes, Alba and coworkers developed polyacrylate based hydrogels to be used for EEG measurements which can record upto 8 hours.[7] Although there is a certain improvement in the recording period with the new hydrogel system, the stability of the aqueous based electrolyte is still a problem when long-term measurements are required.

All these factors reveal that currently used cutaneous electrodes present shortcomings for long-term recordings. Hence, there is a thriving interest to develop new electrolyte systems with low evaporation rates to be used in electrodes aimed for long-term cutaneous recordings.

As explained in detail in the previous chapters, ionic liquids (ILs) are ionic compounds with a negligible vapor pressure and evaporation rate.[8] Such liquids integrated in a gel matrix allow to overcome ambient stability limitations of the actual electrolyte systems used for electrophysiological recordings.[9] In a recent study, Leleux and coworkers showed that organic conjugated polymers can be used as conductive layer on the electrode to decrease the skin-electrode impedance.[10] Following this discovery, the potential of an ion gel or ionic liquid gel assisted PEDOT:PSS electrodes has been successfully demonstrated in cutaneous applications underlying their high performance compared to commercial electrodes with an aqueous-based gel.[9] In this study, Leleux et. al. produced ion gels based on 1-ethyl-3-methylimidazolium ethyl sulfate ionic

liquid and poly(ethylene oxide). These ion gels showed low impedance values over skin and allowed performing the measurements upto 72 hours.

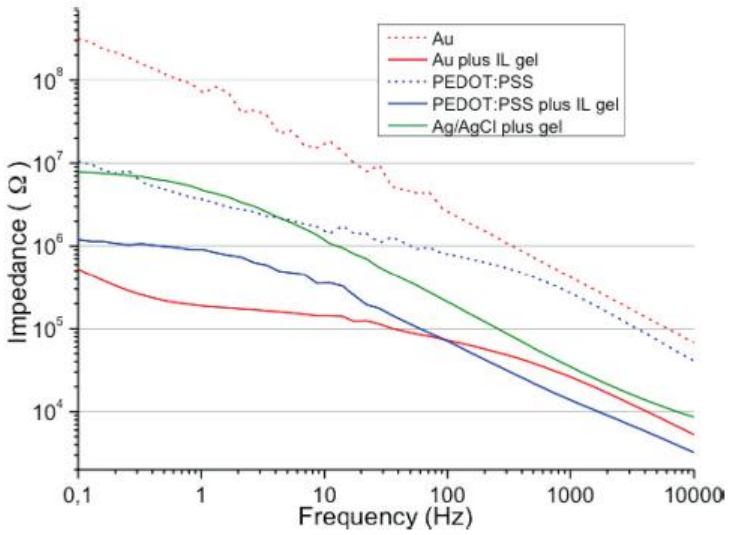

Figure 4.1. Impedance spectra of electrodes over skin. Red curve represents the ion gel based electrode (9)

The reported ion gel was based on 1-ethyl-3-methylimidazolium ethyl sulfate ionic liquid formulated within a poly(ethylene glycol) diacrylate network. The ion gel coating on the electrode allowed to obtain the lowest impedance compared to the bare electrode coated with gold or PEDOT. This discovery opened new opportunities to use ion gel technology in bioelectronics to achieve device performances that cannot be achieved with the conventional technologies.

Chapter 4

Although ionic liquids were initially defined as green solvents, one of the most actual concerns regarding ionic liquids is their toxicology.[11] It is widely accepted that among all the different types of ionic liquids some of them are toxic and hence should not be released to the environment while some others not.[12] Cholinium cation based ionic liquids are known also as bioionic liquids due to their biocompatibility, biodegradability and low toxicity[13,14], as discussed more in detail in chapter 2, which makes them good candidates for bioapplications. Also in chapter 2, we have shown as a preliminary study that the cholinium based ionic liquid monomers and ionic liquids can be used for the preparation of ion gels.

In this work, we focused on the preparation of ion gels based on cholinium ionic liquids and ionic liquid monomers and their use as solid electrolytes in cutaneous electrophysiology. The prepared ion gels are incorporated onto electrodes to lower skin-electrode impedance and perform during long time. Ion gels were obtained by confining cholinium ionic liquid into the crosslinked network of poly(ionic liquid) network prepared by photopolymerization. Various properties such as thermal, electrical and rheological were studied by varying the amount of free ionic liquid in the ion gels. These ion gels were deposited onto the PEDOT:PSS based electrodes and their long-term recording perfomances over skin were investigated.

4.2. Experimental

4.2.1. Materials

2-Dimethylaminoethyl methacrylate (98%, Aldrich), 2-bromoethanol (95%, Aldrich), cholinium hydroxide (80% by weight in methanol, Aldrich), lactic acid (85% solution in H_2O, Aldrich), 2-hydroxy-2-methyl propiophenone (97%, Aldrich), ethyl acetate (99.5%, Aldrich), methanol (99%, Aldrich) were all reagent grade and used without further purification.

4.2.2. Monomer and ionic liquid synthesis

2-cholinium lactate methacrylate ionic liquid monomer and cholinium lactate ionic liquid were synthesized as previously described in chapter 2. The ^1H NMR spectra of the monomer and the ionic liquid are provided below.

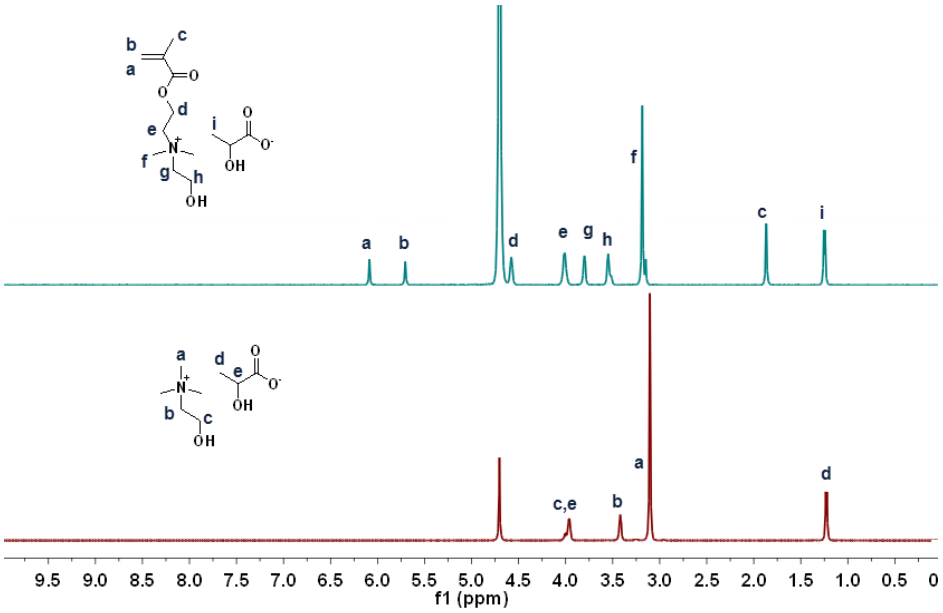

Figure 4.2. ^{1}H NMR spectra of the ionic liquid monomer (top) and the ionic liquid (bottom) (D_2O)

4.2.3. Preparation of ion gels

To prepare the ion gels containing different amounts of free ionic liquid inside, calculated amount of ionic liquid monomer and ionic liquid were mixed in a vial. Ethylene glycol dimethacrylate (3 wt % with respect to the monomer) crosslinker was added together with the photoinitiator (1.5 wt% with respect to the monomer) before exposure to UV light. Dymax UVC-5 conveyor belt system with 800 $mWcm^2$ intensity operating at a wavelength of 365 nm was used for photopolymerization. Sample to lamp distance was 10 mm and the belt speed was fixed at 1

m/min. 5 repetitive cycles were applied to achieve a full polymerization. The final mixture was casted into a mold and photopolymerized. The resulting ion gels were removed from the molds and characterized.

4.2.4. Preparation of electrode and ECG measurements

Electrodes were made according to the previously developed protocol described by Leleux et al.[15] Briefly, we used a laser-cut plastic polyimide (Kapton HN) electrodes with a thickness of 125 mm and an active area of 0.5 cm square. 10 nm of chromium and 100 nm of gold were evaporated on the Kapton electrode. The electrode active area was then coated by drop casting with 5 mL of a solution of poly(3,4-ethylenedioxythiophene) doped with poly(styrene sulfonate) (PEDOT:PSS) from (Clevios PH-1000 from Heraeus Holding GmbH). PEDOT:PSS was mixed with ethylene glycol (from Sigma-Aldrich), 4-dodecylbenzenesulfonic acid (Sigma Aldrich), and 3-methacryloxy propyltrimethoxysilane (Sigma Aldrich) with a ratio of 8/2/0.004/0.1 ,respectively to improve both conductivity, surface energy and surface adhesion. 15 mL of cholinium ion gel solution mixed with the photoinitiator were deposited on top of the PEDOT:PSS layer of 0.5 cm^2 (size of the recording area) and UV cured until the full polymerization, as described above. The resulting layer of ion gel was around 2 mm thick. The connection was added at the other end of the electrode using a

snap button and the insulation was made using a protective paint. The electrodes were characterized accordingly to the ANSI/AAMI EC12:2000/(R) 2005 norm: AC impedance and DC offset voltage are 300 Ω and 25.4 mV, respectively. The skin impedance spectra were acquired using a potentiostat (Autolab equipped with FRA module, Metrohm B.V.), using a 3 electrodes configuration. Two electrodes, working and counter, were placed 2 cm apart from each other on the forearm and a third one, called reference electrode, was located 30 cm away.[16] ECG recordings were performed by placing one electrode on each wrist of a healthy volunteer to form a bipolar Limb Lead I derivation, one of the 12 ECG lead configurations used in clinics.[17,18] To avoid any loose of contact due to the possible mechanical displacement of the electrode connected to electrical wires during long-term evaluations, the electrodes were fixed to the skin with 3 M Steri-Strip and a protective bandage was rolled around each wrist. The ECG was then recorded for 48 seconds several times a day during 72 hours. The CardioTOMM acquisition system was provided by Microvitae Technologies. Signals were then filtered and processed by LabVIEW software using a standard wavelet approach.

4.2.5. Characterization

The ^{1}H NMR measurements were carried out on a Bruker AC-400 instrument with the following experimental conditions: spectral width 20 ppm with 32 K data points, flip angle 90, relaxation delay of 1 s, digital resolution of 0.24 Hz/pt. Thermogravimetric analysis (TGA) was performed by using a TA instruments Q500 device. The samples were heated from room temperature to 800 ºC with a heating rate of 10 ºC min^{-1} under air. Differential scanning calorimetry (DSC) experiments were performed on a TA Instruments Q2000. The sample materials were enclosed in non-recyclable aluminium hermetic pans, the sample masses being in the range of 5–10 mg. The samples were first heated to 150 ºC with a heating rate of 10 ºC min^{-1} and kept isothermal for 5 minutes. The samples were then cooled down to -80 ºC with a cooling rate of 10 ºC min^{-1} and kept isothermal for 5 minutes. Second run heating cycles were taken and analyzed for the detection of the glass transition temperature of the ion gels. Rheology measurements on the prepared ion gels were conducted on a Thermo-Haake Rheostress I viscoelastometer using oscillatory tests. Angular frequency sweeps from 0.01 to 100 rad s^{-1} at constant strain amplitude (g = 0.005) were applied at 25 ºC. G' and G'' values were plotted versus angular frequency. Attenuated Total Reflection Fourier Transform Infrared Spectroscopy (ATR-FTIR) was performed to confirm the success of the photopolymer-

ization. Spectra were recorded on Bruker ALPHA-P equipment from 350 cm^{-1} to 4000 cm^{-1} with a resolution of 2 cm^{-1}. Ionic conductivities (σ) of ion gels at different temperatures were obtained by Electrochemical Impedance Spectroscopy (EIS) using a Bio-logic VMP3 multichannel potentiostatic-galvanostatic system equipped with an impedance module. The experiment was performed using a 2-electrode Swageloks cell in which a coin-like shape membrane was sandwiched in between two stainless steel pistons. Samples were exposed to different temperature in an environmental chamber (BINDER, Model MK 53 (E2)) interfaced with APTCOM3 software. Each temperature was stabilized for at least 1 h before each measurement. The frequency range was varied from 1 MHz to 10 MHz at the bias voltage of 0 V with potential amplitude of 10 mV. Ionic conductivity (σ) for each temperature was calculated using the following expression; $\sigma\ (S\ cm^{-1}) = t/R \times A$, where, t is the thickness of the membrane (cm), A is geometrical area of the membrane (cm^2) and R is the resistance calculated by the intercept of the curve with the real axis on a Nyquist plot (Ω). To observe the percent weight gain due to environmental humidity, the ion gels were left at ambient temperature (24 °C) having relative humidity values between 60-70%. The water uptake was evaluated gravimetrically over 80 hours.

Chapter 4

4.3. Results and Discussion

4.3.1. Preparation of ion gels

Ion gels are materials that are formed by electrolytes. In terms of structure, they are similar to hydrogels, but the water in hydrogels is replaced by a nonflammable and nonvolatile ionic liquid. As explained in the chapter 1, ion gels can be prepared by using many different matrices such as polysaccharides, polyethylene oxide, poly(ionic liquid)s or inorganic siloxane networks. However, poly(ionic liquid)s are preferred due to their excellent compatibility with the free ionic liquid through strong Coulombic interactions preventing the leakage of the ionic liquid. In this work, ion gels were prepared through photopolymerization of the 2-cholinium lactate methacrylate ionic liquid monomer with the cholinium lactate ionic liquid containing small amount of a crosslinker. The amount of free ionic liquid was varied from 0 wt% to 60 wt%. The general procedure for the preparation of ion gels is depicted in the scheme below.

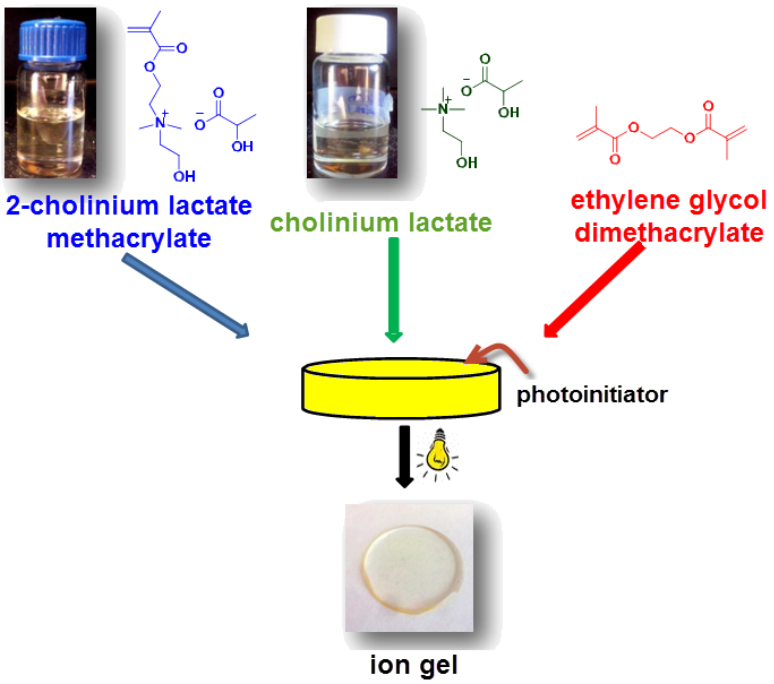

Scheme 4.1. General procedure for the preparation of cholinium based ion gels

The ion gels were coded as IG-0, IG-10, IG-20, IG-30, IG-40, IG-50 and IG-60 where the number represents the weight percent of the free ionic liquid. Photopolymerization is a common technique to produce polymers at room temperature and short reaction times allowing rapid manufacture of materials. Therefore, all ion gels were prepared in less than 2 minutes by using a UV-light curing conveyor belt system. One of the important parameters regarding the synthetic reproducibility and proper design of ion gels through photopolymerization is the conversion

of the monomer to form the polymer matrix. Uncontrolled polymerization will yield non-reproducible ion gels which will result in gels with incoherent properties. The conversion of the polymerization was controlled by ^{1}H NMR and ATR-FTIR spectroscopy. The crosslinked structures of ion gels prevent their dissolution and make it impossible to obtain direct ^{1}H NMR spectra from solution. Therefore, to evaluate non-polymerized content of the monomer, the ion gels were immersed into D_2O for 1 day. The soluble fraction was then analyzed by ^{1}H NMR spectroscopy. Since the 2-cholinium lactate methacrylate monomer is highly water soluble, any unreacted monomer will dissolve in the aqueous phase. The resulting signals are given in the following figure.

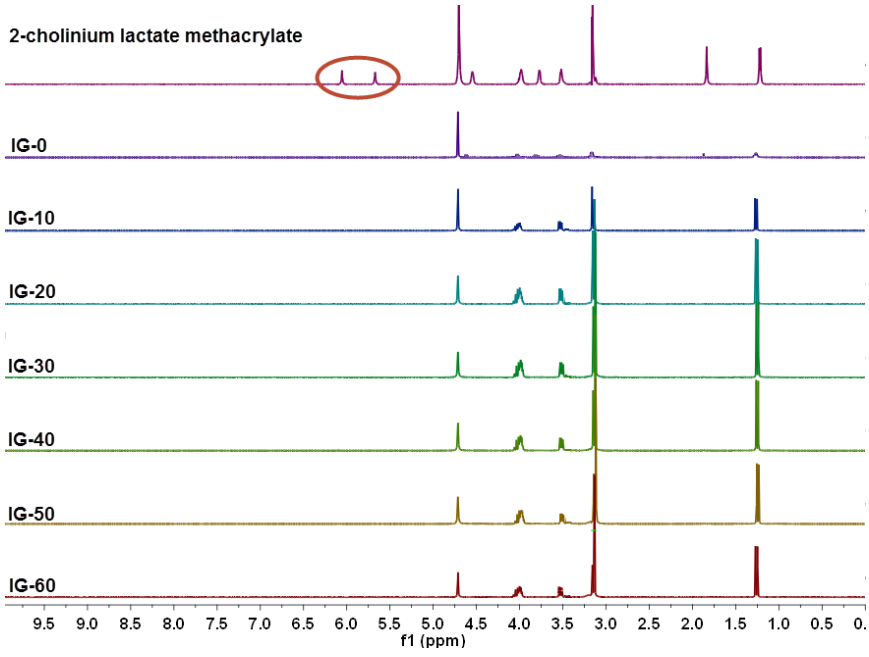

Figure 4.3. ^{1}H NMR spectra of extracted part of the ion gels in D_2O

As it can be seen from the figure 4.3 the signals associated with the reactive methacrylic group disappeared for all the ion gel compositions after exposure to UV light indicating the complete photopolymerization of the monomer.

The further studies using ATR-FTIR spectroscopy affirm the full conversion of the monomer in solid ion gel samples. The spectra are provided below.

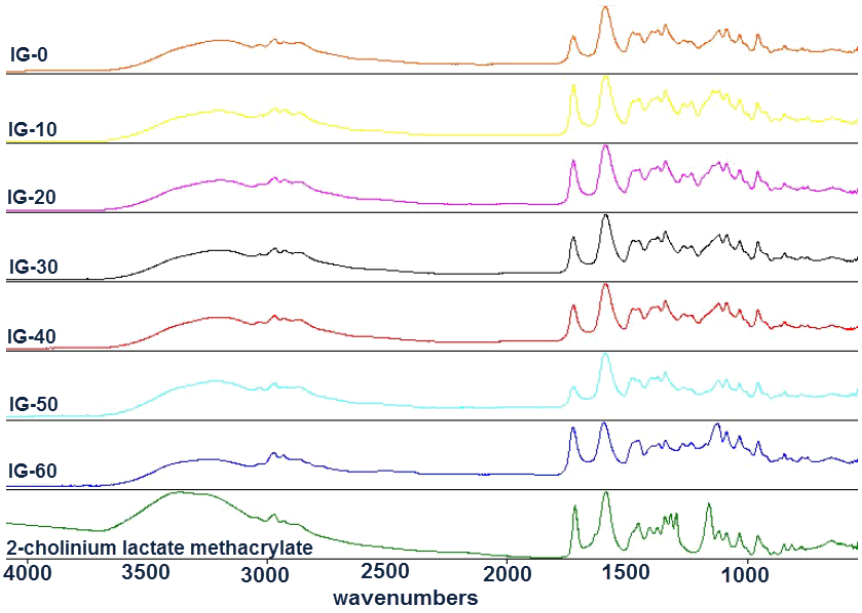

Figure 4.4. ATR-FTIR spectra of the ion gels from 400 to 4000 cm^{-1}

The O-H stretching associated with both monomer and the ionic liquid is observed between 3100 cm^{-1} and 3600 cm^{-1} as a broad signal. The C=O stretching was observed at around 1720 cm^{-1} for all the ion gel samples associated with carboxyl group in the ionic liquid monomer cation. The strong signal having a maxima at 1590 cm^{-1} assigned to the C=O stretching of the carboxylate associated with the lactate anion present in both monomer and the ionic liquid. The C=C stretching signal associated with the reactive monomer group was observed at 1635 cm^{-1}. This region is magnified and given in the following figure.

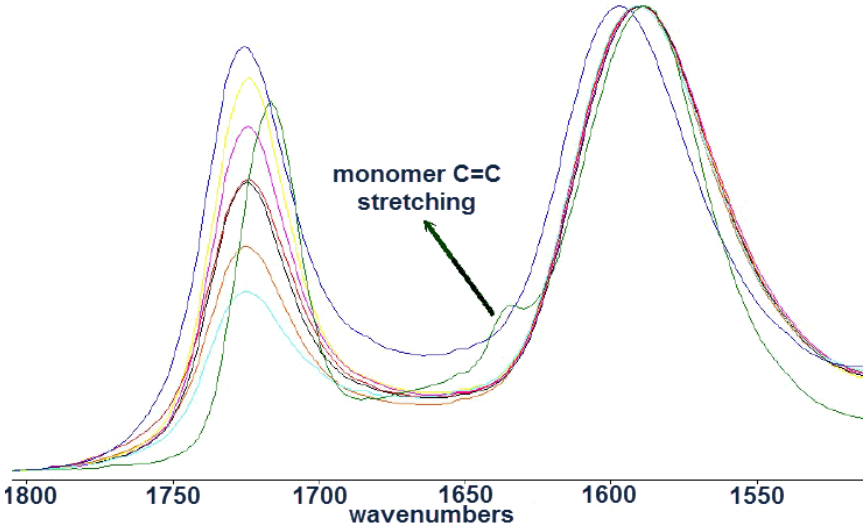

Figure 4.5. ATR-FTIR spectra of ion gels 1500-1800 cm^{-1}

The C=C stretching signals were disappeared for all the ion gels samples. This indicates that the photopolymerization of the ionic liquid monomer to form the polymer matrix was successfully performed.

4.3.2. Rheological properties of ion gels

The mechanical properties of ion gels are one of the most important properties for their practical application as part of the electrode in contact with the skin. This interface has to be soft to conform well with the skin surface and hair, flexible to absorb the encountered mechanical shocks. Therefore, rheological properties of the ion gels were analyzed

by frequency sweep measurements. Elastic (G') and viscous (G'') moduli of the ion gels were examined as a function of angular frequency at 25 ºC. The resulting profiles are provided in the following figure.

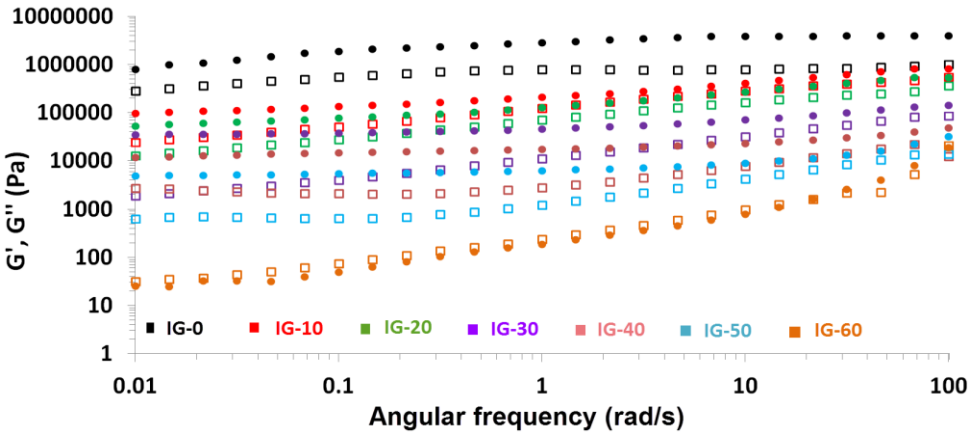

Figure 4.6. Frequency dependence of dynamic storage (G') (circular symbols) and loss (G'') (square symbols) moduli of the ion gels

Ideal gels display almost purely elastic response where the elastic modulus is higher than the viscous modulus and is independent of angular frequency. For the sample that does not contain any free IL (IG-0), highest elastic modulus (G') was obtained which is around 4.08 MPa and is approximately four times greater than the loss modulus (G'') throughout the entire frequency range. Both G' and G'' were frequency independent until 1 rad s^{-1} and after there was a very weak dependency. This confirms that the sample was a gel network of rubbery nature. As expected, introduction of free ionic liquid into the polymer network acts

as plasticizer and reduces the mechanical strength of the ion gels as revealed by the decreased G' and G'' values. With the introduction of 10% IL into the structure, the G' value decreased to 0.83 MPa at 100 rad s^{-1}. The G'' was lower than G' over the entire angular frequency range and both moduli were slightly frequency dependent indicating that the material behaves as a soft solid material. Although increasing the IL content further reduced the elastic modulus down to 0.55 MPa, G'' was lower than the G' over the entire angular frequency range and dependence of both moduli was similar to the previous formulation indicating a soft solid ion gel. The gradual decrease of both moduli was observed while increasing free IL content in the ion gel formulations. All the ion gels until 50% IL displayed similar frequency behaviour over the entire measured angular frequency range. In all cases, the elastic moduli of the ion gels were higher than loss moduli suggesting that the elastic components of the dynamic moduli were greater. The ion gel IG-60 is the sample that contains the highest amount of free IL and displayed the lowest mechanical property relative to the samples containing less IL. At high angular frequencies, the G' and G'' values were almost the same around 0.02 MPa. The G'' became higher than G' over the entire lower angular frequency range and both moduli were frequency dependent indicating that the sample was a pregel. These findings indicated the gel type behaviour of the ion gels due to the crosslinked poly(ionic liquid) matrix

blended with ionic liquid. In conclusion, these cholinium ion gels presented soft solid and elastic behaviours which are ideal mechanical properties for the application as cutaneous electrodes.

4.3.3. Thermal properties of the ion gels

Thermal properties of the ion gels were analyzed by differential scanning calorimetry (DSC) and thermogravimetric analysis (TGA). DSC signals are provided in the following figure.

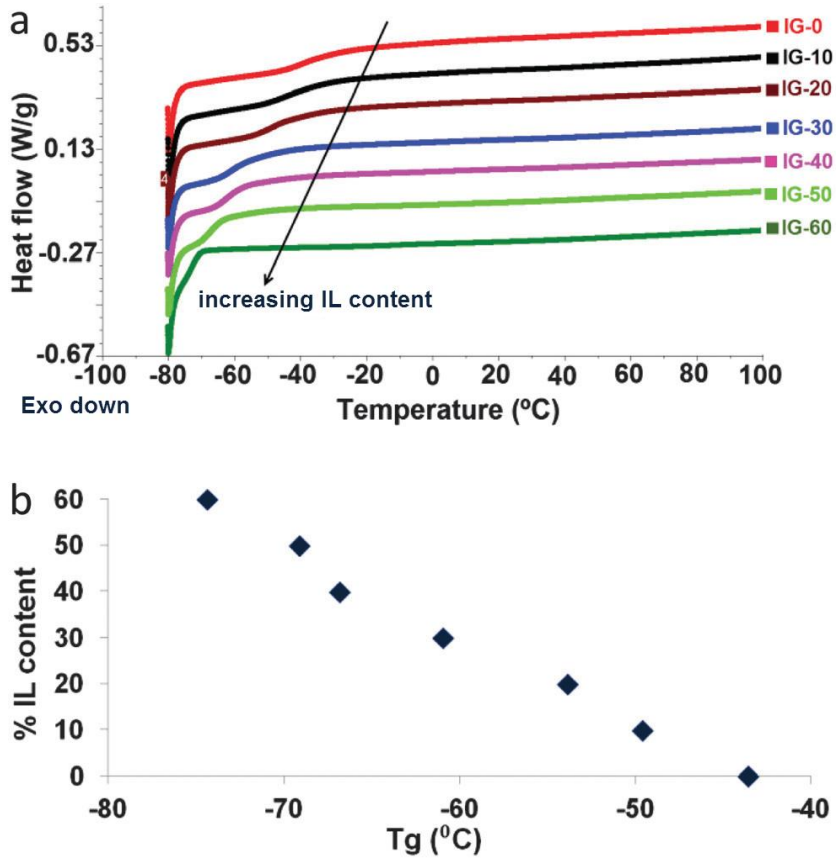

Figure 4.7. (a) Differential scanning calorimetry (DSC) curves of the ion gels containing different amounts of IL. (b) Glass transition temperature change vs. free ionic liquid %.

The glass transition temperature (T_g) of the homopolymer of 2-cholinium lactate methacrylate is around -50 ºC. Similarly, DSC analysis of the sample IG-0 revealed a T_g around -40 ºC which is slightly higher due to the crosslinked nature of the sample. Introduction of free IL acts

as a plasticizer to the polymer matrix decreasing the T_g of the ion gel. Therefore, T_g values gradually decrease with the increasing IL content. The lowest glass transition being found around -70 ºC for IG-60 in which 60% free IL content was blended. Additionally, the change in the glass transition temperature with changing ionic liquid content is provided in figure 4.7b. As clearly seen from the figure, addition of ionic liquid plasticizes the material resulting in a gradual decrease of the glass transition temperature with increasing amount of free ionic liquid in the polymeric matrix. Low T_g behaviour of ion gels provides a broad operational window from -70 ºC to higher temperatures.

To determine the thermal stability of ion gels, TGA measurements were carried out. The TGA signals are provided in figure 4.8. As reported in literature, cholinium based ionic liquids display onset temperatures starting from 170 ºC.[14] For the ion gels composed of cholinium cation combined with lactate anion, the trend observed for the thermal stabilities were similar to the glass transition temperatures.

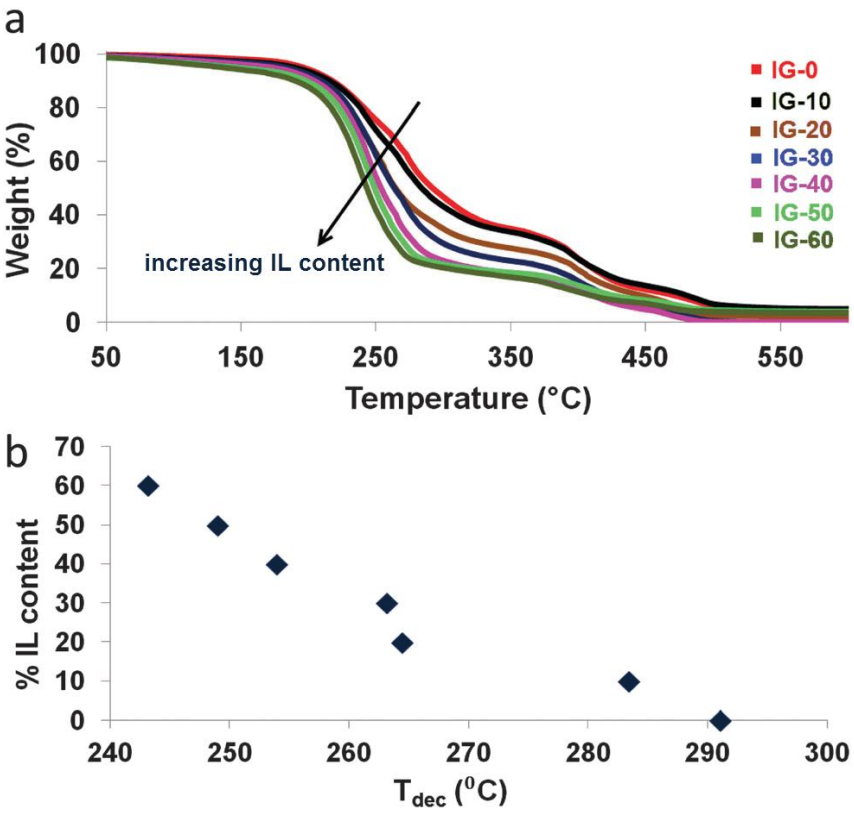

Figure 4.8. (a) TGA profiles of the ion gels. (b) Decomposition temperature vs. free IL content in the gels (the temperature at which 50% weight loss was observed and was taken as the decomposition temperature).

Although the onset temperatures were similar to each other for all the ion gel formulations at around 180 ºC, the weight loss after that point were distinctive as it can be seen from the given figure above. Samples containing higher amounts of free IL displayed a sharper weight loss compared to the samples with low IL contents. The sample IG-0 showed

a decomposition temperature (50% weight loss) at 292 ºC and this temperature gradually dropped down to 250 ºC for IG-60. To better demonstrate the change in the decomposition temperature of the ion gels with changing ionic liquid content, figure 4.8b is provided. As clearly seen, introduction of ionic liquid into the solid matrix gradually decreases the decomposition temperature as the amount of ionic liquid increases. This trend is expected since the polymer backbone will provide additional stability to the ion gel and the amount of polymer inside decreases with increasing free ionic liquid amount.

4.3.4. Electrical properties of the ion gels

Due to the presence of the free ionic liquid confined in the polymer matrix, ion gels present higher ionic conductivities than other solid polymer electrolytes.[20] Therefore, the ionic conductivity of an ion gel becomes one of the most characteristic properties and it is usually related to its good performance in the different device application. For this reason, the ionic conductivities of ion gels were determined by impedance spectroscopy from 0 ºC to 110 ºC as shown in figure 4.9.

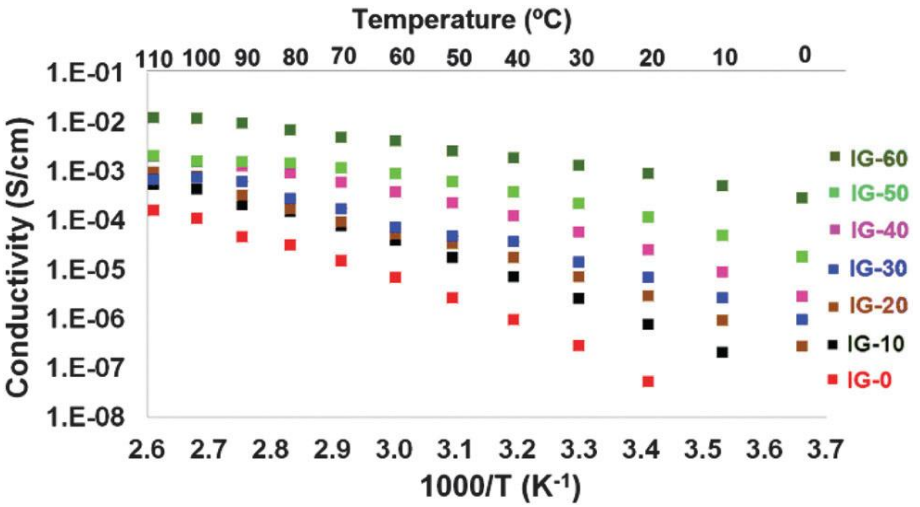

Figure 4.9. Ionic conductivities of ion gels from 0 ºC to 110 ºC

The ionic conductivities change dramatically with the introduction of free ionic liquid and its weight content as expected. The slight curvature observed in the Arrhenius plot is in good accordance with the Vogel–Tamman–Fulcher (VTF) model which is commonly seen in amorphous polymer electrolytes due to the amorphous nature of the polymer matrix. The conductivity values were gradually increasing with the increasing free ionic liquid amount in the ion gel. The ionic conductivity reach values between 10^{-8} S cm^{-1} for the pure poly(ionic liquid) and 10^{-3} S cm^{-1} for ion gels having 60 wt% of free IL. The values range from 10^{-8} S cm^{-1} at 20 ºC to 10^{-4} S cm^{-1} at 110 ºC for the sample that does not contain any free IL. When 20 wt% of cholinium lactate is introduced into the ion gel, the ionic conductivity at 20 ºC was 10^{-6} S cm^{-1} which gradually in-

creased to 10^{-3} S cm^{-1} at 110 ºC. As expected, the highest ionic conductivity values were obtained for the ion gel which contains 60 wt% free ionic liquid IG-60, the values ranging from 10^{-3} S cm^{-1} at 20 ºC to 10^{-2} S cm^{-1} from 20 ºC to 110 ºC, respectively.

4.3.5. Long-term cutaneous recordings

Cholinium ion gels were incorporated onto electrodes made of gold and PEDOT:PSS conducting polymer. The electrodes were made on a thin polyimide film allowing a stable and flexible contact to the skin. The cholinium-based ion gel is then used as the electrolytic interface between the skin and the electrode itself. This interface is an important element in successful transcutaneous signal transduction. Figure 4.10 illustrates the cross section of the electrode.

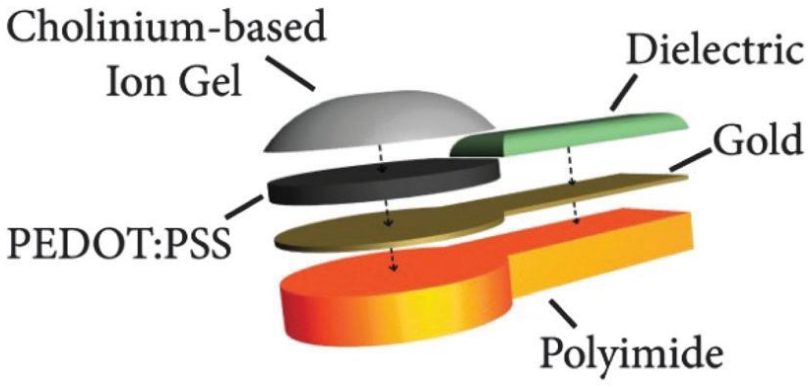

Figure 4.10. Exploded view of the different layers of cutaneous electrode

Polyimide layer allows an easy manipulation of the electrode and its flexibility reduces mechanical stress in wearable conditions (motion, long-term contact etc..). The gold layer offers a good electronic conductivity when PEDOT:PSS layer serves to reduce the electrode contact impedance. Additionally, the PEDOT:PSS layer provides a bifunctional ground to monolithically host ion gel due to its conductive and polymeric nature. In order to compare the performance of these electrodes in cutaneous recordings, we tested the electrode/skin impedance on a healthy volunteer. The electrodes were placed on the subject's arm using a three-electrode configuration, where both counter and reference electrodes were commercial Ag/AgCl electrodes. Figure 4.11 shows typical electrical impedance spectra, both magnitude and phase angle, for the electrodes tested including different ion gels with different free IL contents.

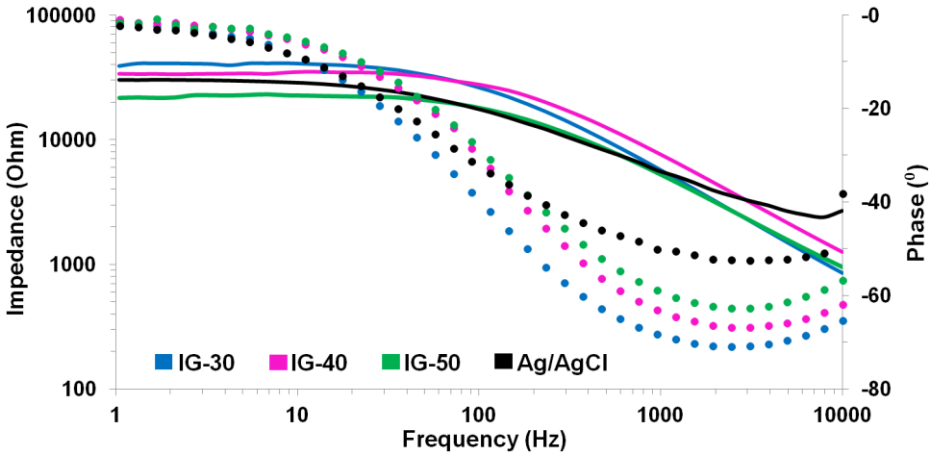

Figure 4.11. Impedance values on skin over frequencies for different ion gels and comparison with a standard medical Ag/AgCl electrode

To record physiological potential variations, a good contact with the skin and low impedance are important to ensure a good ionic/electronic translation. All the tested cholinium ion gels showed good long-term adhesion to the skin. This is an important factor since in long-term recordings the electrodes have to endure some mechanical constraints during movements such as friction and delamination from the skin. Interestingly, impedance values obtained using electrodes containing different cholinium ion gel compositions are comparable to the ones from regular medical electrode, as shown in figure 4.11. Similar to the data presented above the impedance measurements of the ion gels coated electrodes containing different amounts of the free IL displayed a slight decrease of

impedance magnitude at low frequency range with increasing the free IL amount. The phase curves show that ion gel electrodes behave similarly to standard Ag/AgCl electrodes, i.e. their phase shift is close to 0° at low frequencies, as mostly non-polarizable electrodes. The comparison of impedance values with the commercial Ag/AgCl electrode standard indicated that cholinium ion gels can effectively be used in electrophysiological recordings. Although impedance of all gels was comparable to the commercial Ag/AgCl electrode, the lowest impedance was obtained with IG-50 ion gel formulation. This composition presented a good compromise between mechanical properties and ionic conductivity of the material.

It is worth to mention that the ion gels are composed of water soluble ingredients. Therefore, direct exposure of the ion gels to water or excessive sweat will result in loss of gel integrity. However, the exposure of the ion gels to environmental humidity does not affect their integrity. The % weight gain due to moisture uptake was limited up to 4% and did not cause any integrity issues of the gels during the evaluated time period, as shown in figure 4.12.

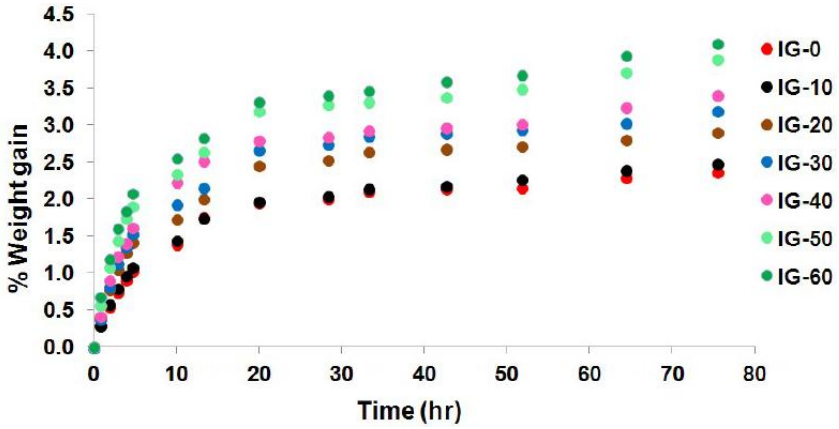

Figure 4.12. The % weight gain of the ion gels when they are left at ambient humidity.

The water uptake from the environment was more important for the ion gels containing higher amount of free ionic liquid. Additionally, the ECG signals recorded during 72 hours did not display any degradation of the signals indicating that the integrity of the ion gel was well preserved upon the exposure to environmental and skin humidity. (figure 4.14)

Different clinical applications cardiac monitoring, nightlong brain activity recordings, prosthesis controlled by muscle activities – require electrodes that can provide a good signal quality for a long period of recording. Most of the current medical electrodes are made with an electrolyte that can dry after a few hours, contrary to ion gels. Dry electrodes were developed in the past decades to overcome limitations related with the gel ambient instabilities.[16,20] However, they usually show high sensi-

tivity to motion artefacts due to the limited conformability to the skin. Recently, highly flexible and extremely conformable nanoscale dry electrodes have been developed by Zucca et al.[21] demonstrating intimate combination of the electrode with skin, repeating its surface topology and showing comparable electrical performance with standard medical ones. The performance of the cholinium ion gel IG-50 was evaluated in cutaneous electrophysiology. Short-term evaluation of this electrode demonstrated similar performance over 3 h of recordings in comparison with medical standard, shown in figure 4.13.

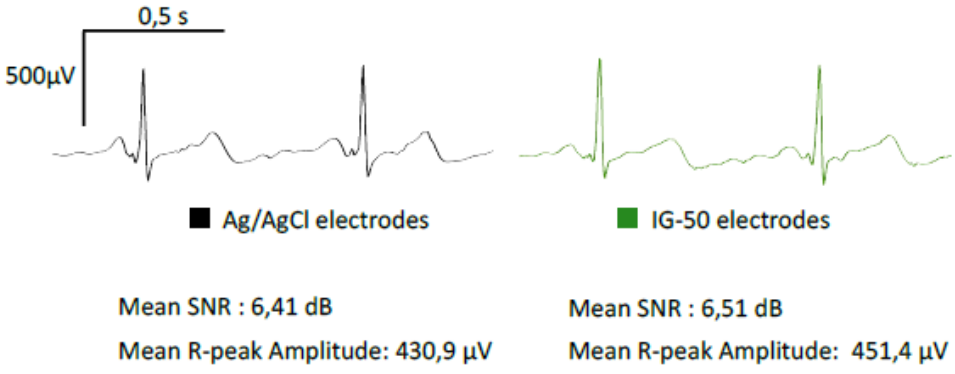

Figure 4.13. Comparison of ECG recording performance: Ag/AgCl medical standard (in Black) vs cholinium ion gel IG-50-assisted (in Green) electrodes. ECG signals were recorded on skin afterward 3h of contact.

To evaluate long-term recording capabilities of IG-50-assisted electrodes, the heart activity was regularly recorded from ion gel-assisted electrodes for 3 days long continuously placed in contact with the skin.

Chapter 4

Electrocardiography is a very common method of monitoring the cardiac function through the electric fields generated by muscular tissues. The progression of cardiac cells depolarization and consecutive muscle contraction throughout the heart give rise to ionic currents that characterize its activity. These small cyclic potential changes are recorded on the skin from electrodes and the signal can be then processed to analyze the different steps of each heart contraction. ECG signals recorded from our electrodes are shown in figure 4.14a.

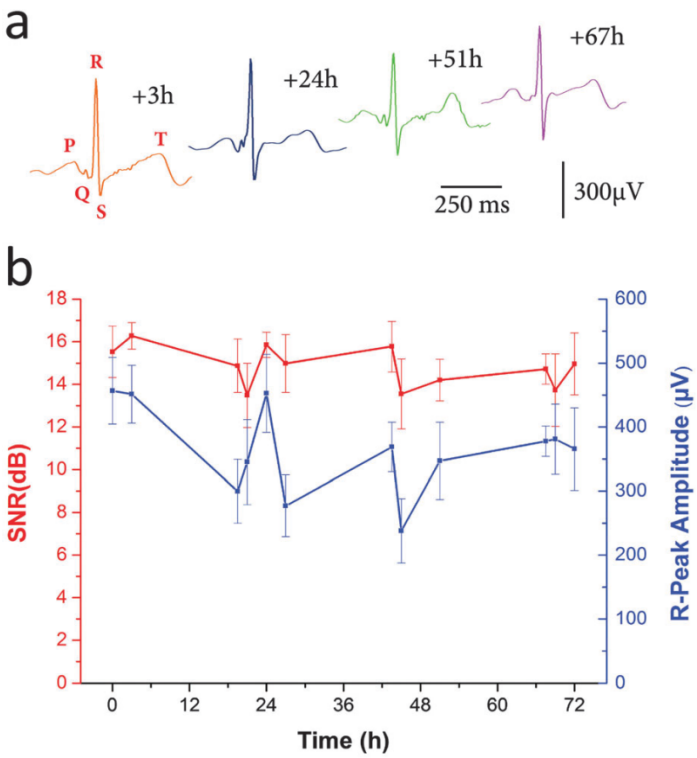

Figure 4.14. Long-term ECG measurement performed with IG-50. (A) ECG signals recorded on skin with highlighted PQRST complexes. (B) Stability of the ECG signals over 72 hours with SNR (red) and R-peaks amplitudes (blue) evolutions.

The PQRST complexes, corresponding to the different depolarization phases of the hearth, can be easily identified. The R peak matches with the main hearth beat and is used to calculate hearth rate in healthcare applications for general public. Cardiologists need to study the intervals between the different waves as well as general features to be able to di-

agnose disorders as ventricular hypertrophy or myocardial infarction. Figure 4.14b shows the evolution of the ECG signal with time. For every measurement Signal-to-Noise Ratio (SNR) was calculated by using the Crest factor, or Peak-to-RMS value, which is the ratio between the R peak amplitude and the RMS value of the signal all along a PQRST complex.[22] The amplitudes of R-peaks over time are also shown. As the recordings were carried out on a person performing regular activities (walking, office working, taking shower. . .) many reasons cause daily variations of SNR and R-peaks amplitudes. The physiological change of the skin impedance, the noise from different electronic sources can interfere with the signal and modify the recording quality. However, the electrodes containing cholinium ion gel allowed obtaining good quality electrophysiological recordings during 72 hours long with the reliable detection of the PQRST cardiac complex.

4.4. Conclusions

New cholinium-based ion gels were synthesized by photopolymerization in less than two minutes. The ion gels showed mechanical properties of an elastic gel soft solid and low glass transition temperatures and thermal stability. As an important property, the ion gels showed values of ionic conductivity values at 20 ºC up to 10^{-3} S cm^{-1}. These properties make the cholinium-based ion gel good candidates to be used as the

electrolytic interface with the skin in transcutaneous electrophysiology. Cholinium ion gels showed good long term adhesion to the skin without any loss of properties caused by the evaporation of the electrolyte in commercial electrodes. Accurate physiologic signals were recorded for a long period of time with a remarkable stability. Due to the recognized low toxicity of cholinium ionic liquids, these ion gels are ideal candidates to assist the long-term cutaneous recordings. However, further evaluations are required to assess the dermotoxicology of the ion gels in clinical applications.

Scientific Contributions

Isik M., Lonjaret T., Sardon H., Marcilla R., Herve T., Malliaras G. G., Ismailova E., Mecerreyes D., *Cholinium-based ion gels as solid electrolytes for long-term cutaneous electrophysiology*, J. Mater. Chem. C., **2015**, 3, 8942.

4.5. References

1- H. Berger , *Arch. Psychiatr. Nervenkr.* 1929, **87**, 527

2- J. M. Gilchrist, *Neurology* 1985 , **35** , 1503 .

3- A. Achaibou, G. Pourtois , S. Schwartz , P. Vuilleumier , Neuropsychologia, 2008 , **46** , 1104 .

4- T. Akerstedt , M. Gillberg , Int. J. Neurosci. 1990 , **52** , 29 .

5- E. T. McAdams, J. Jossinet, A. Lackermeier, and F. Risacher, Med. Biol. Eng. Comput., 1994, **34**, 397–408.

6- L.-D. Liao, I.-J. Wang, S.-F. Chen, J.-Y. Chang and C.-T. Lin, Sensors, 2011, **11**, 5819.

7- N.A. Alba, R. J. Sclabassi, M. Sun and X. T. Sui, IEEE Trans Neural Syst Rehabil Eng, 2010, **18**, 415-421.

8- M. Galinski, A. Lewandowsky and I. Stepniak, Electrochim. Acta, 2006, **51**, 5567.

9- P. Leleux, C. Johnson, X. Strakosas, J. Rivnay, T. Herve, R. M. Owens and G. G. Malliaras, Adv. Healthcare Mater., 2014, **3**, 1377.

10- P. Leleux, J-M. Badier, J. Rivnay, C. Benar, T. Herve, P. Chauvel and G. G. Malliaras, Adv. Healthcare Mater., 2013, **3**, 490-493.

11- T. P. T. Pham, C.-W. Cho and Y.-S. Yun, Water Res., 2010, **44**, 352.

12- S. Stolte, J. Arning, U. Bottin-Weber, A. Muller, W.-R. Pitner, U. Welz-Biermann, B. Jastorff and J. Ranke, Green Chem., 2007, **9**, 760-767; S. Stolte, M. Matzke, J. Arning, A. Boschen, W.-R. Pitner, U. Welz-Biermann, B. Jastorff and J. Ranke, Green Chem., 2007, **9**, 1170–1179.

13- M. Petkovic, J. L. Ferguson, H. Q. N. Gunaratne, R. Ferreira, K. R. Seddon, L. P. N. Rebelo and C. S. Pereira, Green Chem., 2010, **12**, 643.

14- Y. Fukaya, Y. Iizuka, K. Sekikawa and H. Ohno, Green Chem., 2007, **9**, 1155.

15- P. Leleux, J.-M. Badier, J. Rivnay, C. Be´nar, T. Herve´, P. Chauvel and G. G. Malliaras, Adv. Healthcare Mater., 2013, **3**, 490–493.

16- N. Meziane, J. G. Webster, M. Attari and A. J. Nimunkar, Physiol. Meas., 2013, **34**, R47–R69.

17- W. Einthoven, G. Fahr and A. de Waart, Pflu¨ger Arch. ges. Physiol., 2013, **150**, 275–315.

18- A. R. Barens, F. N. Wilson, H. E. B. Pardee, C. C. Wolpferth and P. D. White, Am. Heart J., 1938, **15**, 235–239.

19- A. S. Shaplov, R. Marcilla and D. Mecerreyes, Electrochim. Acta, 2015, DOI: 10.1016/j.electacta.2015.03.038.

20- A. Searle and L. Kirkup, Physiol. Meas., 2000, **21**, 271–283.

21- A. Zucca, C. Cipriani, S. Sudha, S. Tarantino, D. Ricci, V. Mattoli and F. Greco, Adv. Healthcare Mater., 2015, **4**, 941.

22- G. Clifford, F. Azuaje and P. McSharry, Advanced Methods and Tools for ECG Analysis, Artech House Publishing, Boston, London, 2006, p. 384.

5 Innovative Poly(ionic liquid)s by the Polymerization of Deep Eutectic Monomers

Contents

5.1. Introduction……153

5.2. Experimental……...156

5.3. Results and Discussion……160

5.4. Conclusions……..…179

5.5. References…….…..180

Chapter 5

5.1. Introduction

Ionic liquids (ILs) have been investigated as green solvents due to their unique properties such as nonflammability, chemical stability, high solvation capability, and electrical conductivity and most important of all their negligible vapor pressure.[1-2] A subset of ionic liquids is protic ionic liquids which are prepared by combination of a Brønsted acid and a base. Due to their easiness for synthesis, possibility to use cheap and environmentally benign ingredients such as natural carboxylic acids and amines, they have been considered as alternatives to ILs.[3] The search for better alternatives is an everlasting process. For this reason, a third class of ionic liquids named deep eutectic solvents (DESs) emerged as an alternative a few years ago.[4] DESs are molecular complexes formed between quaternary ammonium or phosphonium salts and hydrogen bond donor molecules generally chosen from cheap and safe components. The salt acts as the hydrogen bond acceptor to self-associate with the donor molecule to form the DES via hydrogen bonding. The hydrogen bonding formed between the halide anion of the salt and the hydrogen bond donor molecule causes charge delocalization to occur. This strong interaction is responsible for the decrease of the freezing point of the mixture relative to the melting points of the individual components used for the formation of the DES. DESs possess many common properties with the conventional ionic liquids. As compared to

common solvents, DESs are nonvolatile, nonflammable and easy to scale up since no purification is required and synthesis is 100% atom economic making them attractive in large scale industrial applications.[5,6] The very first report about eutectic mixtures of pyridinium halides with metal halides dates back to 1950s.[7] These eutectic mixtures contain complex chloroaluminate which are large and hence reducing the charge density. In 2002, Abbott and coworkers discovered that the trimethylethanolammonium chloride (choline chloride) urea mixtures form deep eutectic solvents and possess ionic liquid like properties.[8] Following this discovery, cheap deep eutectic solvents formed between choline chloride and natural carboxylic acids are reported as versatile alternatives to ionic liquids.[4] These DESs have been deeply investigated by different groups and proposed for many different applications where ionic liquids or conventional organic solvents are used.[9] Among these applications, CO2 capture,[10] metal oxide solubilization,[11] drug solubilization,[12] purification,[13] catalysis,[14] electrodeposition,[15] material preparation[16] and biopolymer processing[17] can be given as examples. The use of DES in polymer science is a relatively unexplored topic. In some pioneering works, Morales and coworkers used deep eutectic systems for the frontal polymerization of acrylic monomers. DES were formed between choline chloride and acrylic acid (AA) or methacrylic acid (MAA) monomers[18,19] DES assisted frontal polymerization of the monomer was

conducted by heating and choline chloride was recovered from the system upon the termination of the polymerization reaction allowing recycling of one component and reutilizing. Another example to use of DES systems in polymer synthesis is the work of Serrano and coworkers for the synthesis of polyesters assisted by DES.[20,21] Here, DESs were formed between quaternary ammonium and phosphonium salts with octanediol. Upon the formation of the DES, citric acid was dissolved in the preformed mixture and the reaction was conducted at 80 ºC for upto 20 days until the completion of the reaction. The DES assisted synthesis strategy was also used for the synthesis of crosslinked resorcinol-formaldehyde thermosets for carbonization leading to monolithic carbons.[22,23] To summarize the previous examples, DESs have been used so far in polymer science as solvents and functional additives. In this paper we show that the DES strategy can be used for the preparation of new ionic liquid monomers and poly(ionic liquid)s. Thus, we introduce a new concept ‘deep eutectic monomers’ (DEMs) as cheap chemicals to develop innovative poly(ionic liquids). In this work, DEMs were easily prepared by mixing quaternary ammonium monomers and various hydrogen bond donors. As a starting point, we have selected 2-cholinium bromide methacrylate and tri- and tetra-ol ammonium bromides as the quaternary ammonium monomers and N'-hydroxy-2-methylpropanimidamide (amidoxime), citric acid and terephthalic acid as

hydrogen bond donors to prepare DEMs. As an advantage, the formation of liquid monomers allowed the use of mild photopolymerization and polycondensation polymerizations to synthesize new polymeric materials. The potential to use these materials as solid sorbents for carbon dioxide capture was investigated.

5.2. Experimental

5.2.1. Materials

2-dimethylaminoethylmethacrylate (Aldrich), 2-bromoethanol (Aldrich), citric acid (CA) (Aldrich), terephthalic acid (TA) (Aldrich), 2-hydroxy-2-methylpropiophenone (Aldrich), triethanolamine (Acros), 2-bromoethane (Acros), N'-hydroxy-2-methylpropanimidamide (Amidoxime) (Acros) , ethylacetate (Aldrich), methanol (Aldrich) and acetone (Aldrich) were obtained as high purity reagent grade chemicals and used without further purification.

5.2.2. Preparation of quaternary ammonium compounds

Three different quaternary ammonium compounds were prepared. The detailed synthesis for 2-cholinium bromide methacrylate (ChBr) is provided elsewhere.[24] Typically, 2-dimethylaminoethylmethacrylate monomer was quaternized by using 2-bromoethanol to yield the desired compound. In a similar manner, the preparation of quaternary ammoni-

um alcohols was performed. Triethanolamine was quaternized by using either 2-bromoethanol or 2-bromoethane to synthesize tetrakis(2-hydroxyethyl)ammonium bromide (tetraol) or N-ethyl-2-hydroxy-N,N-bis(2-hydroxyethyl)ethanaminium bromide (triol) compounds, respectively. In a typical reaction, calculated amount of triethanolamine was charged into a reaction vessel and calculated amount of the quaternization agent was introduced dropwise over the triethanolamine at room temperature at bulk. After the addition of the whole reagent, the reaction mixture was heated upto 50 ºC under magnetic stirring. The reactions were conducted for 24 hours and the products were obtained as solid. The crude product was dissolved in minimum amount of methanol and precipitated in large excess of ethylacetate to get rid of any unreacted chemical. The precipitates were washed thoroughly 3 times and dried under vacuum at 40 ºC. The final compounds were obtained as white powders in high yields.

5.2.3. Preparation of deep eutectic monomers

Deep eutectic monomers were prepared by simple mixing of the ingredients in a vial. In a typical procedure for the DEMs based on 2-cholinium bromide methacrylate monomer, calculated amount of quaternary ammonium monomer was mixed with calculated amount of carboxylic acid. To homogenize the ingredients, small amount of methanol

was dropped into the mixture and agitated with a magnetic bar. Pressurized air was applied onto the mixture to remove the solvent and the corresponding DEM was obtained as a liquid. The DEM was dried further under vacuum at room temperature. The DEMs composed of tetraol, triol and carboxylic acids were prepared similarly by mixing the ingredients. Calculated amount of quaternary ammonium alcohol was mixed with the desired carboxylic acid and the mixture was placed into an oven at 50 ºC to yield a DEM which is liquid at room temperature. The resulting DEMs were used without further purification. All the DEMs were characterized by means of differential scanning calorimetry, NMR and FTIR to confirm the formation of the deep eutectic monomers.

5.2.4. Characterization

The NMR measurements were carried out on a Bruker AC-300 (for ^{1}H NMR) instrument with the following experimental conditions: spectral width 15 ppm with 32 K data points, flip angle 90, relaxation delay of 1 s, digital resolution of 0.24 Hz/pt. Solid state NMR spectra were recorded on a Bruker 400 AVANCE III WB spectrometer 9.40T. ^{13}C CP/MAS NMR spectra were collected using a 4mmMASDVT probe at a spinning of 12 KHz, using the cross polarization pulse sequence, at 100.63 MHz, a time domain of 2K, a spectral width of 29 KHz, a contact time of 1.5ms and an interpulse delay of 5s. Thermogravimetric analysis (TGA) was

performed by using a TA instruments Q500 device. The samples were heated from 40 ºC to 800 ºC with a heating rate of 10 ºC/min under nitrogen gas flow. Differential scanning calorimetry experiments were performed on a TA instruments Q200. The sample materials were enclosed in nonrecyclable aluminium hermetic pans, the sample masses being around 5-10 mg. The samples were first equilibrated at 0 ºC and heated with a heating rate of 10 ºC/min and kept isothermal for 5 minutes to erase the thermal history. Then cooled down to -80 ºC and kept isothermal for 5 minutes. The samples then heated to the desired temperature with a heating rate of 10 ºC/min and the 2nd heating cycles were taken for the detection of the glass transition temperatures. Attenuated Total Reflection Fourier Transform Infrared Spectroscopy (ATR-FTIR) was performed on Bruker ALPHA-P equipment. The spectra were recorded from 350 cm^{-1} to 4000 cm^{-1} with a resolution of 2 cm^{-1} and 24 scans were taken for each spectrum. Dymax UVC-5 conveyor belt system with 800 mW/cm^2 intensity operating at a wavelength of 365 nm was used for photopolymerization. Sample to lamp distance was 100 mm and the belt speed was fixed at 2 m/min. 5 repetitive cycles were applied to achieve a full photopolymerization. CO_2 adsorption at 0 °C was measured in a Quantachrome Nova 4200e static volumetric analyzer. Prior to the analysis, samples were outgassed at 25 °C for 36 h.

The narrow micropore volume (Vn) was calculated by applying the Dubinin–Radushkevitch equation to the CO_2 adsorption isotherm at 0 °C.

5.3. Results and Discussion

5.3.1. Deep eutectic monomer preparation

The synthesis and preparation of the quaternary ammonium compounds used for the DEM preparation is depicted in figure 5.1 together with the NMR signals associated with the compounds.

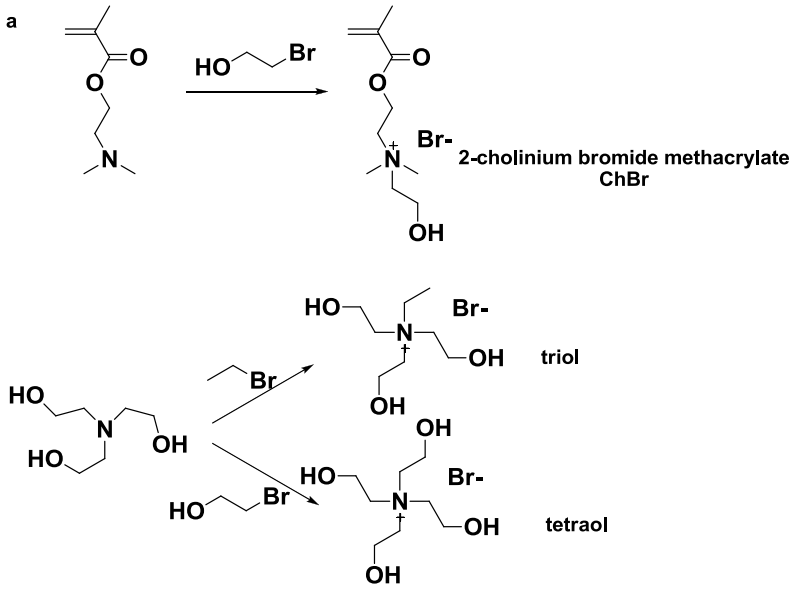

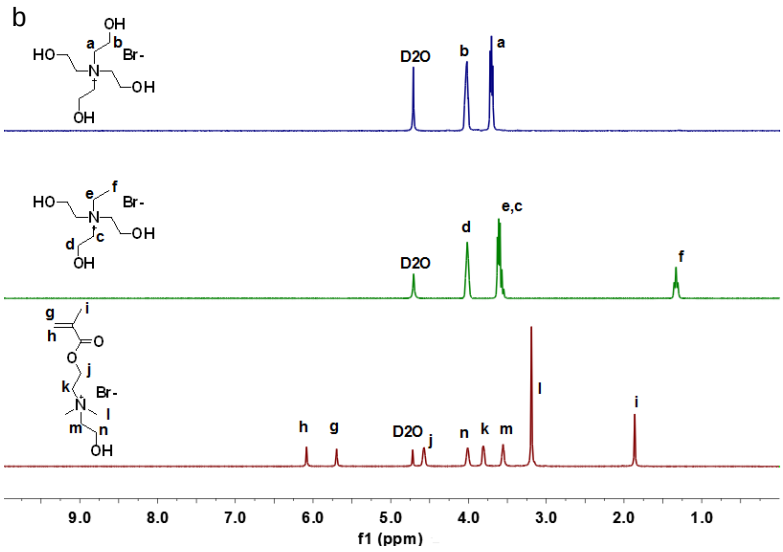

Figure 5.1. a) Synthesis of the quaternary ammonium compounds and b) the corresponding ^{1}H NMR spectra (300 MHz)

Deep eutectic monomers with 2-cholinium bromide methacrylate (ChBr) were prepared through simple blending of the components at room temperature. In a typical preparation, desired amount of the quaternary ammonium component was mixed with the calculated amount of the hydrogen bond donor. To be able to homogenize the ingredients, minimum amount of methanol is added under agitation. The components were mixed thoroughly and the solvent was evaporated by pressurized air. Upon the removal of the methanol, the DEM was obtained as a viscous liquid at room temperature (figure 5.2). The sample was then dried further under reduced pressure at room temperature. The DEMs prepared by using quaternary ammonium alcohols (triol and tetraol) (figure 5.2)

were prepared by heating the DEM mixture at 50 ºC in bulk. As mentioned earlier, quaternary ammonium compounds and different hydrogen bond donor molecules have been used to prepare the desired DEMs. The chemical structures of the compounds used for the preparation are given in the figure below.

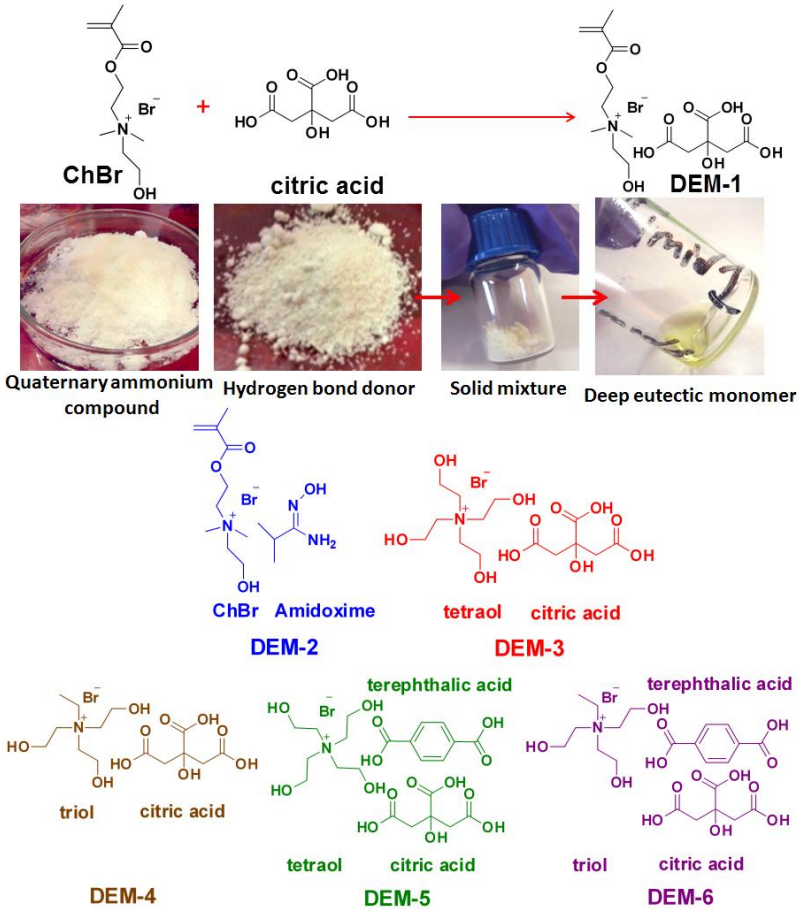

Figure 5.2. DEM preparation depicted and the structures of the chemicals used for DEM preparation

The formation of the DEM was first confirmed visually upon the formation of a homogeneous liquid at room temperature as depicted in figure 5.2. DEMs having different compositions were prepared. The compositions of the DEMs and their properties are given in the table below.

Table 5.1. Deep eutectic monomers prepared and their properties

Code	Composition	Ratio (mol/mol)	T_g[a] (°C)	T_m[b] (°C)	T_m[c] (°C)
DEM-1	ChBr/Citric acid	1.0/1.0	-40	153	90.5
DEM-2	ChBr/Amidoxime	1.0/1.0	-54	61	90.5
DEM-3	Tetraol/Citric acid	3.0/4.0	-26.5	153	40.3
DEM-4	Triol/Citric acid	1.0/1.0	-30.2	153	60.0
DEM-5	Tetraol/Citric acid/terephthalic acid	3.0/2.5/2.0	-28.7	153/300	40.3
DEM-6	Triol/Citric acid/terephthalic acid	4.0/2.5/2.0	-47.9	153/300	60.0

[a]Extracted data from DSC measurements, [b]melting points of the pure hydrogen bond donor molecules [c]melting points of the quaternary ammonium compounds

To further verify the formation, the DEMs are characterized by differential scanning calorimetry (DSC) measurements. DSC is a very useful tool to confirm the formation of DES since the interaction between the hydrogen bond acceptor and donor molecules will result in a lower freezing point than the melting points of the individual components. As it

is clearly seen from the DSC profiles of the deep eutectic monomers, the melting signals associated with the starting crystalline compounds were not present after mixing. Instead, clear glass transition temperatures were observed which were well below the room temperature as a result of the deep eutectic formation. There was no freezing point observed for DEMs within the scan limits of the measurements. As given in the table 1, glass transitions of -40 ºC, -54 ºC, -26.5 ºC, -30.2 ºC, -28.7 ºC, -47.9 ºC were obtained for DEM-1, DEM-2, DEM-3, DEM-4, DEM-5 and DEM-6, respectively. In all the cases, the materials were stable upon storage

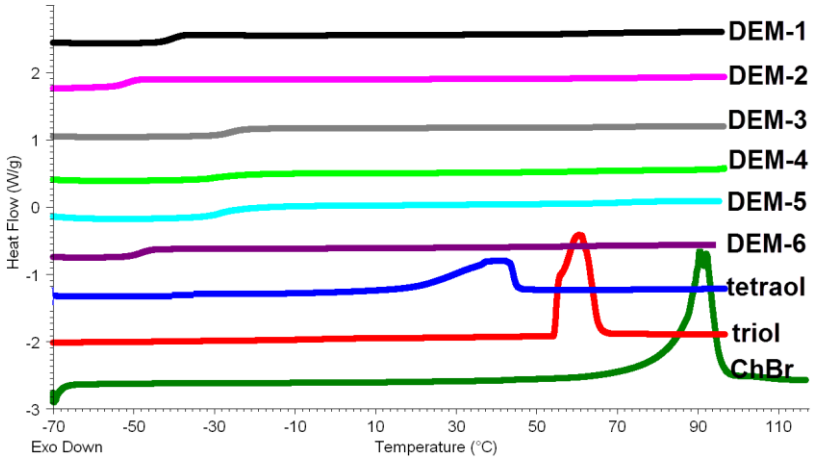

Figure 5.3. DSC scans of the DEMs prepared

Since the formation of the DEMs was verified by DSC measurements, the materials were structurally characterized by means of NMR and

FTIR measurements. As it is seen from figure 5.4, the characteristic chemical shifts associated with the ingredients of the deep eutectic monomers were identified. This verified that the compounds forming the DEM were intact confirming the structural integrity of the samples.

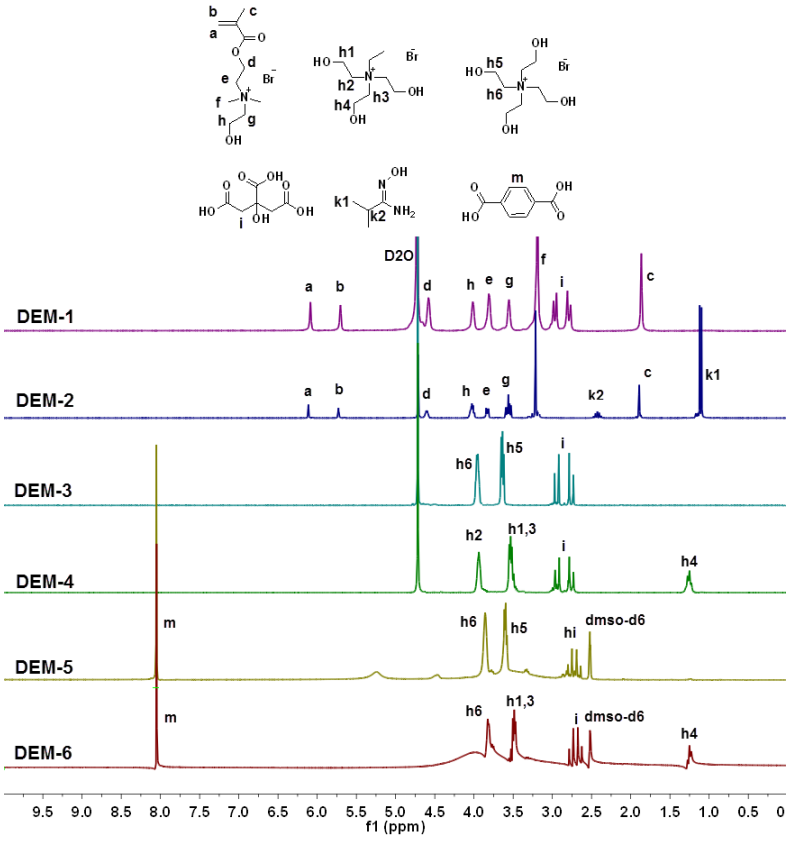

Figure 5.4. ^{1}H NMR spectra of the DEMs prepared

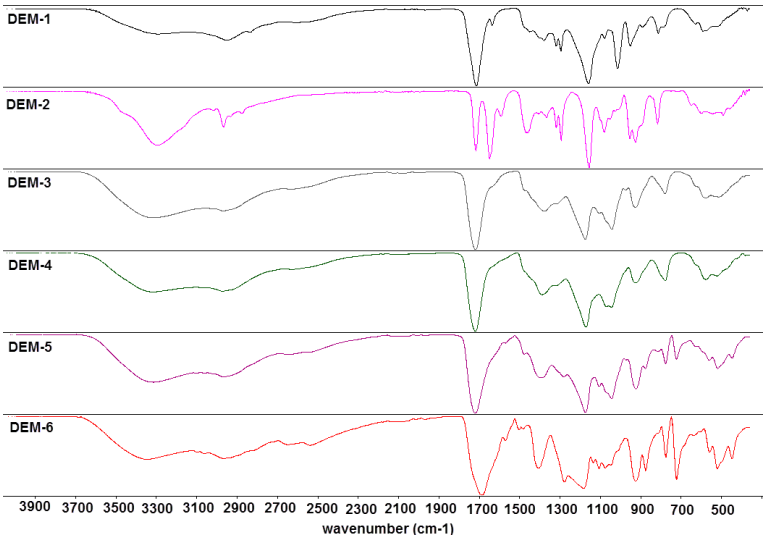

Figure 5.5. FTIR spectra of the DEMs prepared

Similarly, the FTIR characterization (figure 5.5) displayed characteristic bands originating from the functional groups present both in the quaternary ammonium compounds and hydrogen bond donor molecules. The O-H stretching bands associated with the presence of ethanol moieties in the quaternary ammonium compounds and the donor molecules were observed around 3350 cm^{-1} as a broad signal. For all the samples, C=O stretching band was observed around 1700 cm^{-1} associated with the ChBr monomer and the carboxylic acid molecules present in the formulations. In addition, C=N stretching band was observed at 1650 cm^{-1} for DEM-2 which contains the amidoxime molecule. The C=C stretching signal associated with the methacrylic monomer present in DEM-1 and

DEM-2 was observed at around 1630 cm^{-1} confirming the integrity of the compounds. The formation of the complexes was also confirmed by the upfield shift of the DEM signals in ^{1}H NMR spectroscopy as compared to the signals of the individual counterparts (figure 5.6).

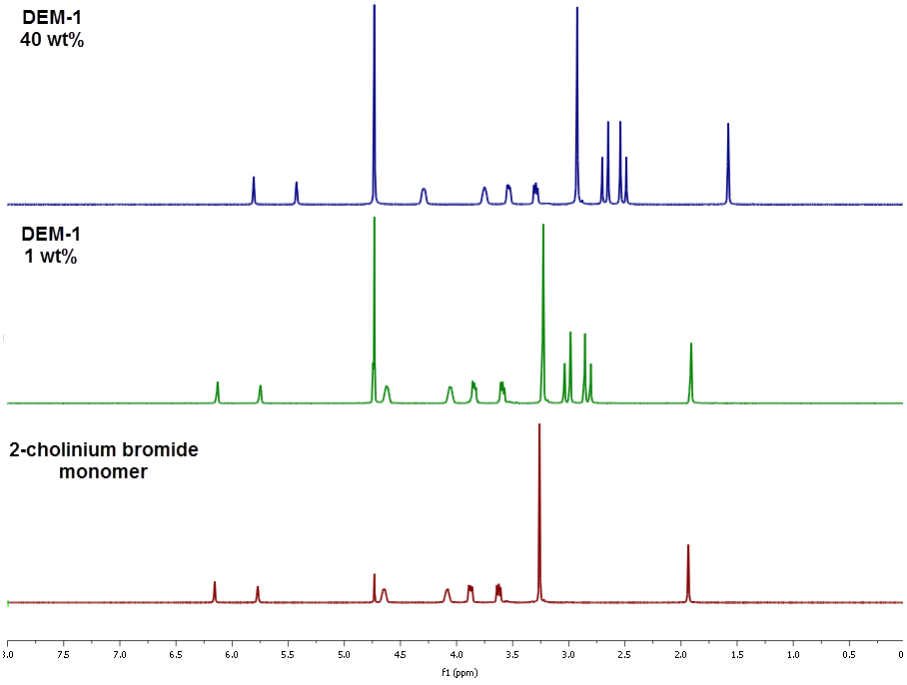

Figure 5.6. ^{1}H NMR signals of DEM-1 with different concentrations in D_2O

As the concentration was increased upto 40 wt%, an upfield shift on ^{1}H NMR signals was observed due to better establishment of the intermolecular interactions as seen in figure 5.6. This shielding effect upon the formation of the deep eutectic interactions with the anion is an indication

of the charge delocalization which causes the liquefaction of the mixture.

The DEM formation through the intermolecular interactions with the hydrogen bond acceptor and donor molecules were also studied by computational modeling. For this, DEM-2 was selected as the model system. All the density functional calculations (DFT) have been carried out with the Gaussian 09 suite of programs. The hydrogen bonding interactions of the donor and acceptor molecules are depicted in figure 5.7.

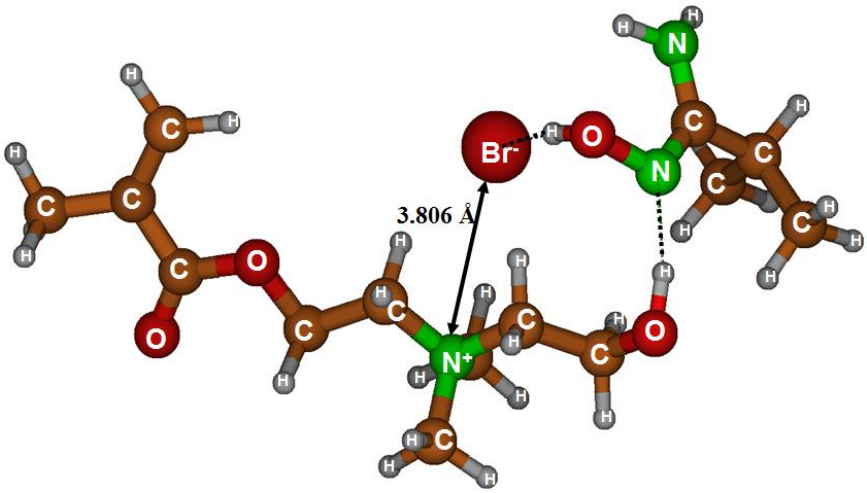

Figure 5.7. Optimized conformation of 2-cholinium bromide methacrylate with amidoxime

As it is seen from the computational result, the hydrogen bonding interaction primarily takes place between the bromide anion (Br^-) and the H

site of the N-OH unit of the amidoxime molecule. In addition, hydrogen bonding between the H site of the O-H of the cholinium cation and the N site of the N-OH unit on the amidoxime takes place. As a result of these strong interactions, the formation of the DEM occurs. The liquefaction upon the formation of the DEM can also be understood by looking at the distance between the cation and the anion. 3.752 Å original distance between the cation (N^+) and the anion (Br^-) was increased to 3.806 Å when amidoxime was added to form the DEM, lowering the coordination strength through charge delocalization. The weakened coordination results in a homogeneous mixture displaying a lower freezing point than the individual components of the system.

5.3.2. Polymerization of deep eutectic monomers

Photopolymerization is a facile technique to obtain polymeric materials and converts an initially liquid monomer mixture into a solid coating. In the cases, the monomers are solid an additional liquid diluent is needed which may be a problem in some applications. Interestingly, the liquid nature of the deep eutectic monomers allows conducting photopolymerization for the DEMs without the need of a diluent. Therefore, photopolymerization of strategy was chosen to polymerize the DEM-1 and DEM-2 based on cholinium methacrylate monomer. The polymerizations were straightforward. Typically, the monomer was mixed with

the desired amount of crosslinker together with the photoinitiator. The resulting liquid was casted into a Teflon mold and photopolymerized in a UV conveyor belt in less than two minutes. The resulting polymers were then dried and characterized. (Figure 5.8a).

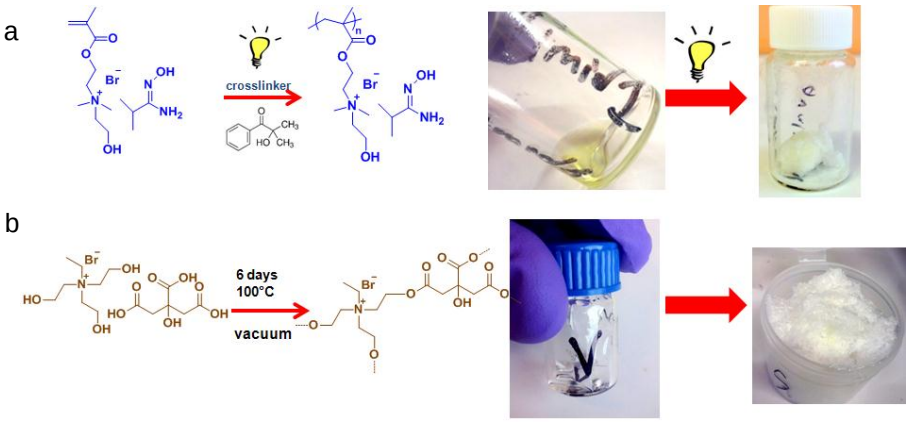

Figure 5.8. Preparation of the polymers by using deep eutectic monomers

The polymers and the monomer conversion were characterized by NMR. First to analyze the remaining monomer in the polymer, the samples are immersed in D_2O and the soluble part was analyzed. Since monomeric 2-cholinium bromide methacrylate is highly water soluble any unreacted molecule will be dissolved in the solvent. The resulting ^1H NMR spectra of the solution is provided in the figure 5.9.

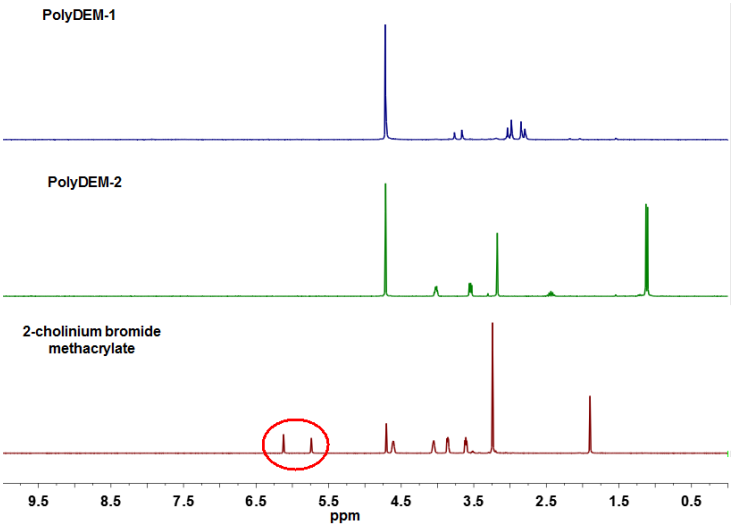

Figure 5.9. ^{1}H NMR signals of the extracted parts of the polyDEM-1 and polyDEM-2

As it is clearly seen, the monomer specific signals between 5.5 and 6.5 ppm associated with the reactive groups disappeared indicating a successful photopolymerization. In addition, solid state ^{13}C NMR spectra are provided in figure 5.10 confirming that the monomers were fully consumed during photopolymerization reaction. The new characteristic signals associated with the polymeric counterparts were also identified indicating the structural integrity of the final polymeric materials.

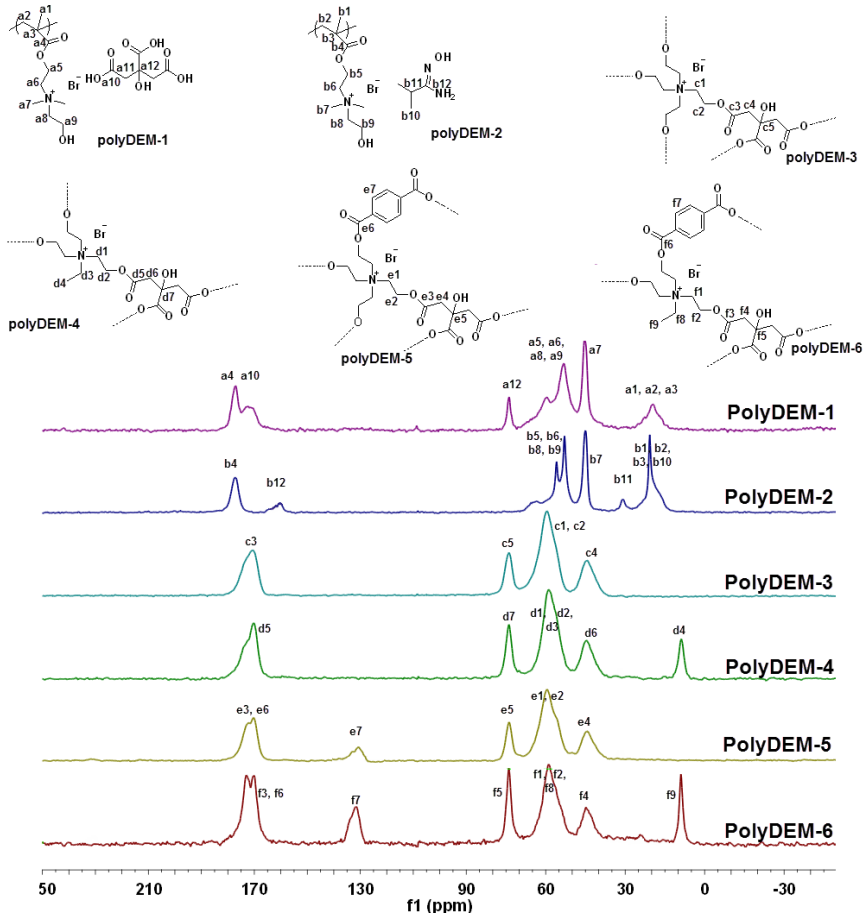

Figure 5.10. Solid state ^{13}C NMR spectra of the polymers prepared

Another approach to synthesize ionic polymeric materials through the use of DEMs as monomers is polycondensation reactions (figure 5.8b). For this purpose, DEM-3, DEM-4, DEM-5 and DEM-6 were used to obtain ionic polyesters. All these DEMs contain the necessary-multifunctional alcohols and carboxylic acid compounds without the need of adding any additional chemical. The reactions were conducted

by heating the DEMs to 100 ºC in a vacuum oven without the addition of catalysts. The samples were kept for 6 days to yield solid materials at the end of the condensation reactions. The obtained polymers are insoluble networks due to the presence of multifunctional monomers. The samples are washed repeatedly with methanol and acetone to remove any unreacted ingredient. In all cases, the yields of the reactions were around 90% indicating a successful esterification reaction. The resulting cross-linked polyesters were characterized by means of FTIR and solid ^{13}C NMR to confirm their chemical structures. The resulting spectra are provided in the figure 5.10 and 5.11. As it is seen from the ^{13}C NMR spectra, the signals associated with the polymer structures are observed indicating a successful polymerization reaction. FTIR revealed that the C=O and CO stretchings associated with the ester groups were around 1720 cm^{-1} and 1150 cm^{-1} , respectively. The presence of deep eutectic interactions allowed the polycondensation reactions to take place well below the melting temperatures of the ingredients since the components were homogeneously dissolved in the solid mixture upon the formation of the deep eutectic monomers. Altogether, this provides an alternative synthetic strategy to be used to produce ionic polyester networks.

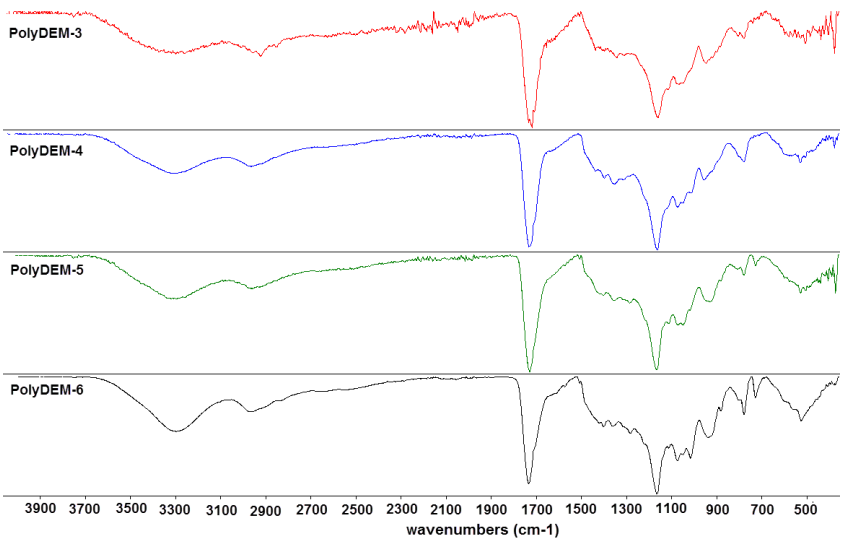

Figure 5.11. FTIR spectra of the polyesters prepared

The thermal properties of the polymers were characterized by means of differential scanning calorimetry (DSC) and thermal gravimetric analysis (TGA) (figure 5.12-5.13).

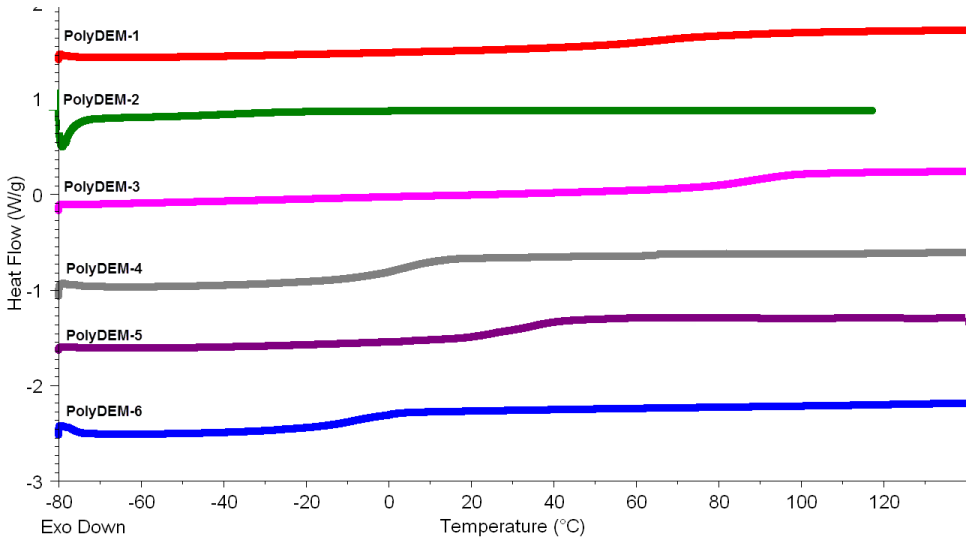

Figure 5.12. DSC scans of the polymers

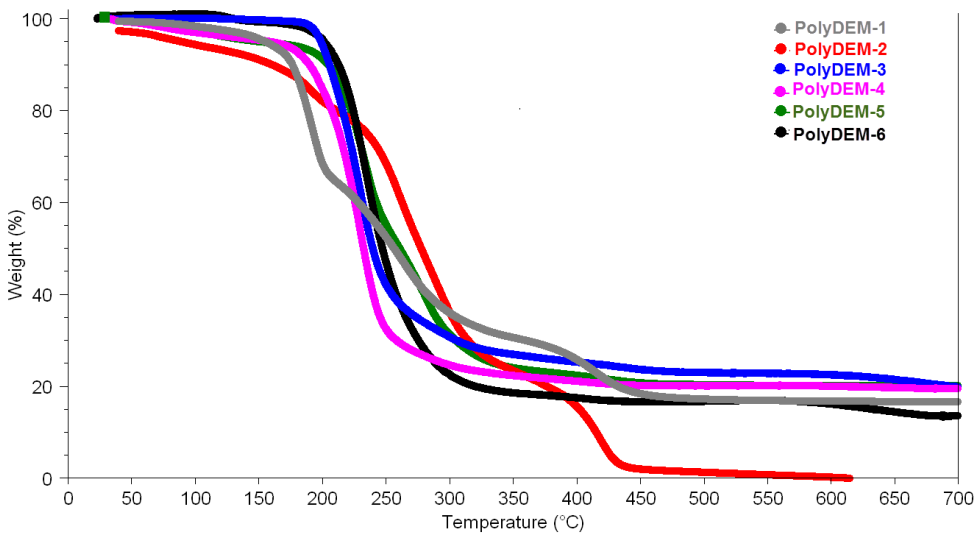

Figure 5.13. TGA scans of the polymers

Table 2. Thermal properties of the polyDEMs prepared

Polymer	T_g(ºC)	T_{onset} (ºC)	T_{dec}[a](ºC)
PolyDEM-1	62	175	257
PolyDEM-2	-36	169	278
PolyDEM-3	85	199	240
PolyDEM-4	2	194	233
PolyDEM-5	35	208	261
PolyDEM-6	-8	212	248

[a] The point where 50% weight loss is observed was taken as the decomposition temperature

As it is seen from the DSC profiles recorded, all the polymers displayed glass transition temperatures (T_g). The temperatures recorded was 62 ºC, -36 ºC, 85 ºC, 2 ºC, 35 ºC and -8 ºC for polyDEM-1, polyDEM-2, polyDEM-3, polyDEM-4, polyDEM-5 and polyDEM-6, respectively. The measured T_gs were broad indicating a morphological heterogeneity in the samples. The temperatures recorded were significantly higher than the values obtained for the starting DEMs. This is related with the formation of crosslinked networks upon the formation of the polymers either through photopolymerization or polycondensation reactions giving more rigid structures. Thermal stabilities of the polymers were analyzed and the TGA profiles are provided in figure 5.13. The lowest onset temperature was observed for polyDEM-2 prepared with the amidoxime. It is known that the degradation of amidoximes results in the formation of hydroxyl amine and nitrile compounds leading to the hydrolysis of the compound. The onset temperature for polyDEM-1 was observed around

175 ºC which is closer to the degradation temperature of the citric acid. As expected, the onset temperatures for polyesters were higher upto 212 ºC due to their highly crosslinked nature. The degradation temperatures for all the polymers were similar having an average value around 250 ºC. Except for polyDEM-2, all the polymers displayed residual masses around 20% at the end of the burning process.

5.3.3. CO_2 Capture

Both poly(ionic liquid)s and deep eutectic solvents[25] are promising materials for carbon dioxide uptake which is a very active area of research nowadays. On the one hand, initial studies to analyze the carbon dioxide capturing capability of poly(ionic liquid)s have shown quite good adsorption values specially when fluorinated counter-anions are involved[26]. On the other hand, DES ionic liquids have also demonstrated promising results.[25] Thus, a logical application for poly(ionic liquids) obtained by polymerized deep eutectic monomers is their use as solid sorbents for carbon dioxide. For that purpose, the poly(ionic liquid) based on the DEM composed of 2-cholinium bromide methacrylate and amidoxime was selected. Molecules containing amidoxime functionality have been proposed as candidates for CO_2 capture due to their high affinity towards CO_2[27] and amidoxime functionalized polyamides were prepared by some groups to be used as solid adsorbents.[28,29] Thus, the

polyDEMs based on amidoxime was found to be non-porous and the CO_2 uptake values at 273 K and 1 bar were found to be 4.5 mg/g (Figure 5.14).

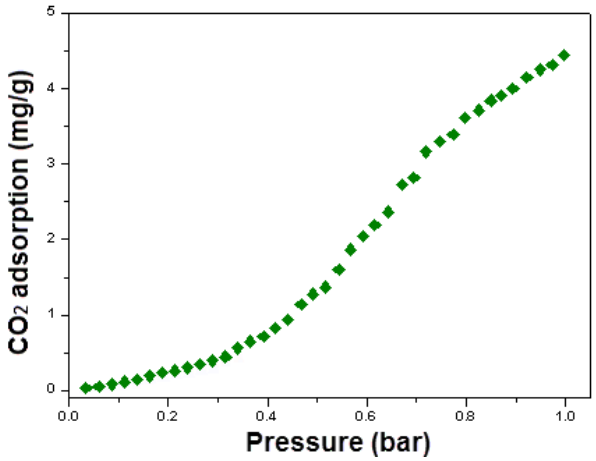

Figure 5.14. CO2 gas adsorption isotherms of polyDEM based on 2-cholinium bromide methacrylate and amidoxime at 273 K

This polymer produced through simple photopolymerization strategy by using an amidoxime overmatches the amidoxime non-porous functionalized polyamides analogs. The advantage to use our poly(ionic liquids) is that amidoxime molecules can be introduced into the solid polymers just by mixing commercially available molecules and the DES formation without the need of tedious covalent attachment step. Therefore, polymers based on DEMs can be a safe and facile alternative to the systems that are both currently under development.

5.4. Conclusions

In this work, we introduce the concept of deep eutectic monomers as a platform for the facile synthesis of new ionic polymeric materials. Various deep eutectic monomers were prepared by using different quaternary ammonium compounds as hydrogen bond acceptors and different carboxylic acids and/or amidoxime as hydrogen bond donors. The strong interactions taking place between the donor and acceptor molecules resulted in the formation of deep eutectic monomers which were viscous liquids at room temperature. The formation of these materials was verified by differential calorimetry measurements and found out that the DEMs only displayed glass transition temperatures in the scanned range and no melting point was recorded. The structural characterization revealed the integrity of the materials to be used as monomers to form polymeric materials. In case of the DEMs prepared with 2-cholinium bromide methacrylate ionic liquid monomer photopolymerization was chosen as a facile approach to produce polymers. For the DEMs prepared with quaternary ammonium alcohols, polycondensation was performed at mild conditions owing to the formation of homogeneous liquids through deep eutectic interactions. Carbon dioxide sorption studies were performed for a selected amidoxime containing polymer as potential application for polymerized deep eutectic monomers. These materials displayed promising results which may lead to

the further development of task-specific polymeric materials by selective design of deep eutectic monomers and polymers in the near future.

Scientific Contributions

Isik M., Ruiperez F., Sardon H., Gonzalez A., Zulfiqar S., Mecerreyes D., *Innovative poly(ionic liquid)s by the polymerization of deep eutectic monomers*, **2016**, submitted.

5.5. References

1- C. Capello, U. Fischer, K. Hungerbuhler, Green Chem., 2007, 9, 927-934.

2- T. Welton, *Chem. Rev.*, **1999**, 99, 2071-2083.

3- T. L. Greaves, C. J. Drummond, *Chem. Rev.*, **2015**, 115, 11379-11448.

4- A. P. Abbott, D. Boothby, G. Capper, D. L. Davies, R. K. Rasheed, *J. A. Chem. Soc.*, **2004**, 126, 9142-9147.

5- E. L. Smith, A. P. Abbott, K. S. Ryder, *Chem. Rev.*, **2014**, 114, 11060-11082.

6- A. Paiva, R. Craveiro, I. Aroso, M. Martins, R. L. Reis, *ACS Sustainable Chem. Eng.*, **2014**, 2, 1063-1071.

7- F. H. Hurley, T. P. Wier, Jr., *J. Electrochem. Soc.*, **1951**, 98, 203-206.

8- A. P. Abbott, G. Capper, D. L. Davies, R. K. Rasheed, V. Tambyrajah, *Chem. Commun.*, **2003**, 70-71.

9- Q. Zhang, K. D. O. Vigier, S. Royer, F. Jerome, *Chem. Soc. Rev.*, **2012**, 41, 7108-7146.

10- L. L. Sze, S. Pandey, S. Ravula, S. Pandey, H. Zhao, G. A. Baker, S. N. Baker, *ACS Sustainable Chem. Eng.*, **2014**, 2, 2117-2123.

11- A. P. Abbott, G. Capper, D. L. Davies, K. J. McKenzie, S. U. Obi, *J. Chem. Eng. Data*, **2006**, 51, 1280-1282.

12- H. G. Morrison, C. C. Sun, S. Neervannan, *Int. J. Phar.*, **2009**, 378, 136-139.

13- A. P. Abbott, P. M. Cullis, M. J. Gibson, R. C. Harris, E. Raven, *Green Chem.*, **2007**, 9, 868-872.

14- S. Garcia-Arguellas, C. Garcia, M. C. Serrano, M. C. Gutierrez, M. L. Ferrer, F. del Monte, *Green Chem.*, **2015**, 17, 3632-3643.

15- E. Gomez, P. Cojocaru, L. Magagnin, E. Valles, *J. Electroanalytical Chem.*, **2011**, 658, 18-24.

16- A. P. Abbott, O. Alaysuy, A. P. M. Antunes, A. C. Douglas, J. Guthrie-Srachan, W. R. Wise, *ACS Sustainable Chem. Eng.*, **2015**, 3, 1241-1247.

17- M. Sharma, C. Mukesh, D. Mondal, K. Prasad, *RSC Advances*, **2013**, 3, 18149.

18- J. D. Mota-Morales, M. C. Gutierrez, I. C. Sanchez, G. Luna-Barcenas, F. del Monte, *Chem. Commun.*, **2011**, 47, 5328-5330.

19- J. D. Mota-Morales, M. C. Gutierrez, M. L. Ferrer, I. C. Sanchez, E. A. Elizalde-Peña, J. A. Pojman, F. del Monte, G. Luna-Barcenas, *J. Polym. Sci. A. Polym. Chem.*, **2013**, 51, 1767-1773.

20- M. C. Serrano, M. C. Gutierrez, R. Jimenez, M. L. Ferrer, F. del Monte, *Chem. Commun.*, **2012**, 48, 579-581.

21- S. Garcia-Arguellas, M. C. Serrano, M. C. Gutierrez, M. L. Ferrer, L. Yuste, F. Rojo, F. del Monte, *Langmuir*, **2013**, 29, 9525-9534.

22- M. C. Gutierrez, D. Carriazo, C. O. Ania, J. B. Parra, M. L. Ferrer, F. del Monte, *Energy Environ. Sci.*, **2011**, 4, 3535.

23- J. Patiño, M. C. Gutierrez, D. Carriazo, C. O. Ania, J. L. G. Fiarro, M. L. Ferrer, F. del Monte, *J. Mater. Chem. A.*, **2014**, 2, 8719.

24- M. Isik, R. Gracia, L. C. Kollnus, L. C. Tome, I. M. Marrucho, D. Mecerreyes, *ACS Macro Lett.*, **2013**, 2, 975-979.

25- R. Ullah, M. Atilhan, B. Anaya, M. Khraisheh, G. Garcia, A. ElKhattat, M. Tariq, S. Aparicio, *Phys. Chem. Chem. Phys.*, **2015**, 17, 20941.

26- S. Zulfiqar, M. I. Sarwar, D. Mecerreyes, *Polym. Chem.*, **2015**, 6, 6435-6451.

27- S. Zulfiqar, F. Karadas, J. Park, E. Deniz, G. D. Stucky, Y. Jung, M. Atilhan, C. T. Yavuz, *Energy Environ. Sci.*, **2011**, 4, 4528.

28- S. Zulfiqar, S. Awan, F. Karadas, M. Atilhan, C. T. Yavuz, M. I. Sarwar, *RSC Advances*, **2013**, 3, 17203.

29- H. A. Patel, C. T. Yavuz, *Chem. Commun.*, **2012**, 48, 9989-9991.

6

Deep Eutectic Monomer Based Poly(ionic liquid)s For Enhanced CO_2 Capture

Contents

5.1. Introduction……185

5.2. Experimental……..189

5.3. Results and Discussion……..193

5.4. Conclusions……220

5.5. References……..222

Chapter 6

6.1. Introduction

Climate change due to global warming is one of the most immediate and important issues to be dealt with by humanity. The increase in the atmospheric carbon dioxide (CO_2) concentration is the major cause of this imminent threat, hence controlling the CO_2 concentration is the key aspect of this problem.[1,2] An easy and efficient way to reduce CO_2 concentration is to capture it prior to emission to atmosphere.[3-6] Although there are different methods such as chemical absorption, physical adsorption, cryogenic fractionation and/or membrane separation, solvent absorption is still the most widely utilized technique to capture and reduce CO_2 emissions.[7-9] The chemicals that are being used for this process generally involve amines, monoethanolamine being the industrial standard for this purpose. Unfortunately, it possesses many disadvantages such as corrosive nature, toxicity, degradability and high energy requirements for regeneration.[10,11] Therefore, development of solid sorbent materials is of the essence.[12,13] It is known that amines show selective and strong binding to CO_2 either through physisorption or chemisorption.[7-9] For that reason, these types of functional groups are essential when designing solid sorbent materials. Many different solid adsorbent systems decorated with amine functionalities are studied from different family of materials such as zeolites, activated carbons, metal

oxides, metal-organic frameworks etc..[14] However, this field is still open and active to new findings for the development of superior materials.

Ionic liquids have emerged as novel solvents for many different applications among which carbon dioxide capture can be given as an example.[15] Compared to conventional volatile compounds used for carbon dioxide capture, ionic liquids are nonvolatile, thus they do not require condensation during the regeneration process allowing to perform faster and easier and to save energy. The cation and anion forming the ionic liquid can be designed and tailor-made materials can be produced that possess high affinities towards carbon dioxide.[16] Task-specific ionic liquids containing reactive components towards carbon dioxide have been used to capture CO_2, yet these materials possess several drawbacks. Some of these can be listed as their complexity and cost for the synthesis and frequent use of unsustainable, environmentally unfriendly, mostly fluorinated, components.[17]

As an alternative to conventional ionic liquids, deep eutectic solvents (DESs) emerged for many different applications including carbon dioxide capture. The use of DESs for carbon dioxide capture is rather new and there are several studies reported in literature. Sze and coworkers designed task-specific ternary DESs by using choline chloride, glycerol and superbase 1,8-diazabicyclo[5.4.0.]undec-7-ene (DBU).[18]

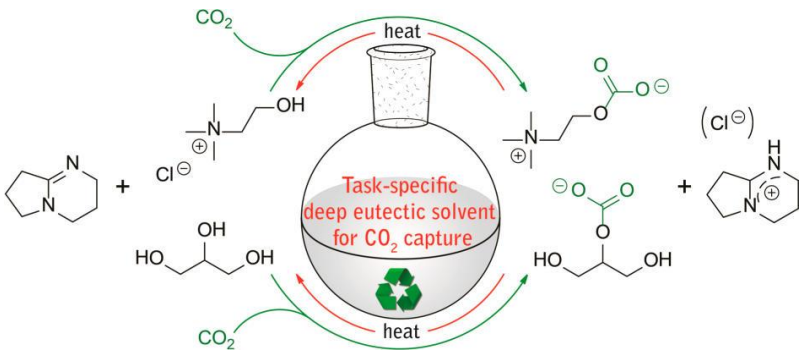

Figure 6.1. Ternary DES and the route for carbon dioxide capture and release (18)

These DESs displayed good carbon dioxide capture performance and the liquid nature of the DES facilitated the release of the carbon dioxide from the medium. However, the strong basicity of the ingredients increases the corrosive behavior of the ternary DES.

In literature, deep eutectic solvents have been prepared mostly with natural carboxylic acids. These DESs have been studied deeply for their physicochemical properties. Ullah and coworkers studied both experimentally and theoretically carbon dioxide capture performance of DES based on choline chloride and levulinic acid.[19]

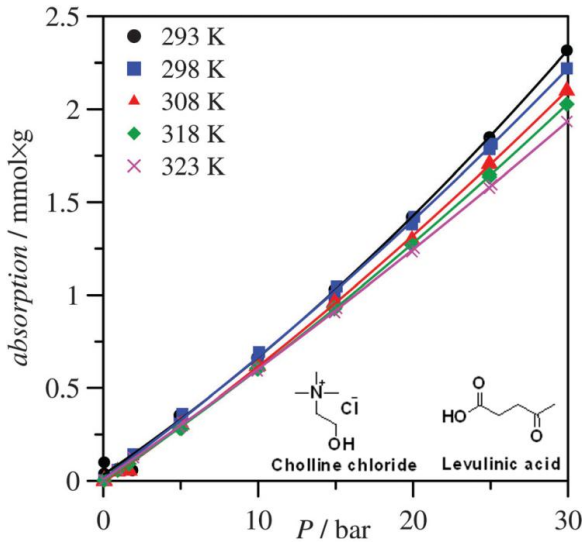

Figure 6.2. High pressure CO_2 solubility in choline chloride:levulinic acid (1:2) DES ionic liquid (19)

The carbon dioxide capture in choline chloride:levulinic acid DES ionic liquid was analyzed at different temperatures. The solubility of CO_2 was about 3 mg/g at 293 K. They also examined the corrosive behaviour of the DES ionic liquid and it was found out that the corrosivity of this solvent showed better performance compared to amine based solvents used in conventional systems.[19] However, the liquid nature of ionic liquids and DESs bring certain drawbacks in terms of application and also the sorbent performances have to be improved further. Therefore, we have decided to use various natural carboxylic acid molecules to form deep eutectic monomers and use them to prepare solid tailor-made

polymeric adsorbents for carbon dioxide capture. In this respect, a variety of DEMs were prepared and characterized to synthesize a library of different polymeric materials through a facile photopolymerization process. These materials were characterized and their performances for CO_2 capture were assessed. Throughout this chapter, the findings and results regarding the synthesis and characterization of DEM based polymers containing carboxylic acids will be discussed.

6.2. Experimental

6.2.1. Materials

2-dimethyalminoethylmethacrylate, 2-bromoethanol, ethylene glycol dimethacrylate, citric acid, malonic acid, oxalic acid, maleic acid, zinc chloride, ethyl acetate, methanol, 2-hydroxy-2-methylpropiophenone (photoinitiator) were obtained from Sigma-Aldrich as reagent grade high purity chemicals and used without further purification.

6.2.2. Deep eutectic monomer (DEM) preparation

The synthesis of the 2-cholinium bromide methacrylate (Cholinium bromide) was explained before in detail. Cholinium bromide quaternary

ammonium monomer was used to prepare the DEMs. Similar to the previous samples, DEMs were prepared through simple mixing of the monomer with the corresponding acid. In a typical preparation, calculated amount of cholinium bromide monomer was mixed with a calculated amount of a carboxylic acid. The solid mixture was homogenized by adding a small amount of methanol and mixed with a magnetic stirrer. The solvent was removed from the mixture by simple air purge and the remaining solvent was removed under vacuum. The resulting monomers were viscous liquids and characterized by ^{1}H NMR, FTIR and DSC to confirm the formation of the DEMs.

6.2.3. Polymerization of DEMs

The formation of DEMs results in homogeneous liquid monomers which allow performing quick photopolymerization reactions to obtain the polymers. In a typical polymerization reaction, the liquid DEM was mixed with the ethylene glycol dimethacrylate crosslinker (10 wt% with respect to the amount of polymerizable group) and the photoinitiator. The resulting solution was casted into Teflon mold. The solution was then exposed to UV light for photopolymerization. The polymer obtained was dried to get rid of any residual solvent or moisture. The resulting polymers were analyzed by ^{1}H NMR, FTIR, TGA and DSC.

6.2.4. Characterization

The NMR measurements were carried out on a Bruker AC-300 (for ^{1}H NMR) instrument with the following experimental conditions: spectral width 15 ppm with 32 K data points, flip angle 90, relaxation delay of 1 s, digital resolution of 0.24 Hz/pt. Solid state NMR spectra were recorded on a Bruker 400 AVANCE III WB spectrometer 9.40T. ^{13}C CP/MAS NMR spectra were collected using a 4mmMASDVT probe at a spinning of 12 KHz, using the cross polarization pulse sequence, at 100.63 MHz, a time domain of 2K, a spectral width of 29 KHz, a contact time of 1.5ms and an interpulse delay of 5s. Thermogravimetric analysis (TGA) was performed by using a TA instruments Q500 device. The samples were heated from 40 ºC to 800 ºC with a heating rate of 10ºC/min under nitrogen gas flow. Differential scanning calorimetry experiments were performed on a TA instruments Q200. The sample materials were enclosed in nonrecyclable aluminium hermetic pans, the sample masses being around 5-10 mg. The samples were first equilibrated at 0 ºC and heated to 80 ºC with a heating rate of 10 ºC/min and kept isothermal for 5 minutes to erase the thermal history. Then cooled down to -80 ºC and kept isothermal for 5 minutes. The samples then heated to 80 ºC with a heating rate of 10 ºC/min and the 2^{nd} heating cycles were taken for the detection of the glass transition temperatures. Attenuated Total Reflection Fourier Transform Infrared Spectroscopy (ATR-FTIR) was per-

formed on Bruker ALPHA-P equipment. The spectra were recorded from 350 cm^{-1} to 4000 cm^{-1} with a resolution of 2 cm^{-1} and 24 scans were taken for each spectrum. Dymax UVC-5 conveyor belt system with 800 mW/cm^2 intensity operating at a wavelength of 365 nm was used for photopolymerization. Sample to lamp distance was 100 mm and the belt speed was fixed at 2 m/min. 5 repetitive cycles were applied to achieve a full photopolymerization. X-Ray diffraction studies were conducted by using Bruker D8 Advance powder diffractometer. 0.1542 nm Cu-Kα radiation was used as the X-ray beam. The scans were performed from 2° up to 80° with 0.05º step size and step time of 5 seconds. The XRD intensities obtained were plotted against scattering angle 2θ.

6.2.5. CO_2 Capture

CO_2 measurements of PolyDEMs were recorded using Micromeritics ASAP 2020 physisorption analyzer at 273 K and 298 K. The samples were degassed at 343 K for 24h prior to analysis. The Brunauer–Emmett–Teller (BET) surface area of polyDEM samples was determined at 77 K with N_2 using Micromeritics ASAP 2020 physisorption analyzer.

6.3. Results and Discussion

6.3.1. DEM preparation and characterization

Preparation of the DEMs was straightforward. The cholinium bromide quaternary ammonium monomer was the hydrogen bond acceptor moiety in the formulation whereas the carboxylic acids were serving as hydrogen bond donor groups. As mentioned earlier, the quaternary ammonium monomer and carboxylic acid were mixed in a vial in solid state and small amount of solvent was introduced to homogenize the system. Mixing the components while purging with pressurized air yielded a viscous liquid. The remaining solvent was removed under reduced pressure. For the preparation of DEMs, 4 different carboxylic acids were chosen. Those natural acids are widely used in literature to make deep eutectic solvents. The chemical structures of the components of DESs are provided in the scheme below.

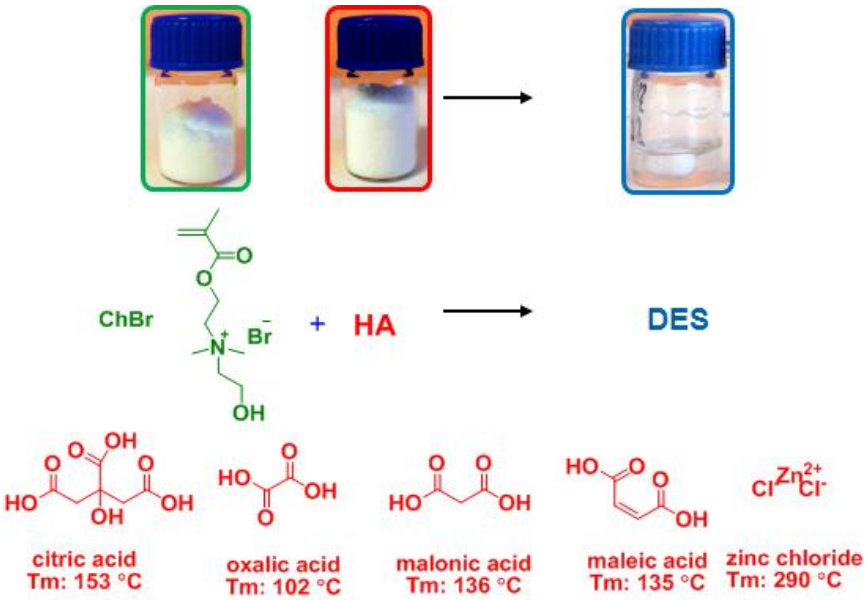

Scheme 6.1. DEM preparation and the structures of the chemicals used

DEMs prepared contained similar molar ratios of cholinium bromide and the acid. Since it is known that metal halides form DESs, $ZnCl_2$ was also used to prepare a DEM. The compositions and some physical properties of the DEMs are provided in the table below.

Table 6.1. Compositions and properties of DEMs prepared

Code	Composition	Molar Ratio	T_g[a] (°C)
DEM-A	ChBr/Citric acid	1/1	-40
DEM-B	ChBr/Citric acid	1/1.5	-37
DEM-C	ChBr/Oxalic acid	1/2	-55
DEM-D	ChBr/Malonic acid	1/2	-23
DEM-E	ChBr/Maleic acid	1/2	-53
DEM-F	ChBr/$ZnCl_2$	1/2	-48

[a]Glass transition temperature of the DEM. All the DEMs were obtained as viscous liquids. Freezing points were not detected for all the samples

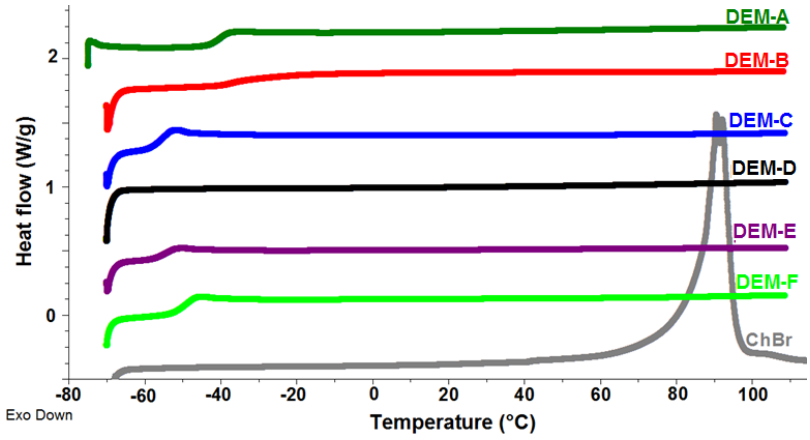

Figure 6.4. DSC signals of the DEM monomers

DSC scans confirmed the formation of the DEMs. As mentioned, the strong intermolecular interactions between the hydrogen bond acceptor and donor moieties results in a freezing point lower than the melting

point of the individual components. The 2-cholinium bromide methacrylate monomer displayed a melting point at 90 ºC as it can be seen in the figure 5.4. In the DEM-A monomer composed of citric acid (T_m: 153 °C) and cholinium bromide monomer displayed a glass transition (T_g) temperature of -40 °C and no freezing point (T_f) was detected in the range scanned. DEM-B had a T_g of -37 °C and no T_f was recorded. Similarly, DEM-C, DEM-D, DEM-E and DEM-F displayed T_gs of -55 °C, -23 °C, -53 °C, and -48 °C, respectively. No T_fs were recorded for all the samples in the DSC scan range. Differential calorimetry characterizations showed that the DEMs were formed for all the compositions resulting in liquid samples at room temperature. The DEMs were also analyzed by ^{1}H NMR to confirm the structures of the samples.

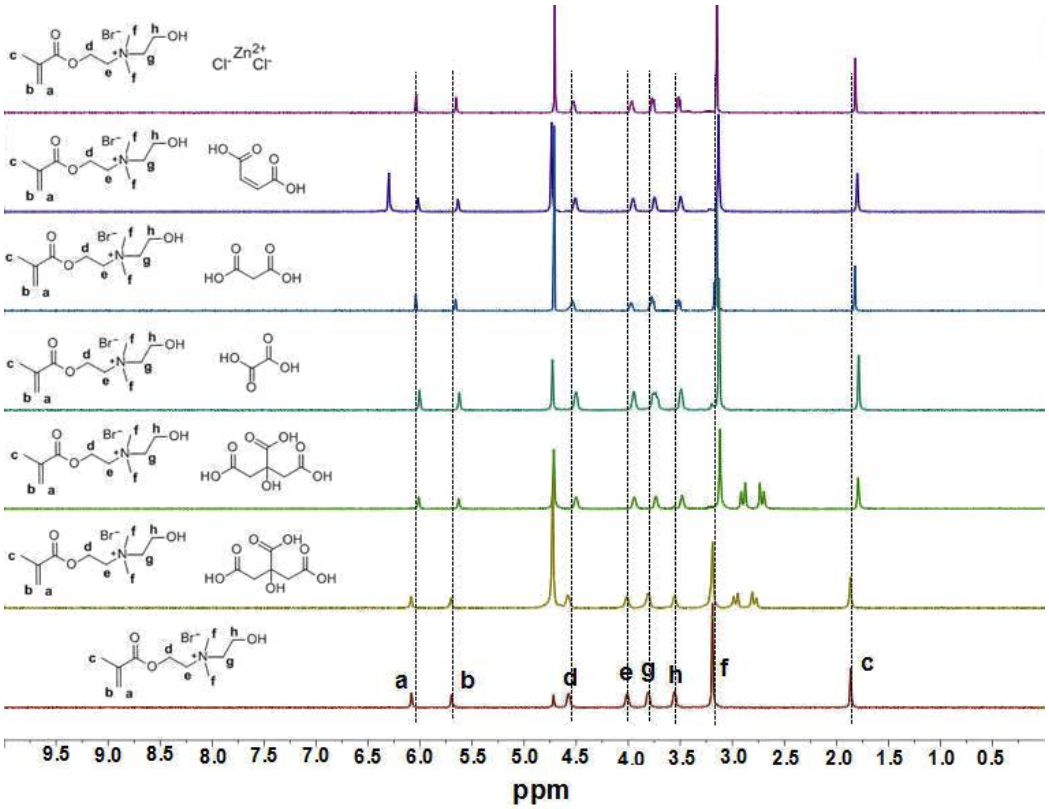

Figure 6.5. ^{1}H NMR signals of the DEMs prepared (300 MHz, D_2O)

As seen from the ^{1}H NMR spectra of the DEMs, the signals associated with the cholinium bromide monomer were clearly observed for all the DEMs indicating that the quaternary ammonium monomer was structurally intact in all the monomers prepared. In addition, signals associated with the citric acid between 2.5-3.0 ppm were observed in DEM-A and DEM-B monomers confirming the presence of the carboxylic acid. There was no additional signal was observed in the case of DEM-C since the carboxylic acid does not contain any methyl proton.

Similarly, DEM-D monomer displayed an additional peak at 3.20 ppm associated with the $–CH_2$ protons of the malonic acid. A clear signal at 6.27 ppm associated with the RCHCHR protons of maleic acid was observed for DEM-E as expected. No additional peak was observed for the DEM-F monomer since there is no additional proton source was introduced to the system. To sum up, ^1H NMR revealed that all the DEMs were successfully prepared with all the chemicals present and intact in the system.

Another interesting point observed from the spectra was the shift of the signals with the addition of carboxylic acids as a result of the intermolecular interaction between the quaternary ammonium monomer and the carboxylic acid. To be able to observe this interaction, two solutions of DEM-E were prepared, solid concentrations ranging from 1% to 60%. The chemical shifts due to change in the concentration of the samples are given in table below.

Table 6.2. ^{1}H NMR spectroscopy data of DEM-E recorded with different concentrations recorded in D_2O

Sample	δ (ppm)									
	HDO	Maleic acid	Cholinium bromide monomer							
		R-C<u>H</u>-C<u>H</u>-R	HO-C<u>H</u>$_2$	-C<u>H</u>$_2$-N(C<u>H</u>$_3$)$_2$-		C<u>H</u>$_2$ -	C<u>H</u>$_2$-OCO-C(C<u>H</u>$_3$)=C-<u>H</u> - <u>H</u>			
ChBr	4.71		3.63	3.88	3.25	4.64	4.08	1.92	5.76	6.14
Maleic acid	4.72	6.33								
DEM-E 60%	4.86	5.67	2.91	3.14	2.52	3.34	3.86	1.13	4.97	5.35
DEM-E 1%	4.72	6.37	3.59	3.81	3.21	4.04	4.59	1.89	5.73	6.11

The formation of the complexes was also confirmed by the upfield shift of the DEM signals in ^{1}H NMR spectroscopy as compared to the signals of the individual counterparts. The spectrum of concentrated samples revealed that the characteristic signals of DEM-E formed between cholinium bromide and maleic acid were upfield shifted as compared to the ones obtained for cholinium bromide and maleic acid in D_2O. This was indicative of strong change in the chemical environment upon the establishment of strong anion-hydrogen bond donor interactions as the concentration of the sample was increased. The rupture of this interaction resulted in a downfield shift as the anion cation introduction is reestablished.

Another characterization performed on the DEMs was FTIR measurements.

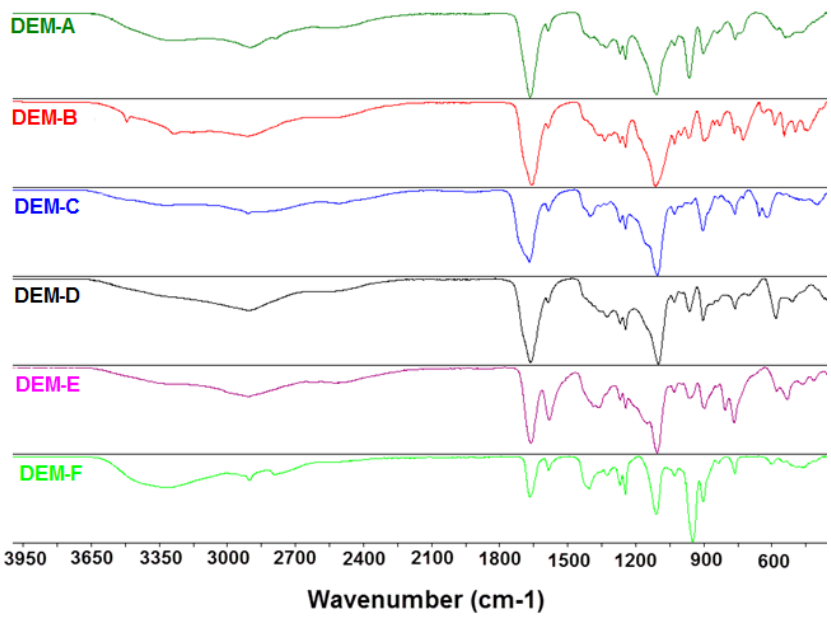

Figure 6.7. FTIR spectra of DEMs from 400 cm^{-1} to 4000 cm^{-1}

The broad band observed between 3050 cm^{-1} and 3570 cm^{-1} was assigned to OH stretching associated with the OH groups in the structures of both cholinium bromide and hydrogen bond donor moieties. Due to presence of hydrogen bonding, this band is observed as a broad signal for all the DEMs prepared. In addition, the C=O stretching associated with both the quaternary ammonium monomer and the hydrogen bond donors is observed around 1715 cm^{-1} for all the DEMs. Due to the presence of polymerizable C=C group in the cholinium bromide, the C=C stretching band associated with this group is observed at 1630 cm^{-1} for all the samples. This signal was more intense in the case of

DEM-E since the composition of this monomer involves maleic acid which also contains a C=C group. The broad peak observed around 1425 cm^{-1} to 1499 cm^{-1} was assigned to CH_2, CH_3 bending vibrations. The C-O stretching signal was observed around 1160 cm^{-1} for all the DEMs as a strong peak. The C-N stretching band was observed around 1295 cm^{-1} for all the DEMs associated with the presence of the quaternary ammonium monomer. FTIR characterization also confirmed the structural integrity of the DEMs prepared with cholinium bromide and hydrogen bond donor molecules.

Computational studies were also performed for DEM-A, DEM-C and DEM-D to find out the conformation of the hydrogen bond donor molecules with the quaternary ammonium monomer. All the density functional calculations (DFT) have been carried out with the Gaussian 09 suite of programs. The geometrical optimizations were performed using the long-range corrected functional ωB97XD, which includes dispersion corrections, together with the 6-31+G(d,p) basis set. Harmonic vibrational frequencies were obtained, at the same level of theory, by analytical differentiation of the gradients in order to determine whether the structures were minima or transition states. All structures showed real frequencies for all of the normal modes of vibration. These frequencies were then used to evaluate the zero-point vibrational energy (ZPVE) and the thermal corrections, at T = 298 K, in the harmonic oscillator approximation.

The electronic energy was refined by single-point calculations using the 6-311++G(2df,2p) basis set. The binding energy of 2-cholinium bromide methacrylate (ChBr) with the hydrogen bond donors was estimated as follows:

$$\Delta E_{CP} = E_0(complex) - E_0(ChBr) - E_0(acid)$$

where E0 refers to the electronic energy, along with the zero-point energy correction of the ChBr/hydrogen bond donor complexes and the individual molecules. ΔE_{CP} is the binding energy including the correction of the basis set superposition error (BSSE) by means of the counterpoise method. The results in the following images describe the hydrogen bonding with carboxylic acids for the anion and cation.

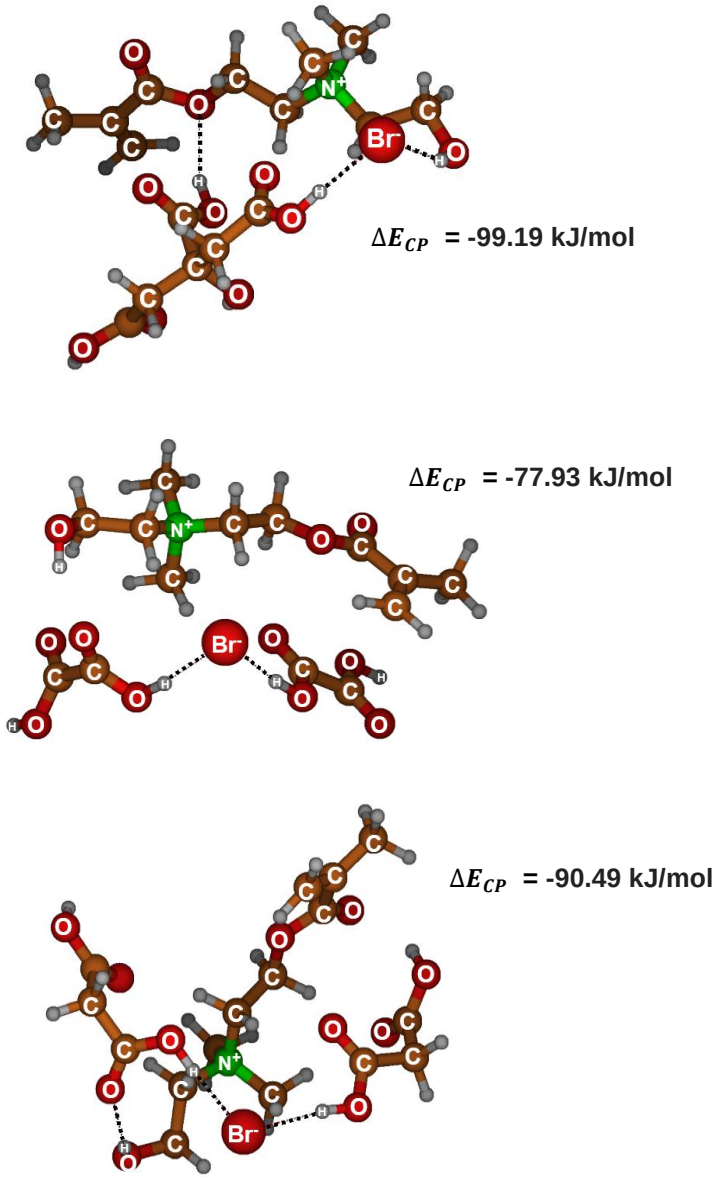

Figure 6.8. Optimized conformation of 2-cholinium bromide with carboxylic acids a) DEM-A (citric), b) DEM-C (oxalic), c) DEM-D (malonic)

The hydrogen bonding interactions of the donor and acceptor molecules are depicted in figure 6.8. As it can be seen for DEM-A, the interaction primarily takes place between the bromide anion (Br^-) and H site of the COO-H of the citric acid molecule. Another interaction between the Br^- and H site of the O-H of the cation is observed. The H site of the donor molecules primarily interacts with the COO site on the cation. The binding energy for the complex formed between the quaternary ammonium monomer and citric acid was calculated as -99.19 kJ/mol. DEM-C formed between the quaternary ammonium monomer and oxalic acid displayed hydrogen bonding between the bromide (Br^-) anion and H site of the COO-H of the two acid molecules present in the system. The binding energy for this system was calculated as -77.93 kJ/mol. The third analyzed system, DEM-D, displayed strong interactions with the Br^- site of the cation through H sites of the COO-H of the malonic acid donor molecules. In addition to these interactions observed, O site of the COO of the acid molecule displayed interaction with the H on the O-H unit of the cation. The binding energy between the quaternary ammonium monomer and the two malonic acid molecules was calculated as -90.49 kJ/mol. It is seen from the computational studies that the main hydrogen bondings are developed in the studied DEM systems are through the anion and the acidic protons of the carboxylic acid donor molecules. The binding energies also showed that the affinities of the

donor molecules towards the quaternary ammonium monomer are as follows citric acid > malonic acid > oxalic acid. This suggests that stronger interactions are established between citric acid and quaternary ammonium than malonic acid or oxalic acid. Another important point to mention is the changes in the distance between the cation and the anion as a result of the formation of the complexes. The original distance between the cation (N^+) and the anion (Br^-) was calculated as 3.752 Å. This value was increased upto 4.194 Å in the case of DEM-A prepared with citric acid. This significant increase suggests that the coordination strength between the ion pairs is decreased causing charge delocalization. Similarly, the cation-anion distances were calculated as 3.965 Å and 4.004 Å for DEM-C and DEM-D, respectively. As clearly seen, the increases in the distance between the cation and anion as a result of the strong interactions yield deep eutectic monomers displaying lower freezing points than the individual components of the system.

6.3.2. PolyDEM preparation and characterization

Photopolymerization, a straightforward and facile strategy, was used for the preparation of the polymers by using the DEMs. The formation of liquid samples upon the formation of DEM allows performing photopolymerization just by casting the components into a mold. To conduct the

polymerizations, the DEM mixture containing the monomer, crosslinker and the photoinitiator was casted into Teflon mold. The sample was exposed to UV light and the polymer was obtained at the end of the process. The preparation of the polymers is depicted in the figure below.

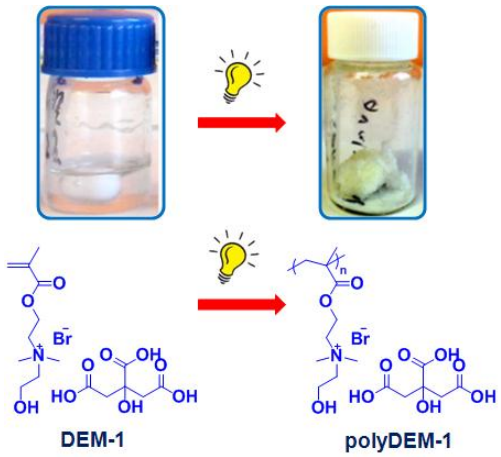

Figure 6.9. Illustration of the preparation of the polyDEM sample

The prepared polymer was placed into vacuum oven at 70 ºC to dry. The polyDEMs were characterized to observe their various properties. Due to their insoluble nature of the backbone of the polymeric samples, the monomer conversion was characterized by the immersion of the polymer samples in D_2O to be able to solubilize any unreacted monomer in the sample. The solution was then analyzed by ^1H NMR.

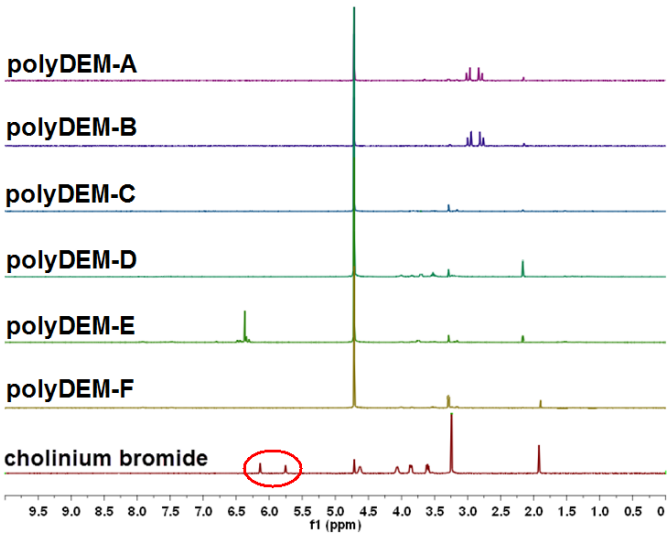

Figure 5.10. ^{1}H NMR spectra of the serums obtained from polyDEMs

Upon the immersion of the samples into D_2O, any unreacted monomer will dissolve in the medium. When the spectra are analyzed, it can be clearly seen that the monomer specific signals associated with H_2C=CR group are not observed in all the polyDEM samples between 5.5 and 6.25 ppm. This indicates that the polymerization of the monomer was quantitative in all the polymers. When the signals of polyDEM-A and polyDEM-B serums are analyzed, it is clearly observed that citric acid acting as the hydrogen bond donor in these DEMs was also dissolved in water giving signals at 2.7-3.0 ppm. There was no signal observed associated with oxalic acid since it does not possess any hydrogen except the acidic protons in the polyDEM-C. A weak signal associ-

ated with malonic acid was observed in polyDEM-D at 3.5 ppm. In case of polyDEM-E, a strong signal was observed at 6.37 ppm confirming the presence of maleic acid which possesses RCH=CHR. In all the polyDES samples, there were small signals observed around similar shifts associated with the cholinium bromide monomer. This suggests that there was a very small fraction of soluble polymer when the samples were immersed in D_2O. In conclusion, NMR characterization confirmed a successful photopolymerization of the DES monomers to obtain the corresponding polyDEMs. In addition, solid ^{13}C NNR spectra were acquired.

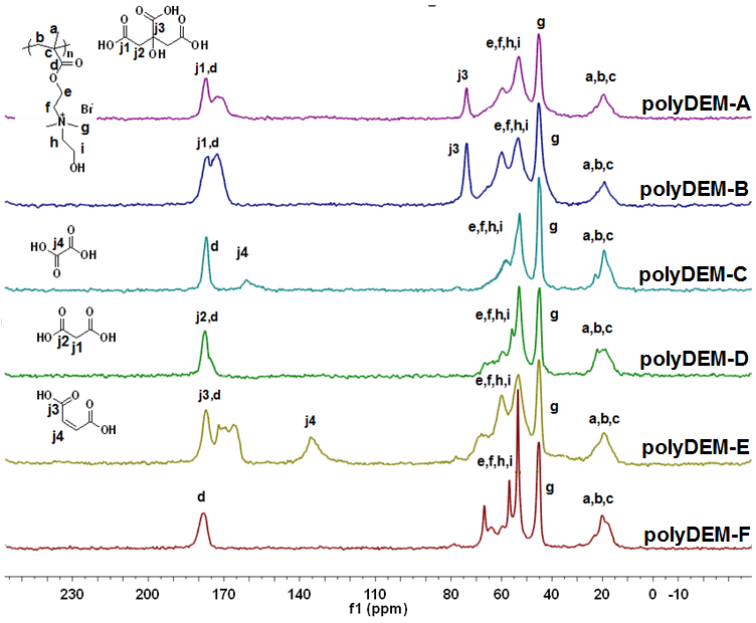

Figure 6.11. Solid state ^{13}C NMR of the polyDEMs

^{13}C NMR characterization of the polyDESs also confirmed the successful polymerization of the DEMs through photopolymerization. The signals associated with the monomer reactive C=C group between 125-136 ppm disappeared as a result of the polymerization. In addition, characteristic signals associated with the hydrogen bond donors in the formulations together with the signals associated with the backbone of the poly(ionic liquid) are observed confirming the structures of the polymers.

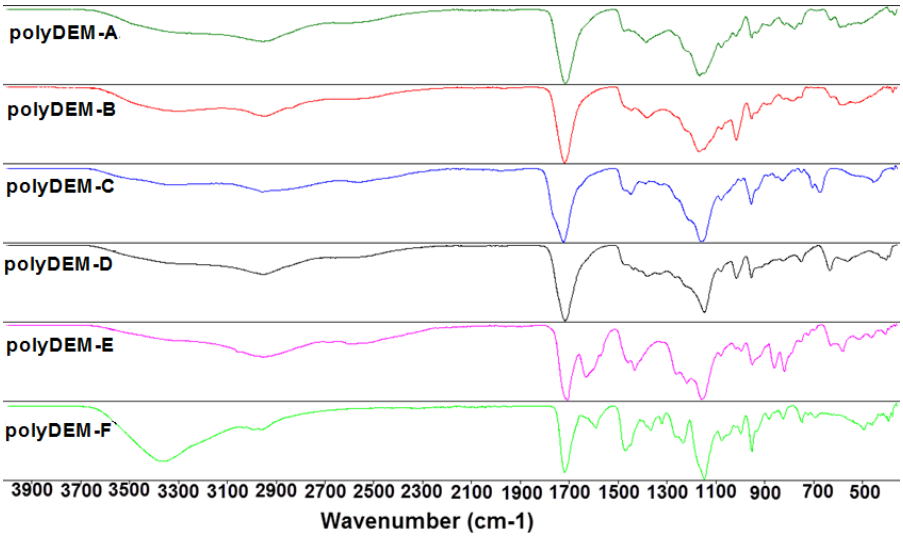

Figure 6.12. FTIR spectra of the polyDEMs from 400 cm^{-1} to 4000 cm^{-1}

Another characterization conducted was FTIR analysis. The OH stretching band as a broad signal was observed between 3000 cm^{-1} and 3650 cm^{-1} due to presence of hydroxyl groups in all DEM components.

The C=O stretching peak was observed at 1716 cm^{-1} for all the samples. The C=C stretching bands observed at 1630 cm-1 in the FTIR spectra of the monomers were disappeared indicating a successful polymerization of the monomers prepared. The C=C stretching band due to the presence of maleic acid in polyDEM-E was observed at 1635 cm^{-1}. The broad peaks observed around 1430 cm^{-1} were assigned to CH_2 bending vibrations. The strong peaks observed at 1150 cm^{-1} were assigned to C-O stretching associated both with the cholinium bromide and the hydrogen bond donor molecules. The FTIR spectra of the polymers after photopolymerization confirmed the structural integrity of the components forming the DEMs.

Differential scanning calorimetry (DSC) measurements were performed to detect the glass transition temperatures of the polymers prepared with DEMs.

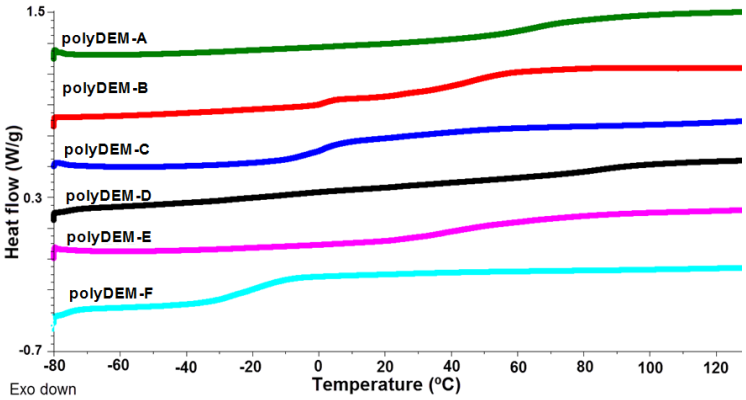

Figure 6.13. DSC scans of polyDEMs from -80 ºC to 120 ºC

The DSC characterization of the polymers revealed that all the polymers possess glass transition temperatures suggesting an amorphous backbone configuration. Although they displayed T_gs, there was no pattern observed with respect to changing hydrogen bond donor in the polyDEM composition. The midpoint of the transition was taken as the glass transition temperature. The values obtained were 62 ºC, 47 ºC, 15 ºC, 83 ºC, 37 ºC and -19 ºC for polyDEM-A, polyDEM-B, polyDEM-C, polyDEM-D, polyDEM-E and polyDEM-F, respectively. PolyDEM-B possessed another transition point at around 2 ºC. The recorded DSC scans revealed that all the samples displayed quite broad glass transitions suggesting a variety of thermal motions as a result of the morphological heterogeneity present in the samples. The recorded values were significantly higher compared to the values obtained for the starting DEMs. This is related with the formation of crosslinked networks upon the formation of the polymers giving more rigid structures.

To determine the thermal stabilities of the samples, thermal gravimetric analysis (TGA) was performed.

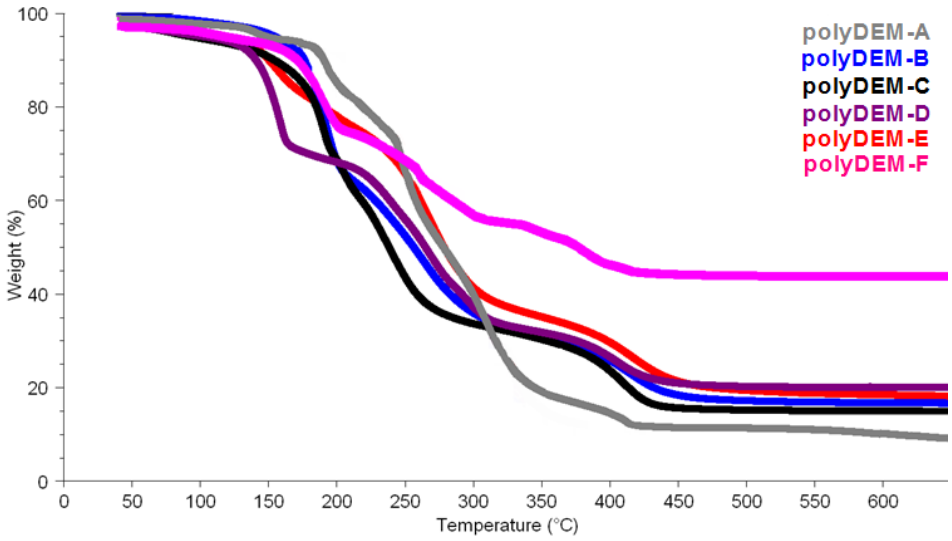

Figure 6.14. TGA profiles of polyDEMs

The TGA profiles showed that the polyDEMs displayed similar thermal stabilities regardless of the DEM component. The onset temperatures dependent on the hydrogen bond donor present in the system. The polymers with citric acid displayed slightly higher onset temperatures due to higher temperature stability of citric acid. The polyDEM-C, polyDEM-D and polyDEM-E containing oxalic, malonic and maleic acid displayed onset temperatures around 150 ºC. The degradation temperatures where 50% weight loss was observed were between 230 ºC and 275 ºC except the polyDEM-F which contains zinc chloride. All the samples displayed residual masses at the end of the TGA process. The pol-

ymers with carboxylic acid had residual masses upto 20% whereas the polyDEM-F displayed 40% residual mass.

Another characterization performed on the polyDEM samples was wide angle X-ray diffraction (WXRD) to analyze the state of the components of the polymers in solid-state. The hydrogen bond donor molecules present in the formulations are small molecules that are normally in crystalline form. Upon the formation of the DES, the crystallization of these molecules is disturbed eventually leading to freezing temperatures much lower than the melting points of individual components.

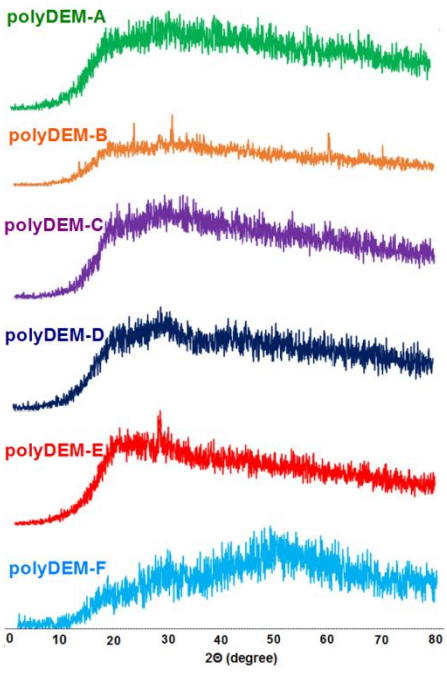

Figure 6.15. X-Ray diffraction profiles of the polyDEMs

XRD profiles revealed that the samples were mostly amorphous and did not show significant crystallization. The polymer which was prepared from DEM-A was totally amorphous displaying only an amorphous halo. PolyDEM-B displayed crystal peaks observed at around 2Θ degrees 14º, 24º, 31º, 60º and 70º as an indication of the partial crystallization of the certain fraction of the citric acid present in the formulation. It is worth mentioning that the difference between polyDEM-A and polyDEM-B in terms of composition is cholinium bromide monomer/citric acid ratio which is 1:1 and 1:1.5, respectively. It is clear that the increase in citric acid ratio for polyDEM-B (1:1.5) resulted in the crystallization of the citric acid suggesting that the strength of interactions between quaternary ammonium molecule and citric acid was not sufficient to lower the lattice energy as efficient as the 1:1 ratio. Only amorphous background was observed for polyDEM-C and polyDEM-D suggesting that the components were stable at the given ratio. The polymer prepared with maleic acid displayed a crystal peak at 29° indicating that the carboxylic acid was partially crystallized. The last sample polyDEM-F only displayed a broad amorphous halo indicating that the sample was totally amorphous.

6.3.3. CO_2 Capture

Testing the potential of PolyDEMs for CO_2 uptake is an emerging area of research. So far, very few attempts have been made with deep eutectic solvents only[19,20] and no attention has been paid to DES based polymers. The studies to analyze the carbon dioxide capturing capability of choline chloride/levulinic acid DES system revealed that the carbon dioxide molecules establish stronger interactions with the acid molecule than the ions. Consequently, this curiosity led us to synthesize six novel polyDEM samples formed with different carboxylic acids through a totally new approach. The use of DEMs rendered possible to produce the solid-state materials through a facile photopolymerization process. Resulting solid samples were characterized in terms of their performances to adsorb carbon dioxide. CO_2 adsorption isotherms of all six PolyDEM samples were measured at 273 K (Figure 6.16a), while the selected ones were also investigated for CO_2 sorption at 298 K (table 6.3 and figure 6.16b).

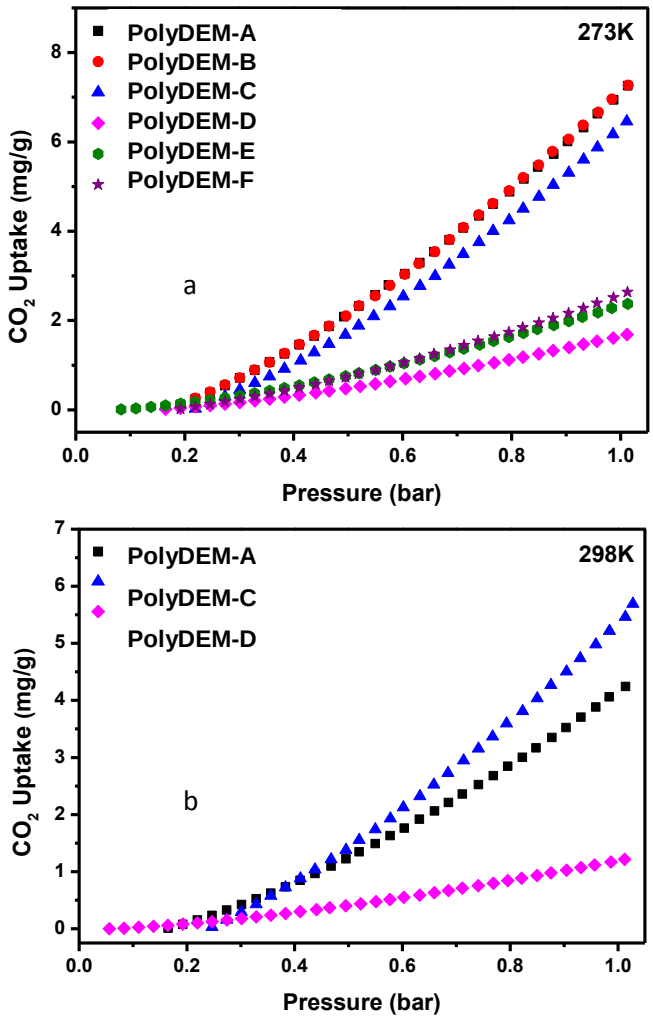

Figure 6.16. a) CO_2 gas adsorption isotherms of PolyDEMs at a) 273 K and b) 298 K for selected polyDEMs.

Table 6.3. Surface area, CO_2 adsorption data at 1 bar and Isosteric heat of adsorption (Q_{st}) of PolyDEM

PolyDEM	SA $_{BET}$ (m^2/g)	CO_2 Uptake (mg/g)		*$Q_{st, CO2}$ (kJ/mol)
		T = 273 K	T = 298 K	
PolyDEM-A	0	7.26	4.24	8.99
PolyDEM-B	0.521	7.27	-	-
PolyDEM-C	0.637	6.46	5.46	2.33
PolyDEM-D	0.178	1.69	1.22	5.50
PolyDEM-E	0.006	2.38	-	-
PolyDEM-F	0.200	2.63	-	-

*Isosteric heat of adsorption (Q_{st}) obtained from CO_2 isotherms data at 273K and 298K using Clausius-Clapeyron equation

Among all samples, PolyDEM A and B exhibited comparable and the highest CO_2 uptake at 273 K and 1 bar (7.26 and 7.27 mg/g) thus illustrating the superiority of using citric acid for the preparation of PolyDEM, respectively. These values of CO_2 sorption are in some cases comparable and higher as compared to other poly(ionic liquid)s already reported in literature[21-25] which are mostly based on highly toxic fluorinated anions. PolyDEM-A, polyDEM-B and polyDEM-C displayed at least two times more CO_2 sorption capacity as compared to the ChCl/Levulinic acid DES system studied in the literature.[19] The CO_2 sorption capacities of PolyDEM follow the decreasing order as given below:

PolyDEM-A~B > PolyDEM-C > PolyDEM-F > PolyDEM-E > PolyDEM-D

Keeping in mind, the conditions required for post combustion CO_2 capture, it is important to determine the sorption potential of any sorbent at 298 K from application viewpoint. The performance of PolyDEM samples at 298 K was monitored by selecting three polyDEM samples A, C and D with highest to lowest CO_2 sorption capacity range at 273 K (Figure 6.15). The CO_2 uptake decreases with increase in temperature in all the three samples depicting physical nature of adsorption.[26] It is important to note that CO_2 sorption of all PolyDEM samples is independent of surface area (Table 6.3). For instance, PolyDEM-A and PolyDEM-B have comparable CO_2 uptake even though PolyDEM-A exhibits zero surface area clearly indicating that CO_2 uptake not only depend on surface area and porosity but also get affected by the presence of heteroatoms, which is evident from the oxygen rich structure of citric acid thus promoting CO_2 sorption in PolyDEM. There already exists number of reports using various functionalities containing nitrogen and oxygen rich CO_2 phillic groups.[27-29] The interaction of carbon dioxide with the solid polyDEM matrix should be maintained in the physisorption regime to accomplish adsorbent regeneration with a minimal energy input. Therefore, isosteric heats of carbon dioxide adsorption (Q_{st}) was also calculated for PolyDEM-A, PolyDEM-C and PolyDEM-D from CO_2 adsorption

isotherms measured at 273 K and 298 K using Clausius-Clapeyron equation. The resulting curves are shown in the figure 6.17.

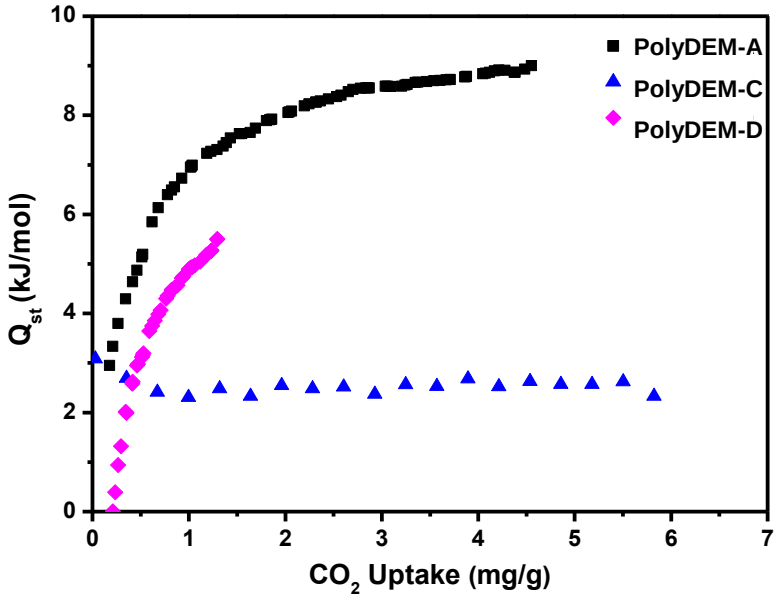

Figure 6.17. Isosteric heat of CO_2 adsorption for selected PolyDEMs

To determine Q_{st} is of paramount importance because it gives information about binding affinity of PolyDEM with CO_2 molecules. The Q_{st} values for PolyDEM-A, PolyDEM-C and PolyDEM-D were found to be 8.99, 2.33 and 5.5 kJ/mol respectively. The values clearly signify the physisorption process because the ones expected for chemisorption process are >40kJ/mol which are far above than the values observed for PolyDEM.

Computational studies were also performed to analyze the interaction of the studied DEM systems with carbon dioxide. The interaction energies of the selected DEMs with CO_2 were determined by using density functional calculations (DFT). The calculated interaction energies reveal the affinity of CO_2 molecule towards DEM systems studied. The calculated ΔE values were -14.97 kJ/mol, -13.20 kJ/mol and -9.29 kJ/mol for DEM-A (citric), DEM-C (oxalic) and DEM-D (malonic), respectively. The computational findings indicate that the DEM system containing citric acid has more affinity towards carbon dioxide. This is followed by the DEM containing oxalic acid and finally the lowest was calculated for the DEM with malonic acid. Thus, the interaction with CO_2 can be listed as follows:

ChBr-citric acid > ChBr-oxalic acid > ChBr-malonic acid

This order is also valid for the experimental findings. As discussed previously, citric acid containing system displayed the highest CO_2 uptake which is followed by the oxalic acid containing system. The lowest CO_2 uptake was observed for the malonic acid containing polyDEM system.

6.4. Conclusions

We presented a promising study on the synthesis and characterization of PolyDEMs using various natural acid molecules. The DEMs were formed between cholinium type quaternary ammonium methacrylic

monomer and carboxylic acids. All the DEMs prepared were liquids at room temperature as a result of strong intermolecular interactions between the components. The formation of the DEMs was confirmed through DSC measurements by the disappearance of the melting point of the monomer and no freezing temperature was recorded in the analyzed temperature range. All the DEMs were structurally confirmed by NMR and FTIR characterization. The resulting monomers were used to conduct photopolymerization at room temperature to obtain polyDEMs. The polymers obtained were used as solid sorbents for carbon dioxide. The CO_2 adsorption studies revealed that the CO_2 uptake capacity of PolyDEMs prepared with citric acid was significantly higher relative to other PolyDEM samples illustrating the exclusive role of citric acid, thus assisting enhanced interaction with CO_2 molecules. The current endeavor is the first mile stone and many other task-specific PolyDEMs can be exploited in the future for efficient CO_2 capture application by the use of green and environmentally benign systems.

Scientific contribution

Isik M, Zulfiqar S, Edhaim F, Ruiperez F, Rothenberger A, Mecerreyes D, *Deep eutectic monomer based poly(ionic liquid)s for enhanced CO2 capture*, **2016**, submitted.

6.5. References

1- R. A. Kerr, Science, 2007, **316**, 188–190.

2- U.S. Department of Commerce, National Oceanic and Atmospheric Administration (NOAA), Trends in Atmospheric Carbon Dioxide, http://www.esrl.noaa.gov/gmd/ccgg/trends/, accessed November 2015.

3- U.S. Department of Energy, Innovative Concepts for Beneficial Reuse of Carbon Dioxide, http://fossil.energy.gov/recovery/projects/beneficial_reuse.html, accessed November 2015.

4- R. Van Noorden, Nature, 2010, **463**, 871–873.

5- K. S. Lackner, Science, 2003, **300**, 1677–1678.

6- J. M. Matter and P. B. Kelemen, Nat. Geosci., 2009, **2**, 837–841.

7- G. T. Rochelle, Science, 2009, **325**, 1652–1654.

8- A. B. Rao and E. S. Rubin, Ind. Eng. Chem. Res., 2006, **45**, 2421–2429.

9- C. Lastoskie, Science, 2010, **330**, 595–596.

10- S. Lee, T. P. Filburn, M. Gray, J. W. Park and H. J. Song, Ind. Eng. Chem. Res., 2008, **47**, 7419–7423.

11- J. C. Abanades, E. S. Rubin and E. J. Anthony, Ind. Eng. Chem. Res., 2004, **43**, 3462–3466.

12- Q. A. Wang, J. Z. Luo, Z. Y. Zhong and A. Borgna, Energy Environ. Sci., 2011, **4**, 42–55.

13- C. T. Yavuz, B. D. Shinall, A. V. Iretskii, M. G. White, T. Golden, M. Atilhan, P. C. Ford and G. D. Stucky, Chem. Mater., 2009, **21**, 3473–3475.

14- a) X. Si, C. Jiao, F. Li, J. Zhang, S. Wang, S. Liu, Z. Li, L. Sun, F. Xu, Z. Gabelica, C. Schick, Energy Environ. Sci., 2011, **4**, 4522; b) Q. Yan, Y. Lin, C. Kong, L. Chen, Chem. Commun., 2013, **49**, 6873; c) S. Yang, J. Sun, A. J. Ramirez-Cuesta, S. K. Callear, W. I. F. David, D. P. Anderson, R. Newby, A. J. Blake, J. E. Parker, C. C. Tang, M. Schroder, Nature Chemistry, 2012, **4**, 887-894.

15- X. Zhang, X. Zhang, H. Dong, Z. Zhao, S. Zhang, Y. Huang, Energy Environ. Sci., 2012, **5**, 6668.

16- a) A. Shariati and C. J. Peters, J. Supercrit. Fluids, 2004, **30**, 139–144; b) J. E. Kim, J. S. Lim and J. W. Kang, Fluid Phase Equilib.,

2011, **306**, 251–255; c) M. B. Shiflett and A. Yokozeki, J. Chem. Eng. Data, 2008, **54**, 108-114.

17- a) E. D. Bates, R. D. Mayton, I. Ntai and J. H. Davis, J. Am. Chem. Soc., 2002, **124**, 926–927; b) J. M. Zhang, S. J. Zhang, K. Dong, Y. Q. Zhang, Y. Q. Shen and X. M. Lv, Chem.–Eur. J., 2006, **12**, 4021–4026; c) B. E. Gurkan, J. C. de la Fuente, E. M. Mindrup, L. E. Ficke, B. F. Goodrich, E. A. Price, W. F. Schneider and J. F. Brennecke, J. Am. Chem. Soc., 2010, **132**, 2116–2117.

18- L. L. Sze, S. Pandey, S. Ravula, S. Pandey, H. Zhao, G. A. Baker, S. N. Baker, ACS Sustainable Chem. Eng., 2014, **2**, 2117-2123.

19- R. Ullah, M. Atilhan, B. Anaya, M. Khraisheh, G. Garcia, A. ElKhattat, M. Tariq, S. Aparicio, Phys. Chem. Chem. Phys., 2015, **17**, 20941.

20- G. Garcia, M. Atilhan, S. Aparicio, Int. J. Greenhouse Gas Contr., 2015, **39**, 62-73.

21- J. Tang, H. Tang, W. Sun, M. Radosz and Y. Shen, J. Polym.

Sci. Part A: Polym. Chem., 2005, **43**, 5477–5489.

22- E.I. Privalova, E. Karjalainen, M. Nurmi, P. Mäki-Arvela, K. Eränen, H. Tenhu, D.Y. Murzin and J-P. Mikkola, ChemSusChem, 2013, **6**, 1500–1509.

23- J.M. Zhu, K.G. He, H. Zhang and F. Xin, Adsorpt. Sci. Technol., 2012, **30**, 35–41.

24- I. Azcune, I. Garcia, P. M. Carrasco, A. Genua, M. Tanczyk, M. Jaschik, K. Warmuzinski, G. Cabanero and Ibon Odriozola, ChemSusChem., 2014, **7**, 3407 – 3412.

25- J. Tang, H. Tang, W. Sun, M. Radosz and Y. Shen, Polymer, 2005, **46**, 12460–12467.

26- S**.** Zulfiqar, M. I. Sarwar, C. T. Yavuz, *RSC Adv*. 2014, **4**, 52263–52269.

27- S. Zulfiqar, S. Awan, F. Karadas, M. Atilhan, C. T. Yavuz, M. I. Sarwar, RSC Adv., 2013, **3**, 17203-17213.

28- R. Dawson, D. J. Adams, A. I. Cooper, Chem. Sci., 2011, **2**, 1173-1177.

29- S. Zulfiqar, F. Karadas, J. Park, E. Deniz, G.D. Stucky, Y. Jung, M. Atilhan, C. T. Yavuz, Energy Environ. Sci., 2011, **4**, 4258-4531.

7

General Conclusions

Chapter 7

This PhD thesis aimed at designing innovative ionic polymeric materials by using monomers coming from renewable sources. The most important results obtained during this PhD project are highlighted in this chapter.

Although many different ionic liquid monomers have been designed and their corresponding poly(ionic liquid)s (PILs) are reported in literature, most of the PILs are based on imidazolium cation and high toxicity fluorinated anions suggesting that the use of lower toxicity cation and anion combinations are overlooked. Therefore, ionic liquid monomers based on environmentally friendly cholinium cation were prepared (chapter 2). Cholinium cation was combined with different anions based on natural carboxylates. Similarly, non-cholinium based quaternary ammonium ionic liquid monomers were prepared for comparison. The corresponding ionic liquid monomers were polymerized and the resulting PILs were characterized. All the monomers were polymerized through free radical polymerization in water yielding relatively high molecular weight poly(ionic liquid)s. It was found out that the presence of hydroxyl groups both on the cation and the anion resulted in the formation of PILs with very low glass transition temperatures, decreasing down to -70 °C. This effect was most predominant for the PIL combining cholinium cation with lactate anion. Thermal stabilities of the PILs were found to be similar to each other, though there were slight deviations depending on

the composition, and they all displayed the common degradation profile of quaternary ammonium compounds. The ionic liquid monomer composed of cholinium cation and lactate anion was also used for two different applications. The liquid nature of the monomer allowed the preparation of cellulose coatings to be prepared through photopolymerization. At low cellulose loadings, transparent coatings were obtained indicating a good synergy between the ionic liquid monomer and the cellulose. As another possible application, the same monomer was used to produce ion gels through photopolymerization.

Another polymeric system based on the monomers coming from renewable sources was block copolymers of 2-cholinium lactate methacrylate with lactide (chapter 3). Cholinium based block copolymers were prepared by combining polylactide and 2-cholinium lactate methacrylate ionic liquid monomer. The block copolymer was synthesized through sequential polymerization of the monomers by using a dual functional RAFT agent. The organocatalyzed ring opening polymerization of the L-lactide was achieved through the initiation with the hydroxyl functionality present on the chain transfer agent. The use of a binary catalyst system allowed the reaction to be conducted at mild and living conditions. The production of low polydispersity macro chain transfer agents allowed the controlled radical polymerization of the ionic liquid monomer. The GPC characterization of the final polymers showed that all the polymers were

obtained with reasonable polydispersities suggesting a good control over the polymerization. The final polymers had lactic acid moieties in each repeat unit even though they display different behaviour. All the polymers were water soluble due to the presence of ionic block and they all displayed self-assembled nanostructures in water since the block co-polymers were amphiphilic. The molecular weight of the samples was effective on the size of the nanostructures. The homogeneity of the self-assembled structures was found to be affected the by the presence of some aggregations in the system. This indicates the importance of the preparation method in agreement with the findings in literature. These block copolymers are formed from biocompatible cholinium cation combined with lactate anion and lactic acid, therefore these materials can be good candidates for bioapplications.

Cholinium is one of the safest cations among the family of many cationic structures used in the literature. Therefore, ionic liquid monomer combining cholinium cation and lactate anion was used for the preparation of ion gels (chapter 4). The liquid nature of the monomer at room temperature allowed the preparation of the ion gels through photopolymerization in a practical way. To have a good compatibility with the polymer matrix, a low toxicity ionic liquid combining cholinium and lactate moieties was used as the free ionic liquid in the ion gel formulations. The presence of the same cation and anion structures allowed having a

very good compatibility leading to an ion gel with long-term structural integrity. The ion gels were produced with tunable mechanical, thermal and electrical properties. The amount of free ionic liquid inside led us to easily alter the physical properties of the final materials. The conductivity values were increased upto reasonable values by increasing the free ionic liquid inside the sample. The good conductivity obtained from the ion gels allowed using these materials as solid electrolytes for long-term cutaneous electrophysiology. The nonvolatility and high mechanical stability of the ion gels rendered possible to apply it onto the electrode and perform measurements upto three days. This cannot be achieved by conventional techniques and materials available. It was also shown that the deposition of the ion gel to the electrode significantly reduced the skin-electrode impedance providing a high resolution for the measurements.

In recent years, there have been significant afford to develop alternative solvents to ionic liquids. Deep eutectic solvents (DESs) have been so far the biggest breakthrough as alternatives since the beginning of the 21st century. Since then many people used these promising materials for many different applications. The use DES in polymer chemistry is relatively san unexplored topic. Considering the significant literature work on DES, we have decided to use this chemistry to produce poly(ionic liquid)s (chapter 5-6). To achieve that quaternary ammonium

alcohols and 2-cholinium bromide methacrylate were used as hydrogen bond acceptors and different hydrogen bond donors were incorporated to obtain the corresponding deep eutectic monomers. All the monomers were liquid at room temperature. The liquid nature of the DEMs allowed performing photopolymerization at bulk conditions. As an alternative approach, polycondensation was also utilized to obtain ionic polyesters. Considering the functional molecules present in the formulations, we have decided to use these materials as solid adsorbents for CO_2 capture. Although the samples were all nonporous, materials displayed comparable or even better CO_2 uptake compared to PILs reported in literature which are mostly based on highly toxic fluorinated anions. The next step for these materials should be the production of porous analogs which possibly will boom the sorption capacity of these materials as alternative to the conventional solid systems used.

During this research work, promising and innovative ionic polymers composed of low toxicity and renewable ingredients were obtained and their properties were investigated. These materials have been used for different applications and promising results were achieved. In all cases, special exertion was given to facile preparation approaches to achieve the final desired materials. The results obtained from different applications of the materials in different fields revealed promising results comparing to the findings in literature. As it is clearly demonstrated, there

are still different opportunities to produce state-of-the-art ionic polymeric materials by using innovative approaches; the next step should be the selective design of the compositions based on the obtained results to enhance the performances in the desired applications.

Annexes

NOMENCLATURE

^{13}C NMR	Carbon nuclear magnetic resonance
^{1}H NMR	Proton nuclear magnetic resonance
ATR	Attenuated total reflectance
ATRP	Atom transfer radical polymerization
BA	Benzoic acid
BF_4	Tetrafluoroborate
ChBr	2-cholinium bromide methacrylate
CMRP	Cobalt mediated radical polymerization
CO_2	Carbon dioxide
CTA	Chain transfer agent
DBU	1,8-Diazabicyclo[5.4.0]undec-7-ene
DEM	Deep eutectic monomer
DES	Deep eutectic solvent
DFT	Density functional theory
DLS	Dynamic light scattering
DSC	Differential scanning calorimetry

E’	Elastic modulus
E’’	Viscous modulus
ECG	Electrocardiography
EDX	Energy dispersive X-ray spectroscopy
EIS	Electrochemical impedance spectroscopy
FTIR	Fourier transform infrared
GPC	Gel permeation chromatography
IL	Ionic liquid
M_n	Number average molecular weight
M_w	Weight average molecular weight
NMP	Nitroxide mediated polymerization
PEDOT	Poly(3,4-ethylenedioxythiophene)
PF_6	Hexafluorophosphate
PIL	Poly(ionic liquid)
PLA	Polylactide
PSS	Poly(styrene sulfonate)
Q_{st}	Isosteric heat of adsorption
RAFT	Reversible addition-fragmentation chain transfer
ROP	Ring opening polymerization

Annexes

SEM	Scanning electron microscope
SNR	Signal-to-noise ratio
TEM	Transmission electron microscope
T_f	Freezing temperature
TFSI	Trifluoromethanesulfonylimide
T_g	Glass transition temperature
TGA	Thermogravimetric analysis
T_m	Melting temperature
WAXD	Wide angle X-ray diffraction
XRD	X-ray diffraction
ω	Angular frequency

Mehmet IŞIK

Phone: +34 678 365 796 (GSM)

E-mail: mhmtisik@gmail.com

Address: POLYMAT- Joxe Mari Korta Center,
San Sebastian-Donostia, Basque Country, Spain

EDUCATION

03.2013 - Present	PhD in Polymer Science and Technology (Marie Curie ESR) POLYMAT, Supervisor: Prof. David Mecerreyes University of the Basque Country, San Sebastian, Spain **Thesis title:** Synthesis of Innovative polyelectrolytes using monomers coming from renewable sources
09.2009 - 08.2011	**M.S.** in Materials Science and Engineering, Graduate School of Sciences & Engineering, Koç University, İstanbul, Turkey **Thesis title:** Synthesis of ABA type triblock copolymers by ring opening polymerization and investigation of the structure-property behavior of the copolymers
09.2004 – 06.2009	**B.S.** in Chemistry, College of Sciences, Koç University, İstanbul, Turkey

EXPERIENCE

03.2013 - Present	**POLYMAT - UPV/EHU,** San Sebastian, Spain **Marie Curie Early Stage Researcher**, Renaissance-ITN -Synthesis and characterization of polyelectrolytes -Ion gels, synthesis and characterization -Polyelectrolytes as solid adsorbents for carbon dioxide capture -Ionic polyurethane foams, preparation and characterization -Porous polyureas
03.2014-04.2014	**IMDEA Energy Institute,** Madrid, Spain **Visiting Researcher,** Electrochemical Processes Unit Impedance spectroscopy measurements of ion gels in climatic chamber

09.2011 – 10.2012	**Koç University,** Istanbul, Turkey **Research Assistant,** Polymer Science & Technology Lab -Modification of various thermoplastic and thermoset polymer surfaces to obtain superhydrophobic, self-cleaning surfaces -Design and synthesis of low molecular weight Jeffamine based polyureas as carbon fiber sizing agents -Synthesis of semi-fluorinated poly(urethane urea)s and preparation of self-cleaning surfaces by electrospinning
09.2009 – 08.2011	**Koç University,** Istanbul, Turkey **Research Assistant,** Polymer Science & Technology Lab -Synthesis of ABA type triblock copolymers and investigation of bulk and surface structure-property relations -UV/Ozone modification of silicone-urea copolymer films and electrospun fibers -Synthesis and characterization of multiphase polymers
Teaching Assistant	Organization of "Organic Chemistry I & II, Physical Chemistry I & II" laboratories. Instruction and grading of the students
09.2005 – 06.2009	**Koç University**, Istanbul, Turkey , **Undergraduate Research Assistant**, Polymer Science & Technology Lab - Synthesis and characterization of water chain extended poly(urethane-urea)s - Synthesis and characterization of perfluoroether containing poly(urethane-urea)s - Electrospinning and characterization of poly(fluoro-ether)s
09.2008 – 06.2009	**Koç University**, Istanbul, Turkey **Undergraduate Teaching Assistant** Preparation and organization of Organic Chemistry I and II, and analytical chemistry laboratories

ACADEMIC ACHIEVEMENTS

Publications during PhD

Isik M, Gracia R, Kollnus LC, Tome LC, Marrucho I, Mecerreyes D, *Cholinium based poly(ionic liquids): Synthesis, characterization and application as biocompatible iongels and cellulose coatings*, **ACS Macro Letters**, 2013, 2 (11), 975-979.

Isik M, Sardon H, Mecerreyes D, *Ionic liquids and cellulose: dissolution, chemical modification and preparation of new cellulosic materials*, **Int J Mol Sci**, 2014, 15 (7), 11922-40.

Isik M, Gracia R, Kollnus LC, Tome LC, Marrucho I, Mecerreyes D, *Cholinium Lactate Methacrylate: Ionic Liquid Monomer for Cellulose Composites and Biocompatible Ion Gels,* **Macromol Symp** (Special issue:Polymers and Ionic Liquids), 2014, 342 (1), 21-24.

Isik M, Sardon H, Saenz M, Mecerreyes D, New *amphiphilic block copolymers from lactic acid and cholinium building units*, **RSC Advances**, 2014, 4, 53407-53410.

Daniela C, Kermagoret A, Debuigne A, Riva R, German I, Isik M, Jérôme C, Mecerreyes D, Taton D, Detrembleur C, *Direct Route to Well-Defined Poly(ionic liquid)s by Controlled Radical Polymerization in Water,* **ACS Macro Lett**., 2014, 3(12), 1276-1280.

Tome LC, Isik M, Freire CSR, Mecerreyes D, Marrucho IM, *Novel pyrrolidinium-based polymeric ionic liquids with cyano counter-anions: High performance membrane materials for post-combustion CO_2 separation*, **J Membrane Sci**, 2015, 483, 155-165.

Isik M, Sardon H, Mecerreyes D, *Ionic Liquid and Cellulose Technologies: Dissolution, Modification and Composite Preparation,* Book Chapter in: Applications of Ionic Liquids in Polymer Science and Technology, **Springer**, 2015.

Diaz M, Ortiz A, Isik M, Mecerreyes D, Ortiz I, *Highly conductive electrolytes based on poly([HSO_3-BVIm][TfO])/[HSO_3-BMIm][TfO] mixtures for fuel cell applications,* **Int J Hydrogen Energ**, 2015, 40, 11294.

Daniela C, Kermagoret A, Debuigne A, Jerome C, Mecerreyes D, Isik M, Taton D, Detrembleur C, *All Poly(ionic liquid)-Based Block Copolymers by Sequential Controlled Radical Copolymerization of Vinylimidazolium Monomers*, **Macromolecules**, 2015.

Isik M, Lonjaret T, Sardon H, Marcilla R, Herve T, Malliaras G.G., Ismailova E, Mecerreyes D, *Cholinium-Based Ion Gels as Solid Electrolytes for Long-Term Cutaneous Electrophysiology,***J Mater. Chem. C**, 2015.

Joao K.G, Tome L.C, Isik M, Mecerreyes D, Marrucho I, *Poly(ionic liquid)s as phase splitting promoters in aqueous biphasic systems*, **Phys. Chem.Chem. Phys**., 2015.

Isik M, Margarida A. C. F, Kari V, Paulis M, Mecerreyes D, *Preparation of poly(ionic liquid) nanoparticles and their novel application as flocculants for water purification*, **Polym. Chem.**, 2016

Isik M, Ruiperez F, Gonzalez A, Sardon H, Zulfiqar S, Mecerreyes D, *Innovative Poly(ionic liquid)s by the Polymerization of Deep Eutectic Monomers***,** Submitted, 2016.

Isik M, Zulfiqar S, Edhaim F, Ruiperez F, Rothenberger A, Mecerreyes D, *Deep eutectic monomer based poly(ionic liquid)s for enhanced CO_2 capture*, Submitted, 2016.

Previous Publications

Yilgor E, M. Isik, I. Yilgor, *Novel synthetic approach for the preparation of poly(urethaneurea) elastomers*, **Macromolecules,** 2010 43 (20), 8588-8593.

Yilgor E, O. Kaymakci, M. Isik, S. Bilgin, I. Yilgor, *Effect of UV/Ozone irradiation on the surface properties of electrospun webs and films prepared from polydimethylsiloxane-urea copolymers*, **Appl. Surf. Sci**., 2012, 258 (10), 4246-4253.

Yilgor I, Bilgin S, Isik M, Yilgor E, *Facile preparation of superhydrophobic polymer surfaces*, **Polymer**, 2012, 53 (6), 1180-1188.

Yilgor I, Bilgin S, Isik M, Yilgor E, *Tunable wetting of polymer surfaces*, **Langmuir**, 2012, 28 (41), 14808-14814.

Bilgin S, Isik M, Yilgor E, Yilgor I, *Hydrophilization of silicone-urea copolymer surfaces by UV/Ozone:Influence of PDMS molecular weight on surface oxidation and hydrophobic recovery*, **Polymer**, 2013, 54 (25), 6665-6675

Yilgor E, Isik M, Soz C.K, Yilgor I, *Synthesis and structure-property behavior of polycaprolactone-polydimethylsiloxane-polycaprolactone triblock copolymers*, **Polymer**, 2016.

Conference Participations

Oral Presentation- 3rd Bilateral Workshop on Novel Materials in collaboration with Max Planck Institute (2008).
Koç University, İstanbul, Turkey
Presentation Title: Synthesis of polyurethane-urea using water as the chain extender

Oral Presentation- **IUPAC World Polymer Congress – MACRO2012 (2012)**
Virginia Tech, Blacksburg, Virginia, USA
Presentation Title: Influence of block lengths on the morphology and properties of PCL-PDMS-PCL triblock copolymers

Oral Presentation- Green chem. and nanotechnologies in polymer chemistry (2014)
Polytechnic Institute, San Sebastian, Spain
Presentation Title: Lactic acid based amphiphilic block copolymers: synthesis, characterization and self assembly in water

Oral Presentation- Green biopolymers and energy conversion and storage (2015)
Linkoping University, Linkoping, Sweden
Presentation Title: Cholinium based ion gels as solid electrolytes for long-term cutaneous

Oral Presentation- ACS National Meeting and Exposition-Boston (2015)
Boston, MA, USA
Presentation Title: Cholinium based ion gels: Synthesis, characterization and application as electrolytes for electrocardiography (ECG)

Poster Presentation- **EUPOC 2013- Polymers and Ionic Liquids (2013)**
Gargnano, Lago di Garda, Italy (Best poster award)
Presentation Title: Cholinium based poly(ionic liquids):Synthesis, characterization and application as biocompatible iongels and cellulose coatings

SKILLS

Operational Skills:

Atomic Force Microscopy (AFM), Scanning Electron Microscopy (SEM), Gel Permeation Chromatography (GPC), Differential Scanning Calorimetry (DSC), Thermo gravimetric Analysis (TGA), UV/VIS Spectrometry, Infrared Spectroscopy (FT-IR), Dynamic Mechanical Analysis (DMA), Electrospinning, X-Ray Diffractometry (XRD), X-Ray Photoelectron Spectroscopy (XPS), White Light Interferometry (WLI), Impedance Spectrometer, Rheometer, Microwave Plasma, Optical Microscopy, Goniometer, Surface Tensiometer, Instron Stress-Strain Analyzer.

Languages: Turkish (native), English (fluent), Spanish (intermediate)

SCHOLARSHIPS

- 03.2013 - 03.2016 **Marie Curie ESR Fellowship** for PhD Studies
- 09.2009 – 09.2011 **Merit scholarship** from Koç University for M.Sc. studies
- 09.2004 – 06.2009 **Merit scholarship** from Koç University for B.Sc. education
- 09.2008 – 01.2009 Vehbi Koç Scholar Award, Koç University, Istanbul

INTERESTS

- Member of “United Aikido Organization”
- Reading, history, music, cinema